PREFACE

We would like to offer the readers the scientific activity report of the Frank Laboratory of Neutron Physics for 2015. The first part of the report presents a brief review of the experimental and theoretical results achieved in the main scientific directions – condensed matter physics, neutron nuclear physics, applied research and development and creation of elements of neutron spectrometers for condensed matter investigations. The second part includes the reports on the operation of the modernized IBR-2 pulsed reactor, the development of the IREN neutron source and researches carried out on EG-5 facility. A list of publications for 2015, the information regarding the seminars and conferences organized in FLNP and a statistical view on the FLNP personnel structure are presented as well.

In 2015 the main achievements of the Laboratory were:

- successful fulfillment of the user program at the IBR-2 spectrometers;
- development of spectrometer complex at the IBR-2 reactor;
- development of IREN facility.

In 2015 the IBR-2 reactor operated for physical experiments for 2646 hours, the IREN facility 237 hours and EG-5 accelerator - 510 hours.

FLNP has cooperation agreements in the field of neutron investigations with almost 200 scientific institutes and universities from more than 40 countries from all over the world. A significant contribution to this cooperation is made by the JINR Member States.

The FLNP staff consists of more than 450 employees in this about 150 less than 35 years of age. The scientific staff includes 84 Ph.D. and 19 D.Sc. researchers and 74 researchers and specialists from 14 of the JINR Member States (besides the Russian Federation) and associated members.

The organization of annual conferences and schools covering all FLNP research fields helps to recruit young specialists — one of the top priority tasks of the FLNP Directorate.

All these facts confirm that the Laboratory continues to develop successfully and dynamically, carrying out investigations in the interests of the JINR Member States.

V.N. Shvetsov

Director

Members of the Directorate of the Frank Laboratory of Neutron Physics:

SHVETSOV
Valeryi
Nikolaevich
Director
since 2013

Deputy Directors for Science

CULICOV
Otilia
Ana
since 2013

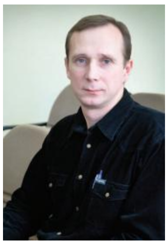

LYCHAGIN
Egor
Valerievich
since 2013

KUČERKA
Norbert
since 2014

KOZENKOV
Sergey
Vyacheslavovich
Deputy Director
for General Issues
since 1989

VINOGRADOV
Alexander
Vital'evich
Chief Engineer
since 2007

CHUDOBA
Dorota
Marta
Scientific secretary
since 2013

1. SCIENTIFIC RESEARCH

CONDENSED MATTER PHYSICS

The main objectives of research in the framework of the theme involved the application of neutron scattering techniques and complementary methods to investigate the structure, dynamics and microscopic properties of nanosystems and novel materials, which are of great importance for the development of nanotechnologies in the fields of electronics, pharmacology, medicine, chemistry, modern condensed matter physics and interdisciplinary sciences.

In 2015, the greater part of experimental research was carried out on the spectrometers of the modernized IBR-2 reactor in accordance with the Topical Plan for JINR Research and International Cooperation and FLNP User Program. A number of scientific experiments were performed in neutron and synchrotron centers in Russia and abroad under the existing cooperation agreements and accepted beam time application proposals. Also, the activities on the modernization of the available spectrometers and the development of new instruments were carried out in accordance with the development program plan for the IBR-2 spectrometers. Most attention was given to the realization of the top-priority projects (creation of the final configuration of a new DN-6 diffractometer for studying microsamples and a multipurpose GRAINS reflectometer).

Within the framework of investigations under the theme the employees of the FLNP Department of Neutron Investigations of Condensed Matter (NICM) maintained broad cooperation with many scientific organizations in Russia and abroad. The cooperation, as a rule, was documented by joint protocols or agreements. In Russia, especially active collaboration was with the thematically-close organizations, such as RRC KI, PNPI, SSC RF IPPE, MSU, IMP UB RAS, IC RAS, INR RAS and others.

A list of the main scientific topics studied by the employees of the NICM Department includes:

- Investigation of the structure and properties of novel functional materials;
- Investigation of the structure and properties of materials under extreme conditions;
- Investigation of fundamental regularities of real-time processes in condensed matter;
- Investigation of atomic dynamics of materials for nuclear power engineering;
- Computer simulation of physical and chemical properties of novel crystalline and nanostructured materials;
- Investigation of magnetic properties of layered nanostructures;
- Investigation of structural characteristics of carbon- and silicon-containing nanomaterials;
- Investigation of molecular dynamics of nanomaterials;
- Investigation of magnetic colloidal systems in bulk and at interfaces;
- Structural analysis of polymer nanodispersed materials;
- Investigation of supramolecular structure and functional characteristics of biological materials;
- Investigation of structure and properties of lipid membranes and lipid complexes;
- Investigation of texture and physical properties of Earth's rocks, minerals and engineering materials;
- Non-destructive control of internal stresses in industrial products and engineering materials;
- Introscopy of internal structure and processes in industrial products, rocks and natural heritage objects.

1. Scientific results

1.1. Structure investigations of novel oxide, intermetallic and nanostructured materials

The magnetic, structural, and vibrational properties of YMn_2O_5 multiferroic with a strong magnetoelectric coupling have been studied by means of neutron, x-ray diffraction, and Raman spectroscopy at pressures up to 30 GPa in a temperature range from 10 to 300 K [1] (**Fig. 1**). The application of high pressure (P > 1 GPa) resulted in a suppression of commensurate and incommensurate antiferromagnetic (AFM) phases with a propagation vector q = (~1/2, 0, ~1/4) and appearance of a new commensurate AFM phase with q_p = (1/2, 0, 1/2). This observation is in sharp contrast to a general trend towards the stabilization of the commensurate AFM phase with the propagation vector q = (1/2, 0, 1/4) found in other RMn_2O_5 compounds under pressure. At higher pressures P > 16 GPa a structural phase transition accompanied by anomalies in the pressure behavior of some unit cell parameters and vibrational modes was observed. The obtained data allowed us to analyze the role of competing magnetic interactions in the formation of the magnetic ground state of RMn_2O_5 multiferroics.

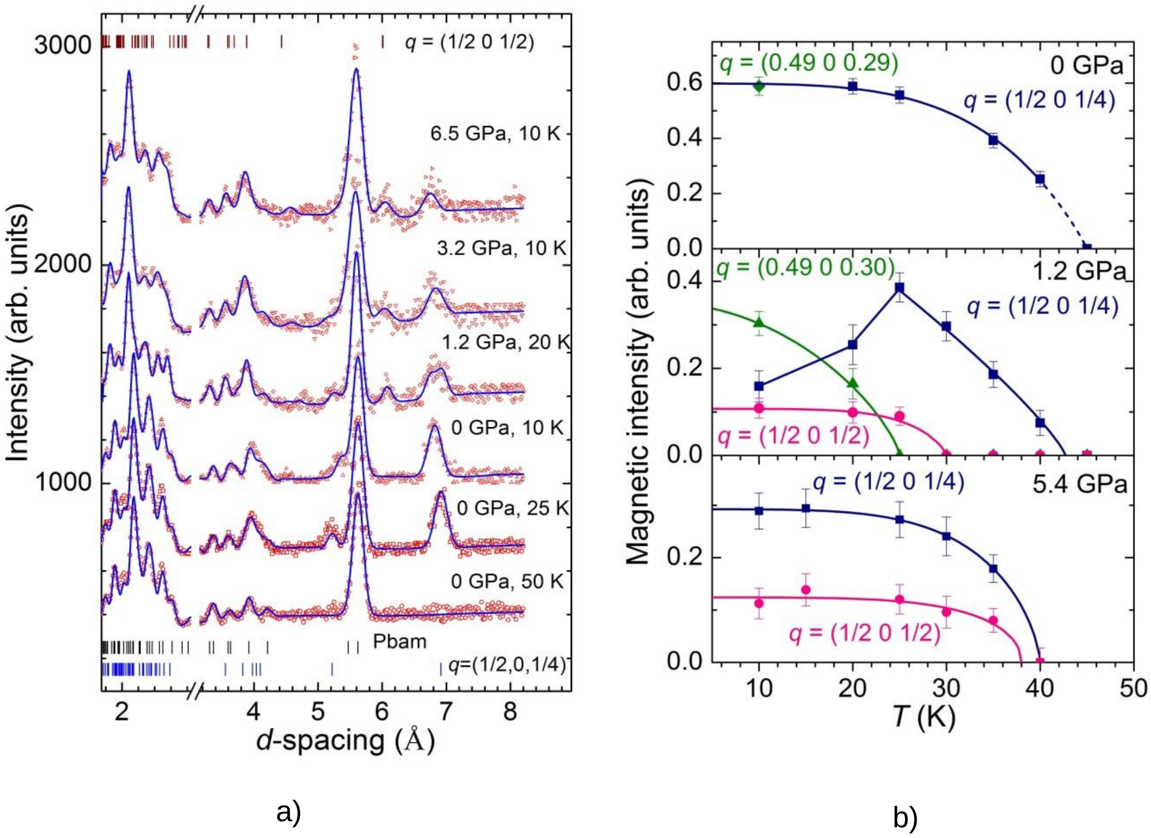

Fig. 1. Neutron diffraction spectra of YMn_2O_5 obtained at different pressures and temperatures with the DN-12 diffractometer and treated with the Rietveld method (a). Temperature dependences of integrated intensity of peaks $(1–q_x, –1, –q_z)/(1–q_x, 1, –q_z)/(\pm q_x, 1, \pm q_z)$ of commensurate and incommensurate AFM phases with a propagation vector q = (~1/2, 0, ~1/4) and a peak $(–q_x, 1, 1–q_z)$ of commensurate AFM phase with a propagation vector q_p = (1/2 0 1/2) under various pressures (b).

1. SCIENTIFIC RESEARCH

The structural characteristics of promising high-voltage cathode materials on the basis of $LiNi_{0.5}Mn_{1.5}O_4$ - $LiNi_{0.5-x}Mn_{1.5-y}M_{x+y}O_4$ (M=Co, Cr, Ti, Al, Mg; x+y=0.05) synthesized in the Institute of Solid State Chemistry and Mechanochemistry, SB RAS (Novosibirsk) have been studied in order to improve their electrochemical properties [2]. Unsubstituted $LiNi_{0.5}Mn_{1.5}O_4$ is characterized by a high potential (4.7 V) corresponding to a flat plateau in a charge-discharge characteristic at an average capacity of 120 mAh/g, which significantly increases the specific stored energy of the battery compared to other materials ($LiCoO_2$ ~3.8 V, $LiFePO_4$ ~3.2 V at the same capacity). Depending on the method of synthesis $LiNi_{0.5}Mn_{1.5}O_4$ may have either a primitive cubic $P4_332$ symmetry with an ordered arrangement of cations (in this case the synthesis temperature should not exceed 700°C) or a face-centered cubic Fd-3m symmetry and disordered arrangement of cations (formed at temperatures above 800°C). Due to the structural transformations during cycling the $LiNi_{0.5}Mn_{1.5}O_4$ compound with a $P4_332$ space group shows poorer electrochemical behavior than $LiNi_{0.5}Mn_{1.5}O_4$ with a Fd-3m structure. Samples for the study were synthesized at T < 800°C by means of a small substitution of other transition metals for Ni and Mn cations and mechanical activation of the reagent mixture in a planetary mill. As a result of the treatment of the neutron diffraction spectra using the Rietveld method it has been revealed that all the samples under study have a two-phase structure, with a phase having an Fd-3m space group being a dominant one and a secondary phase with a $P4_332$ space group ranging from 1 to 20% depending on the substitution metal and the synthesis temperature. It has been found that the dopants preferably substitute for Ni ions, which in turn results in the appearance of a NiO impurity phase in a small amount (1-2%). The average crystal size was 70-80 nm for the samples synthesized at 700°C, and 100-150 nm for the samples synthesized at 800°C. As expected, large microstrains were found to be more frequent in the samples with lower synthesis temperature.

A study of the evolution of the crystalline structure of the cathode material $LiNi_{0.8}Co_{0.1}Al_{0.1}O_2$ in the process of electrochemical cycling has been carried out using neutron diffraction (**Fig. 2**). The experiments were performed on the RTD (Real-Time-Diffractometer) diffractometer. Compositions of $LiNi_xCo_yAl_{1-x-y}O_2$ type are just starting to be introduced in mass production of lithium-ion batteries as a positive electrode (cathode), gradually replacing the widespread lithium cobaltate. Earlier such compounds were studied in real time during electrochemical cycling only in model cells by x-ray diffraction. Neutron diffraction makes it possible to study structural changes in the electrode materials both in specialized electrochemical cells and immediately in finished products. This study investigated a Li-Ion 18650 cylindrical rechargeable battery, where graphite is used as a negative electrode and $LiNi_xCo_yAl_{1-x-y}O_2$ with $x \approx 0.8$ and $y \approx 0.1$ (the values were specified during the treatment of the obtained diffraction data) as a positive electrode. The crystal structure of $LiNi_xCo_yAl_{1-x-y}O_2$ in a completely discharged battery corresponds to a space group R-3m with unit cell parameters a = 2.8453(1) and c = 14.1878(2) Å. On the basis of the analysis of experimental data obtained in the course of several charge-discharge cycles performed at different rates (C/3 and C/10, where C is the full capacity) it has been shown that the intercalation of lithium into graphite proceeds with the successive formation of several LiC_n phases. The formation of final LiC_6 phase during charging is easily detected by a step-like appearance of a diffraction peak at $d \approx 3.67$ Å. The phase separation in the cathode material $LiNi_{0.8}Co_{0.1}Al_{0.1}O_2$, which can be observed, for example, in $LiNi_{0.8}Co_{0.15}Al_{0.05}O_2$, has not been found. At the same time, the unit cell parameters of the two materials change during charging in a similar manner, and the expansion and subsequent contraction of the unit cell proceed anisotropically. When charging, at first the cell expands along the hexagonal c axis and slightly contracts in the basal plane (a and b axes). Towards the end of charging, there occur an abrupt contraction along the c axis and some expansion along the a and b axes.

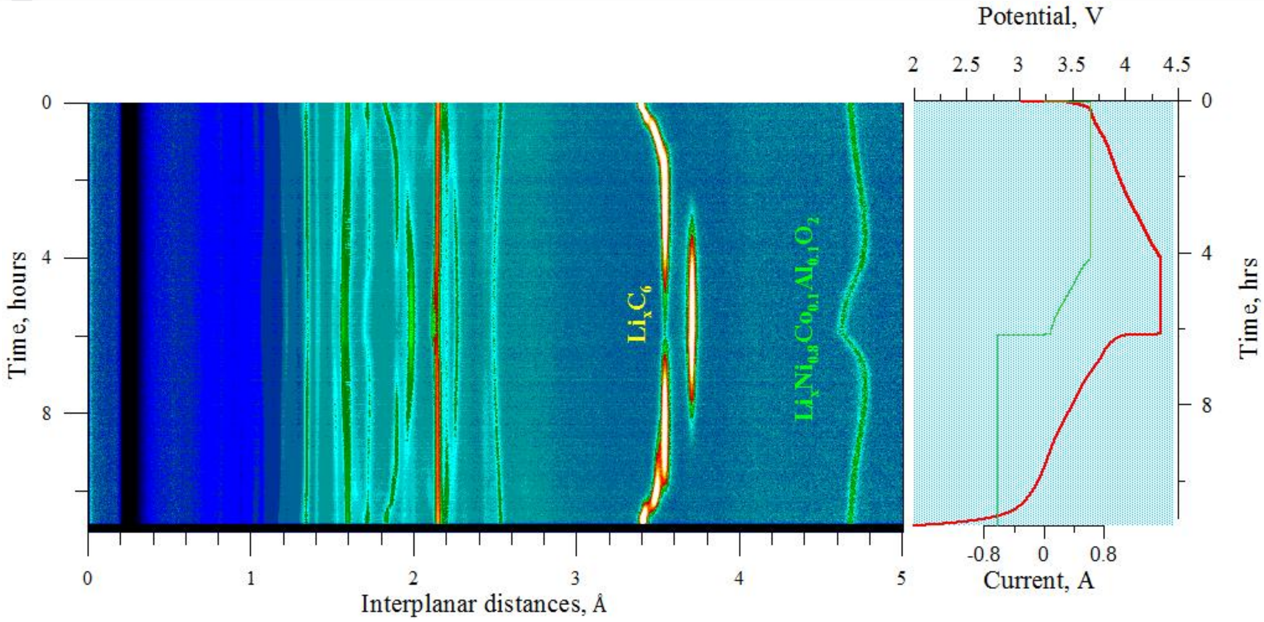

***Fig. 2**. The evolution of neutron diffraction spectra obtained in the real-time (operando) study of $LiNi_{0.8}Co_{0.1}Al_{0.1}O_2$ cathode material using high-intensity neutron diffraction. At the right: charge-discharge curve of the power source during the experiment.*

Methods for obtaining different compounds in the nanostructured state have been developing in recent years. The $VC_{0.875}$ compound was the first carbide in whose coarse-grained powder a nanostructure was created as a result of the disorder-order transformation ($VC_{0.875} \rightarrow V_8C_7$). The atomic-vacancy ordering makes it possible to create the nanostructure in the $VC_{0.875}$ bulk carbide. However, until recently it was unclear whether the superstructure V_8C_7 remains after milling the ordered vanadium carbide to a nanopowder with the average particle size of 400-500 Å and less.

The crystal structure and microstructure of coarse- and nanocrystalline disperse ordered carbide V_8C_7, which was prepared by milling the initial coarse-crystalline powder for 10 h in a planetary ball mill, were studied with the HRFD diffractometer [3,4]. According to the scanning electron microscopy data, the initial powder ~V_8C_7 consists of large particles with a size of 3–5 μm, the microstructure of which is a set of curved lobes with diameters from 400 to 600 nm and thicknesses of about 15–20 nm. The nanopowder V_8C_7 obtained by milling for 10 h consists of nanoparticles with sizes of 20–60 nm united in friable agglomerates with the size from ~400 nm to ~1 μm.

All obtained spectra of the coarse-grained powder ~V_8C_7 include weak superstructure reflections of the ordered phase V_8C_7. For the coarse-grained vanadium carbide ~$VC_{0.875}$ (V_8C_7), the dependence of the width of diffraction peaks on the interplanar distances, $\Delta d^2(d^2)$, is linear, indicating that there is no size effect. For the nanopowder the diffraction peaks are strongly broadened and the dependence $\Delta d^2(d^2)$ is parabolic, from which it follows that the average size of the nanopowder particles is about 190 Å. Also, the presence of the disordered phase $VC_{0.875}$ with the structure B1, the lattice period of which is $a_{B1} < a_{V_8C_7}/2$, was found in the samples under study. The analysis revealed that the disordered phase represents small-size inclusions (~500 Å) in the matrix of the ordered phase V_8C_7, and its content in the coarse-crystalline powder is (21 ± 3) wt %. The real structure of the ordered phase is characterized by a lowered content of carbon as compared to the ideal one, which corresponds to the chemical composition $V_8C_{7-\delta}$, where $\delta \cong 0.03$.

The vanadium carbide nanopowder also contains the ordered and disordered phases (**Fig. 3**), but as a result of milling, the amount of the latter is (45 ± 10) wt %. The periods of cubic unit cells of phases V_8C_7 and $VC_{0.875}$ in the nanopowder are slightly smaller than in the coarse-crystalline powder.

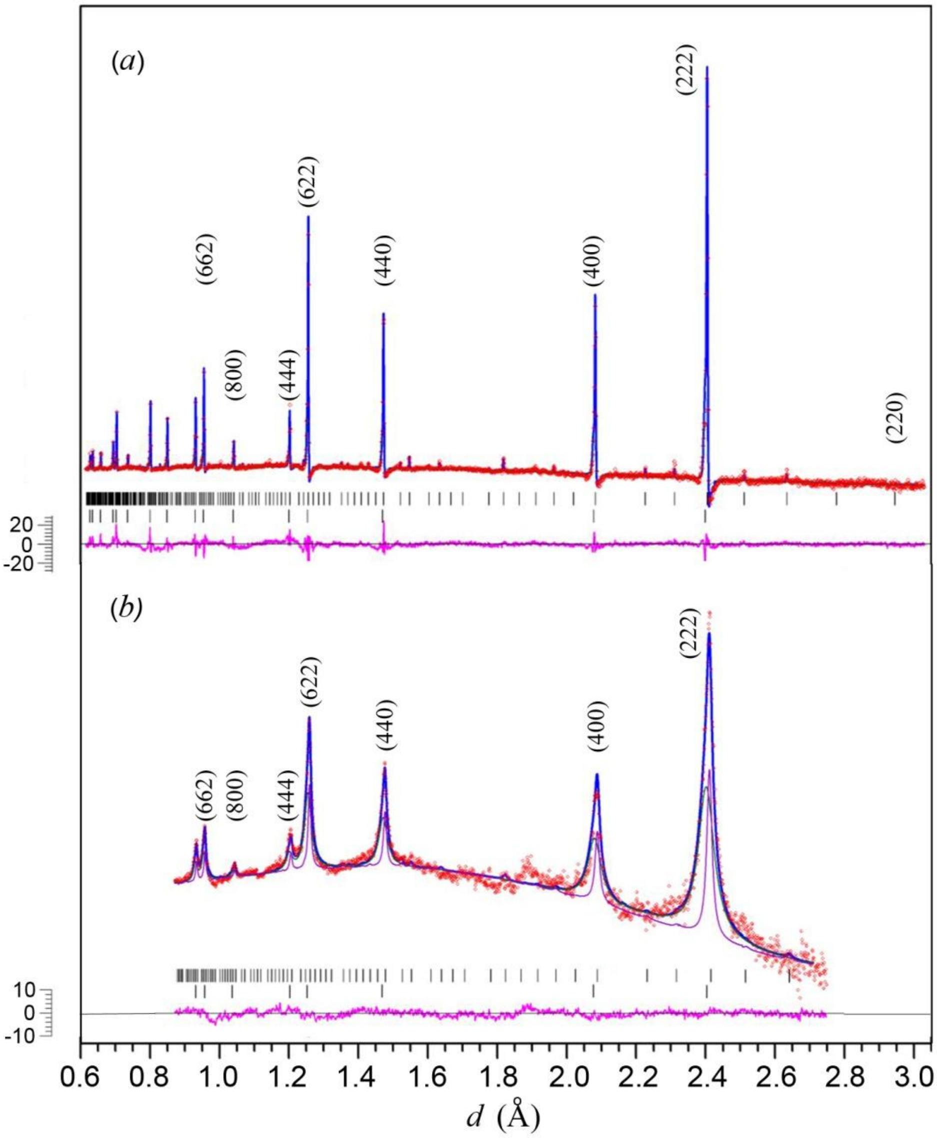

***Fig. 3**. Refinement of the neutron diffraction patterns of vanadium carbide powders (measurements in a high-resolution mode by detectors placed at the scattering angle $2\theta = 152°$): (a) initial coarse-grained powder and (b) nanopowder. The disordered phase is present in the samples along with the main ordered phase. Contributions of the ordered (narrow peaks) and disordered (wide peaks) are shown for the nanopowder. Vertical marks in the upper and lower rows indicate the positions of reflections of the ordered phase $V_8C_{7-\delta}$ ($\delta \cong 0.03$) and the disordered phase $VC_{0.875}$, respectively.*

Taking into account the limitations on the accuracy of determination of the filling of positions of C atoms it is believed that the nanocrystalline ordered phase has the same composition $V_8C_{7-\delta}$, $\delta \cong 0.0$ as that in the coarse-grained powder. The displacements of carbon atoms C3 and C4 in the lattice of the nanocrystalline ordered phase $V_8C_{7-\delta}$ are small. At the same time, the displacements of the same atoms are larger in the coarse-grained ordered phase. This is due to the noticeable deformation distortions of the lattice during milling of the powder.

The structural investigation of a solid solution of $BaFe_{12-x}Al_xO_{19}$ barium ferrites with a partial replacement of iron by diamagnetic aluminum ions (x = 0.1 - 1.2) has been performed using the neutron diffraction method [5]. In the entire investigated range of aluminum concentrations barium hexaferrite retains the structure of magnetoplumbite, and its magnetic structure can be described by the Gorter's model with the orientation of moments along the hexagonal axis. The total magnetic moment per formula unit decreases with the replacement of iron ions with diamagnetic aluminum ions. The increase in the unit cell volume with increasing *x* can be explained by the larger ionic radius of Al ions replacing Fe ions. At low temperatures (10 – 150 K) the Invar effect has been observed, i.e. the coefficient of thermal expansion is practically zero. With growing concentration of Al ions an increase of microstrains in crystallites has been found, which is connected with the different ionic radii of Fe and Al ions.

The crystal and magnetic structure of nanostructured manganites $La_{1-x}Sr_xMnO_3$ (x = 0.28, 0.37) has been studied in the pressure range of 0 - 4.5 GPa and temperature range of 5 - 300 K [6]. The physical properties of these compounds in the nanostructured state differ significantly from those in the bulk holding much promise for applications in biomedical technologies. In both compounds the ferromagnetic ordering is formed at temperatures close to room temperature, and at low temperatures (T < 270 K) the appearance of an additional A-type AFM phase is observed (**Fig. 4**). At higher pressures the volume fraction of AFM phase increases and that of FM phase decreases. The obtained results were interpreted in the framework of the "core-shell" model of the formation of nanoparticles in which the core is ferromagnetic and the shell is antiferromagnetic. The observed behavior of the volume of magnetic phases points to an increase in the thickness of the shell of nanoparticles under pressure.

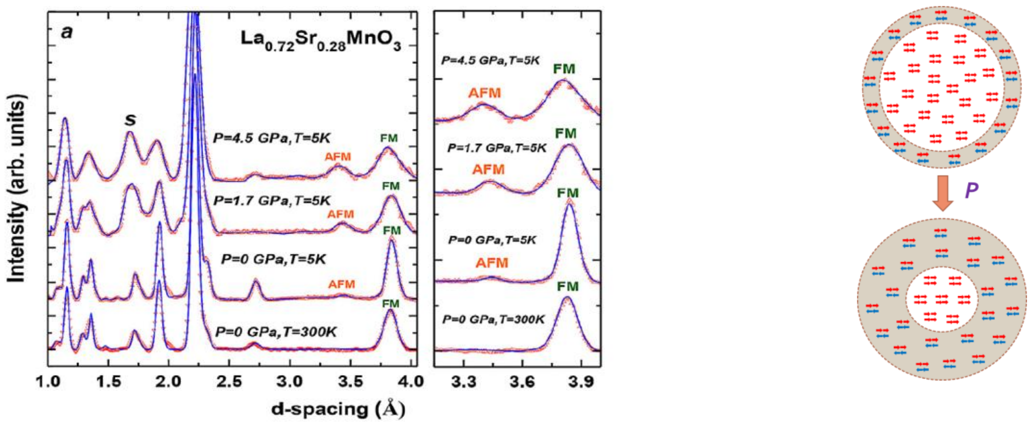

a) b)

Fig. 4. Neutron diffraction spectra of nanostructured manganite $La_{0.72}Sr_{0.28}MnO_3$ obtained at different pressures and temperatures with the DN-12 diffractometer and treated using the Rietveld method (a). "Core-shell" model of nanoparticles and their structural evolution under pressure (b).

1.2. Investigations of magnetic fluids and nanoparticles

In the framework of the study of the adsorption of magnetic nanoparticles on solid surfaces the experiments on neutron reflectometry with a horizontal sample plane were continued for the interface of magnetic fluids with crystalline silicon using different treatment of the surface of a solid support.

Thus, when contacting a solid hydrophilic surface, aqueous magnetic fluids characterized by the presence of a number of stable aggregates in solution form a single adsorption layer of non-aggregated nanoparticles at the interface [7]. Moreover, in the experiments with different configurations (‘crystal on top’ or ‘crystal at bottom’) a substantial difference in the critical angle of total reflection is observed pointing in the second case to an increase in the concentration of nanoparticles of the magnetic fluid at the interface due to the gravitational effect (**Fig. 5**). One can conclude that in contrast to magnetic fluids on weakly polar solvents, where the adsorption mechanism is mainly determined by gravitational sedimentation, in the aqueous magnetic fluids adsorption occurs mainly due to the electrostatic interaction between the nanoparticles with the substrate surface. The study has been carried out in collaboration with the Institute of Experimental Physics, Slovak Academy of Sciences (Kosice, Slovakia), Faculty of Physics of the Taras Shevchenko National University of Kiev (Kiev, Ukraine), research Institutes of the Romanian Academy of Sciences (Bucharest-Timisoara, Romania) and the Max Planck Institute for Solid State Physics (Stuttgart, Germany).

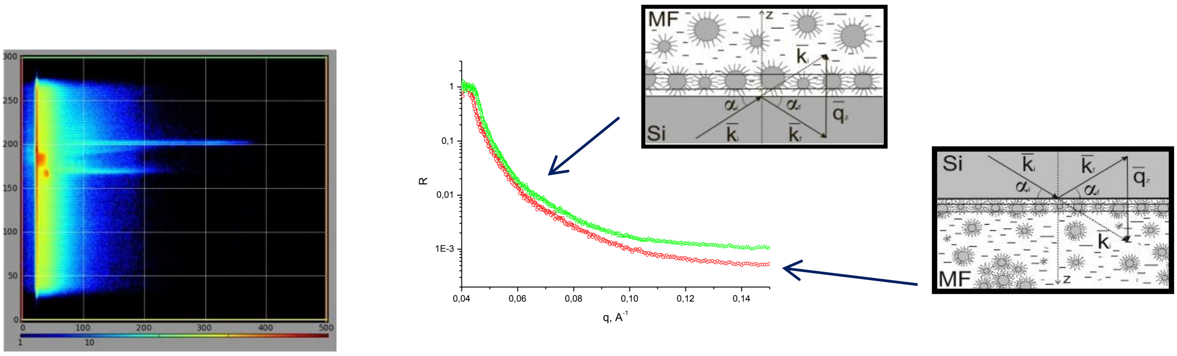

a) b)

***Fig. 5**. (a) 1D spectrum (GRAINS, IBR-2) of the reflected beam of unpolarized neutrons at the interface of the aqueous magnetic fluid (magnetite/sodium oleate/D_2O) with silicon in the coordinates “height of the detector Z - time of flight”; (b) Reflectivity as a function of the momentum transfer for the system magnetic fluid/silicon crystal measured in configurations ‘crystal on top’ and ‘crystal at bottom’ with corresponding representations of the structural organization of nanoparticles of the magnetic fluid at the interface with silicon.*

Using small-angle neutron scattering, changes in the structural organization of transformer-oil-based magnetic fluids have been observed under the action of an external DC and AC electric field (**Fig. 6**) [8]. The investigations have been carried out to clarify the effect of the voltage breakdown enhancement in liquid transformers when adding nanoparticles, specifically magnetite nanoparticles stabilized by oleic acid, to a liquid carrier. It has been shown that after the application of a DC electric field along with a macroscopic phase separation the aggregation at the size level of 100 nm takes place strongly dependening on the field strength. After the electric field is switched off, after a time (of the order of a few hours) the system returns to its original structural state. In the case of an AC electric field, the aggregates also appear at sufficiently low frequencies, and the process terminates when the frequency exceeds a certain critical value. Thus, in addition to the effects of aggregation in an external magnetic field, which is typical for magnetic fluids, a similar sensitivity to the electric field for magnetic fluids based on dielectric carriers has been detected, which opens up new potential possibilities for regulating the properties of these complex systems using external control parameters. The study has been carried out in collaboration with the Institute of Experimental Physics, Slovak Academy of Sciences (Kosice, Slovakia), Faculty of Physics of the Taras Shevchenko National

University of Kiev (Kiev, Ukraine), and the Research Centre of Jülich - Department of Neutron Research (Munich, Germany).

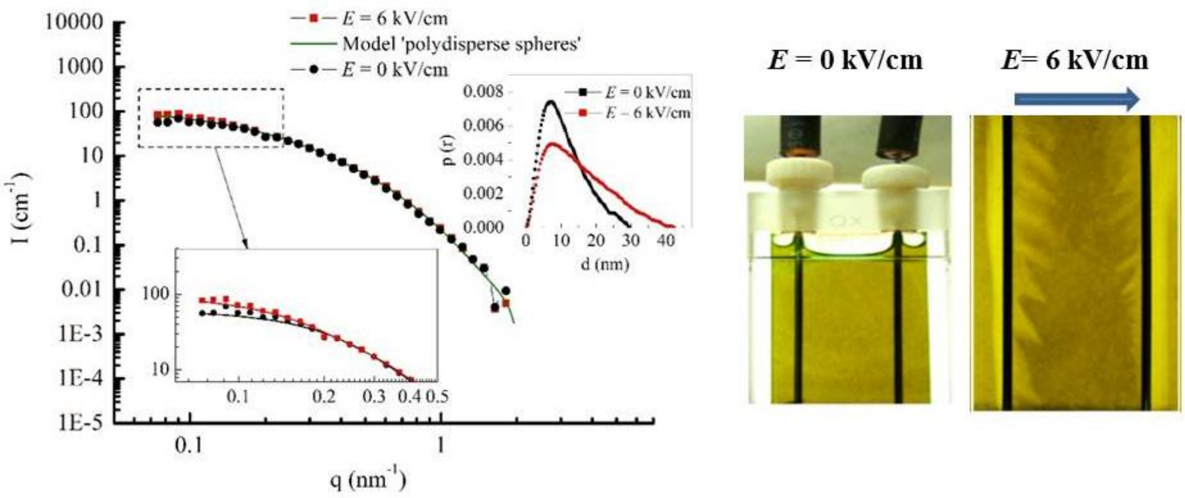

a) b)

***Fig. 6**. The effect of an external electric field on the structure of the magnetic fluid magnetite/oleic acid/transformer oil for (a) nanoscale: small-angle neutron scattering (YuMO, IBR-2), magnetite concentration of 1%, and (b) macrolevel: visual observation of phase separation in a quartz cell (1 mm thick), magnetite concentration of 0.05%. The inset in (a) shows the correlation functions reconstructed from the scattering curves (in the form of pair distance distribution functions) for a fluid in two states: “without a field" and "in a field", which point to an increase in the characteristic size as a result of aggregate formation under the applied field, as well as the presence of anisotropy in the aggregate shape.*

Molecular dynamic (MD) simulations of the low-polarity organic solutions of saturated mono-carboxylic acids with alkyl chain lengths C14 (myristic acid) and C18 (stearic acid) used in the stabilization of magnetic fluids have been applied for the interpretation of the experimental curves of small-angle neutron scattering (SANS) from these systems [9]. In particular, the comparison of the acid structural parameters obtained in the analysis of the SANS curves from the solutions in deuterated benzene and decaline has revealed that in the second solvent there is a significant (up to 15%) increase in the limiting partial volume of the acid molecules despite their close effective conformational lengths. Thus, it has been found that the considered C14 and C18 acids due to the rapid attenuation of the dispersive interaction with distance are characterized by a lower affinity (lyophilic properties) to decalin which exhibits a more complex structure as compared to benzene. Also, the formation of a liquid crystalline phase in concentrated solutions (concentration ranges of 7 – 25 vol.% for C14 and 3 - 10 vol.% for C18) based on deuterated solvents has been considered. The lower values observed in the experiments for the formation of the liquid crystal phase in the solutions based on decalin as compared to benzene can be explained by the structural features of the solvate shells around the acids obtained from the MD simulations. The study has been carried out in collaboration with the Wigner Research Centre for Physics of the Hungarian Academy of Sciences (Budapest, Hungary) and Faculty of Physics of the Taras Shevchenko National University of Kiev (Kiev, Ukraine).

1.3. Investigations of carbon nanomaterials

Small-angle neutron scattering has been applied to characterize the structure of commercial aqueous dispersions of detonation nanodiamonds (DND) [10]. It has been found (**Fig. 7**) that the fractal organization of clusters in the solutions repeats the results of the previous similar experiments on the DNA dispersions of different types, which is indicative of a unique mechanism of the cluster formation during the dispersion synthesis. To explain this mechanism, a modified model of diffusion-limited aggregation (DLA-model) extended for the first time to the case of clusters of polydisperse structural units (DNA particles) has been proposed. It has been shown that along with the polydispersity of DNA particles a sufficiently high polydispersity of the clusters is required to fit the scattering curves by this model. The "light" and "heavy" cluster fractions separated by centrifugation reveal the same kind of clusters at different size scales. The effect of the scattering structure-factor characterizing the cluster-cluster interaction in concentrated suspensions of "light" and "heavy" cluster fractions has been described. The study has been carried out in collaboration with the Department of Chemistry of the Moscow State University (Moscow, Russia) and the Faculty of Physics of the Taras Shevchenko National University of Kiev (Kiev, Ukraine).

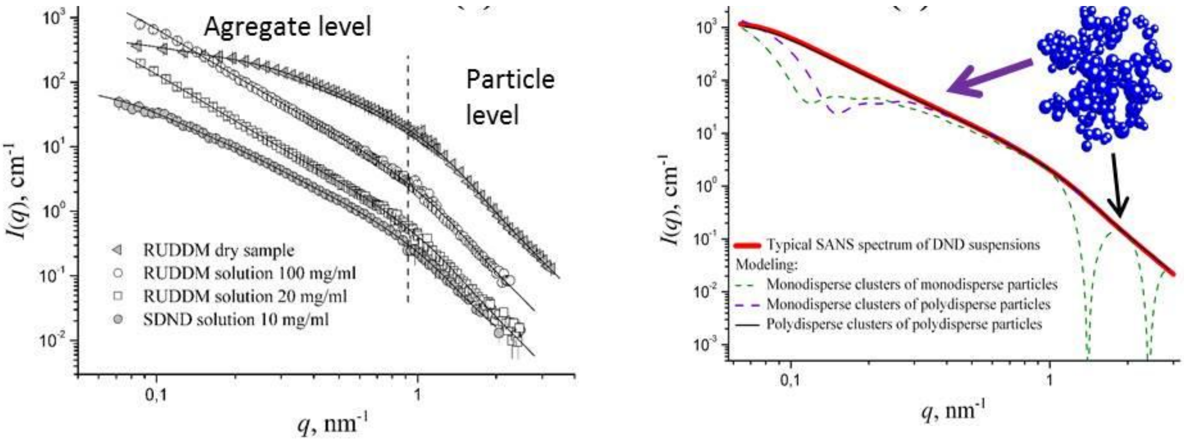

a) b)

***Fig. 7**. (a) Experimental curves of small-angle neutron scattering (YuMO, IBR-2) from commercial aqueous dispersions of detonation nanodiamonds, RUDDM (Real-Dzerzhinsk Ltd.) and SDND (PlasmaChem GmbH), are compared with the model curves (solid lines) calculated in the exponential/power-law approximation for the two structural levels (indicated in the graph). (b) Calculated curves of small-angle scattering for the model of diffusion-limited aggregation with monodisperse/polydisperse structural units and monodisperse/polydisperse clusters are compared with the curve calculated in the exponential/power-law approximation with the parameters obtained from the analysis of experimental data.*

Complex investigations (including UV-Vis spectrometry, atomic force microscopy, small-angle neutron and X-ray scattering, dynamic light scattering) of mixtures of aqueous solutions of fullerene C60 (obtained by the solvent substitution method) with antitumor antibiotics cisplatin [11] and doxorubicin [12] have been carried out. The formation of complexes of C60 with antibiotics has been revealed and confirmed by complementary quantum mechanical calculations. From the studies performed in collaboration with the Faculty of Biology of the Taras Shevchenko National University of Kiev (Kiev, Ukraine), it has been concluded that these complexes are responsible for the enhanced anticancer effect of fullerene-antibiotic mixtures as compared to pure antibiotics. It has been assumed that in this case the fullerene improves targeted delivery of antibiotics, promotes antibiotic accumulation in tumor tissues and increases the duration of drug exposure on tumors, thereby reducing toxic effects of anticancer drugs on vital organs.

In the framework of the research of cluster formation in fullerene solutions the kinetics of dissolution of C60 in a polar solvent, N-methyl-2-pyrrolidone (NMP), has been studied by varing temperature and speed of the component stirring during the preparation of the solution [13]. This system is characterized by a transition from a molecular solution to a colloidal solution, whose detailed description is of great interest from both fundamental and practical viewpoints. Based on the proposed model of the evolution of the C60/NMP solution, as a result of the competition between dissolution and complex formation, a diagram of the corresponding rates depending on the conditions of the solution preparation has been plotted (**Fig. 8**).

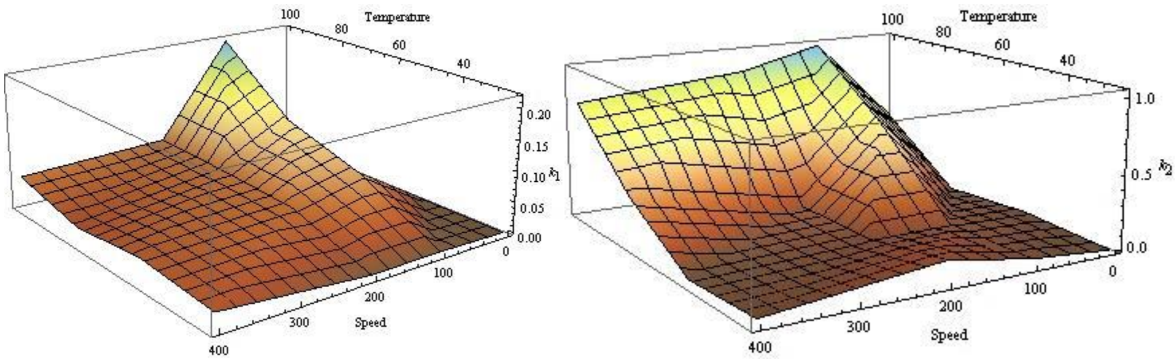

Fig. 8. *Diagram of the rates of dissolution (k1) and complex formation (k2) in C60/NMP solution (concentration 0.3 mg/ml) depending on the stirring speed and temperature. The speed values have been obtained from the analysis of the absorption peak intensity in UV-Vis spectra at a wavelength of 330 nm.*

1.4. Investigations of layered nanostructures

Neutron studies on the modification of the magnetic state in the ferromagnetic layered nanostructure Ta/V/$Fe_{0.7}V_{0.3}$/V/$Fe_{0.7}V_{0.3}$/Nb/Si under the influence of superconductivity were continued (**Fig. 9**).

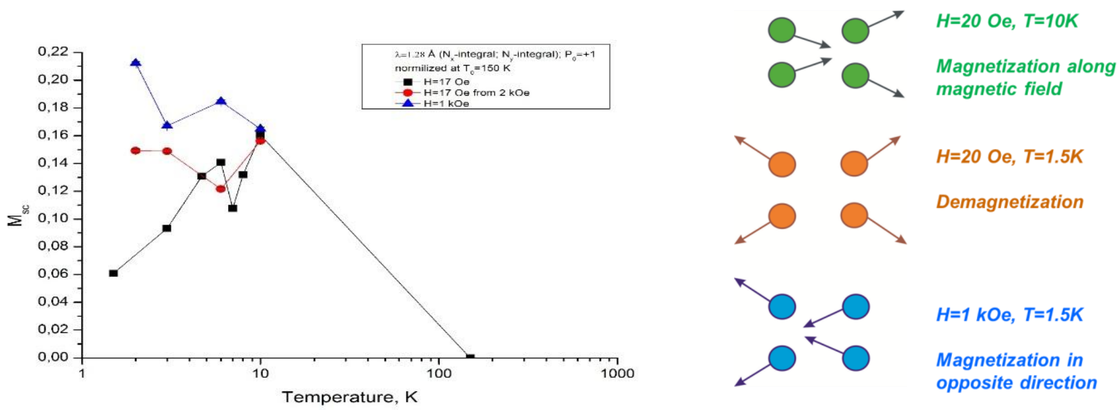

Fig. 9. *Temperature dependences of neutron scattering from magnetic clusters in ferromagnetic layered nanostructure Ta/V/$Fe_{0.7}V_{0.3}$/V/$Fe_{0.7}V_{0.3}$/Nb/Si in various magnetic fields (left) and a schematic representation inllustrating the behavior of the magnetic moments of the clusters (right).*

In the temperature range of 1.5-8 K where niobium and vanadium layers are superconducting, different temperature dependences of neutron scattering from the clusters in this magnetic nanostructure have been detected for the cases of (i) structure in a weak magnetic field of 20 Oe, (ii) structure with residual magnetization after magnetization in a field of 2 kOe, and (iii) structure in a constant magnetic field of 1 kOe. This indicates that the influence of superconductivity on the state of the magnetic clusters in the layered structure depends on the magnetic field strength. Using the real time reflectometry the temperature dependences of neutron scattering have been measured. They showed a characteristic relaxation time within several tens of minutes for the magnetic state of the layered structure Ta/V/$Fe_{0.7}V_{0.3}$/V/$Fe_{0.7}V_{0.3}$/Nb/Si. The dependences associated with the creep of the magnetic flux in the magnetic non-superconducting structure and oppositely directed creep in the superconducting structure have been observed.

1.5. Investigations of biological nanosystems, lipid membranes and complexes

An ability to separate cells from the environment is one of the most important functions of biological membranes. The violation of the membrane integrity causes the cell death. However, local and short-term changes in the membrane integrity leads to the creation of a new structure by cell fusion/fission. Fusion is the basis of the most important physiological processes such as exocytosis, secretion, formation of secondary lysosomes. In addition, *in vitro* targeting cell fusion by various fusion agents is widely used to solve a number of problems in biomedicine and biotechnology. Dimethyl sulfoxide (DMSO) is one of the fusion agents. In the presence of DMSO, pores in membranes appear, thereby increasing permeability and reducing stiffness of the membrane, which in turn initiates the fusion process. DMSO is toxic to living cells. Diethyl sulfoxide (DESO) is less toxic than, for example, DMSO and glycerol, to *E. coli*. Apparently, the mechanism of the interaction of DESO and DMSO with biological membranes is identical. The SANS analysis of the influence of the DMSO and DESO concentration on structural and phase transitions in phospholipid membranes has been carried out. It has been shown that fusion occurs at a lower molar concentration for DESO than for DMSO. DESO (like DMSO) increases the temperature of the main phase transition (T_f). However, in the presence of DMSO the phase transition occurs at a lower temperature (T_f = 35.2°C and 33.6°C) and in a narrower temperature range than in the presence of DESO at the same molar concentration of sulfoxides.

The process of the spontaneous formation of phospholipid vesicles in the presence of calcium ions has been studied by small-angle neutron scattering. For the first time, the behavior of the intermembrane distance in a transitional region for membranes in both liquid and gel phases has been investigated in detail. It has been shown that the transition of a system from the bound state to the unbound state in both phases is of continuous character. If for the liquid phase this result predicted in many theoretical works was expected, the data obtained for the gel phase contradict most of the previously published works. The theoretical investigations concerning the gel phase indicate that the addition of calcium ions to multilayered lipid membranes should cause for the membranes a sharp transition from the bound state to the unbound state, since there are no ondulations in the gel phase (membrane is "harder" than it is in the liquid phase). However, our studies have shown that the influence of the ondulation forces on the membrane interaction shoud be taken into account. Thus, our experimental results confirm the hypothesis of R. Lipowski (1986) about a possible continious character of the transition. The critical concentrations of calcium ions (0.3 mM for the gel phase and 0.4 mM for the liquid phase) when the analyzed transition takes place have been obtained. In addition, the binding constants for calcium ions with lipid membranes (22 M-1 in the gel phase and 24 M-1 in the liquid phase) have been determined.

The visual pigment rhodopsin is a typical representative of the vast family of receptors coupled to G-proteins (GPCR). GPCR in membranes function in dimeric or oligomeric states. However, for rhodopsin and for the whole A class of rhodopsin-like GPCR the functional role of the dimeric state has not yet been established. A supramolecular organization of rhodopsin in photoreceptor membranes is currently much debated. The structural organization of the photoreceptor membranes has been investigated by small-angle neutron scattering with the contrast variation (**Fig. 10**).

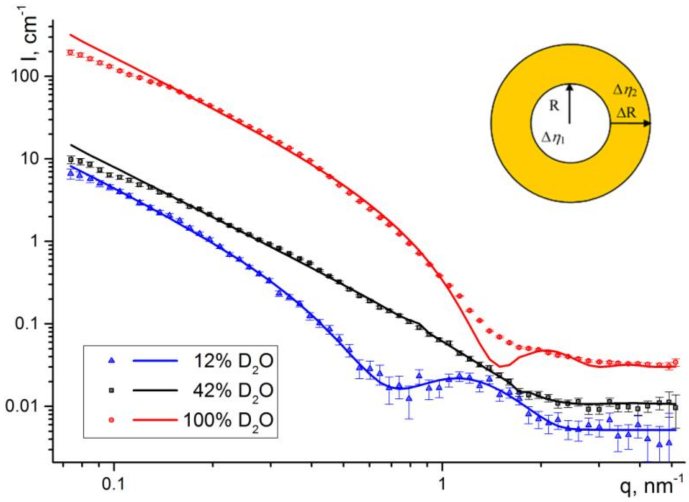

***Fig. 10**. Small-angle neutron scattering curves from a photoreceptor membrane measured with the contrast variation.*

It has been found that rhodopsin has an unusually high packing density in the photoreceptor membrane with the distance between protein molecules of about 56 Å [14]. With a high probability the data obtained assume a monomeric character of rhodopsin molecules in the photoreceptor membrane.

1.7. Atomic and molecular dynamics

In recent years, much interest has been shown in the study of hydrogen-bonded, donor-acceptor type supramolecular co-crystals for their potential use as functional materials with semiconducting and/or ferroelectric properties arising due to the electron- and proton-transfer phenomena. A comprehensive study of the crystal structure and molecular dynamics of co-crystals of bromanilic acid with 2,6-dimethylpyrazine (BrA: 2,6-DMP) 1:1 has been carried out using the methods of single-crystal X-ray diffraction, neutron spectroscopy (NERA spectrometer) and complementary spectroscopic methods, **Fig. 11**. [15]. To interpret the experimental results, theoretical calculations have been performed as well.

The structural analysis has revealed that the system under study crystallizes in the monoclinic P21/c space group, with four molecular units per unit cell. The crystal structure can be described as an infinite net of antiparallelly oriented hydrogen bonded molecular chains (**Fig. 11**). The intermolecular analysis has revealed the nonequivalency of the moderate strength hydrogen-bonding interactions and the presence of multiple specific intermolecular forces. The theoretical calculations using Hirschfeld surface approximation and reduced density gradient approaches have exposed the role of stacking interactions and weak van der Waals forces in the stabilization of the crystal structure.

The analysis of vibrational properties was performed using the methods of neutron and optical spectroscopy (mid-, far- and terahertz ranges).

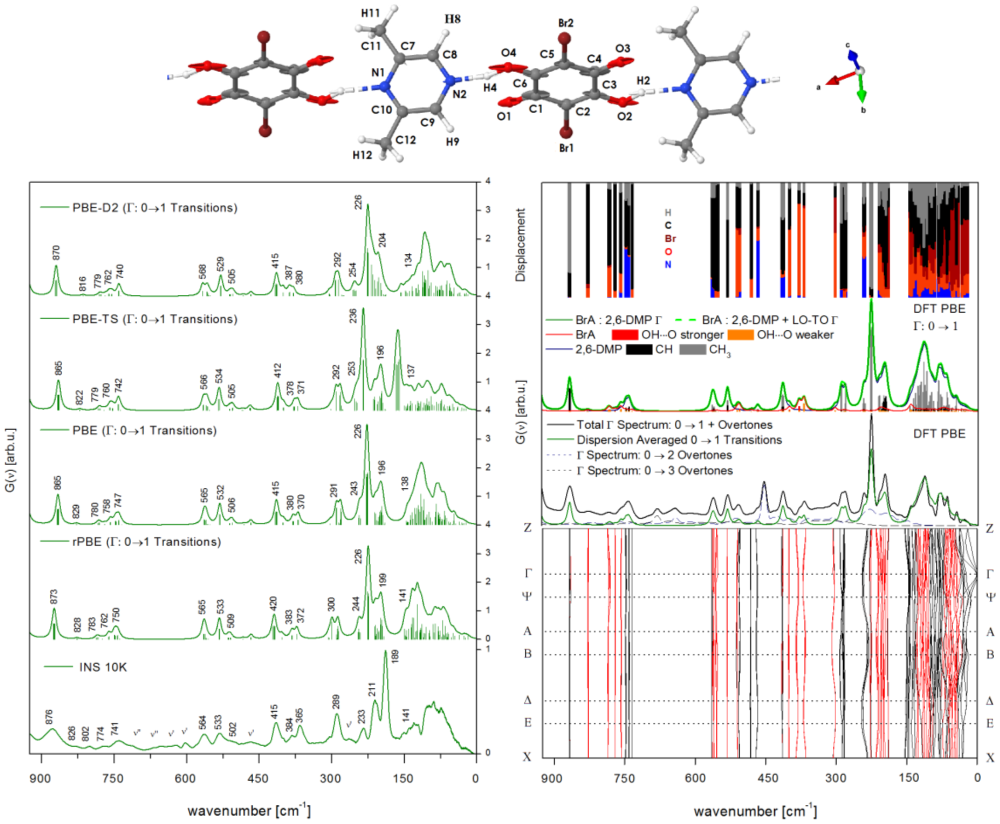

Fig. 11. *Molecular structure, inelastic neutron scattering spectra (NERA 10K) and theoretical calculated vibrational spectra (for 0 → 1 transitions) of BrA:2,6-DMP (1:1) in the frequency range below 925 cm^{-1}. The theoretical spectra are given for both constrained (rPBE; PBE) and fully (PBE-TS; PBE-D) optimized crystal structures. Also, calculated phonon dispersion curves along with the vibrational density of states decomposed into partial density contributions of each molecular fragment are selectively presented. In addition, the dispersion averaged spectrum is given along with the total Γ-point spectrum including the overtone contributions.*

The theoretical analysis of the vibrational spectra was made in the framework of DFT in the semilocal approximation taking into account semiempirical van der Waals corrections. Despite the quasiharmonic approximation, good agreement between the theoretical and experimental spectra was achieved. In particluar, the significant influence of the long-range dipole coupling on the IR spectrum and the effect of the structure on the vibrations with small wave numbers have been revealed.

1.8. Applied research

Among traditional applied investigations in the NICM Department are the experimental studies of internal stresses and texture of rocks and minerals, determination of internal stresses in bulk materials and products, including engineering materials and components of machines and devices. For the most part, these investigations are carried out using neutron diffraction.

On the FSD diffractometer the experiments have been continued on the investigations of distributions of residual stresses in welds that are induced by various beam welding methods (**Fig. 12**). The investigations have been carried out in cooperation with the Institute of Electronics, BAS (Sofia, Bulgaria). Residual stresses in a toothed gear of a sports car transmission gearbox after electron beam welding have been studied. It has been found that in the weld region and adjacent heat-affected zone (HAZ) the residual stresses and microstrains have minimum values. In the region remote from the weld the residual stresses are rather large, and their maximum levels reach values of about 500 MPa, which may point to non-optimal parameters of the beam welding.

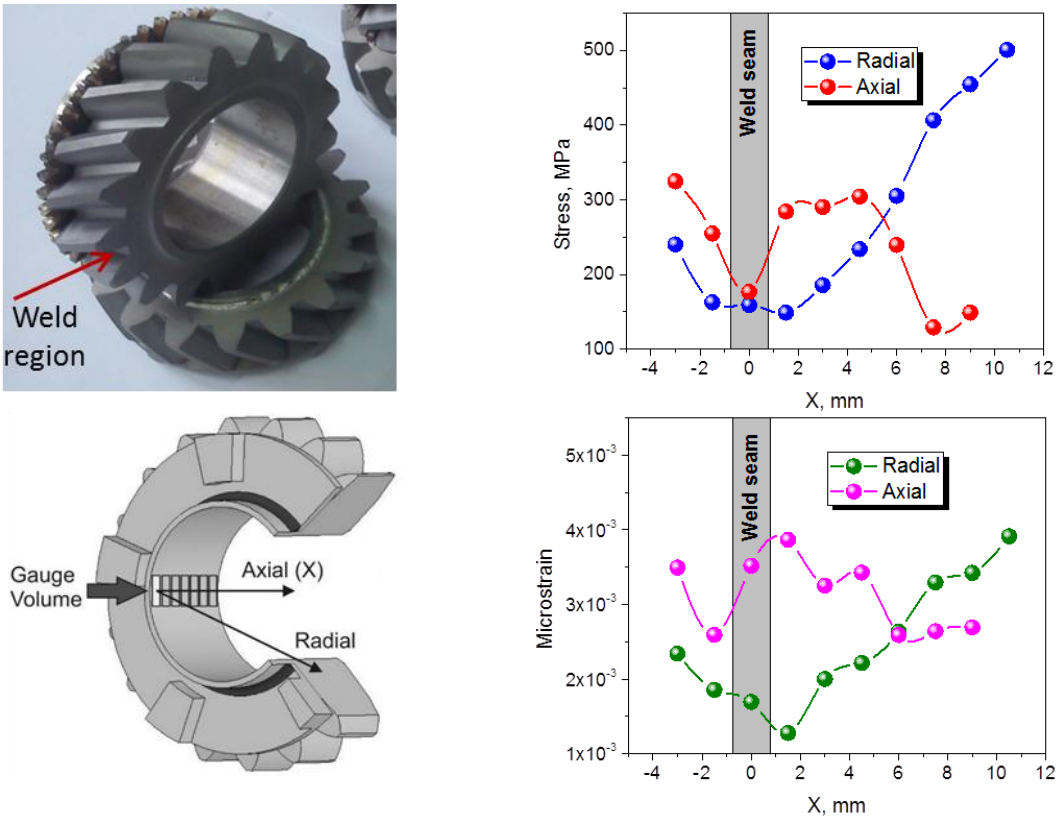

a) b)

***Fig. 12**. a) Photo of toothed gears welded by electron beam welding and scheme of the measurement of residual stresses in the toothed gear. b) Distribution of residual stresses (top) and microstrains (bottom) in the toothed gear welded by electron beam welding.*

A detailed study of residual stresses has been performed for a plate of size 100x100x10 mm of structural steel S355J2+N welded by laser beam welding (**Fig. 13**). The distribution of residual stresses along the scan coordinate X is of an alternating character, and the maximum-largest is the component of the stress tensor σ_x (~ 400-460 MPa) directed along the weld line and having mainly stretching character in the heat-affected zone. The analysis of the behavior of the peak widths near the weld has shown that the peak broadening depends on the direction [hkl] in the crystal, which is a typical manifestation of the orientation factor of dislocations in respect to the scattering vector. In the given sample the maximum level of microstrains in the material reaches $4.8 \cdot 10^{-3}$, and the position of the maximum in the microstrain distribution coincides with the location of the weld center. Using the obtained data on microstrains the dislocation densities in the material have been calculated.

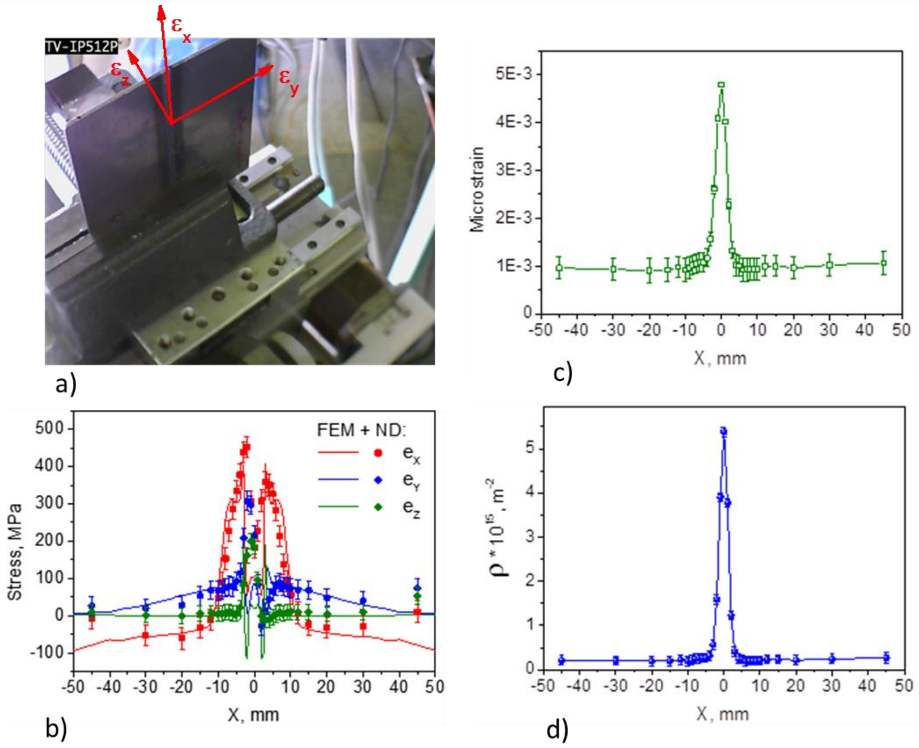

Fig. 13. The sample under study (plate welded by LBW) during the experiment at FSD (a). The arrows indicate the strain tensor components. Experimentally measured distribution of residual stress tensor components in the plate (symbols) welded by LBW (b). For comparison, the results of numerical simulation using the finite element method FEM (solid lines) are presented. Distribution of microstrains in the crystal lattice (c) and dislocation densities (d) obtained from the diffraction data in the plate welded by LBW.

In addition to the neutron diffraction experiments and in the framework of the existing cooperation numerical calculations have been performed by the finite element method - FEM (group of Prof. V.Mikhailov, Brandenburg University of Technology, Germany). The comparison of the neutron data and calculations using FEM shows a good agreement, which supports the validity of the developed theoretical model of the laser welding process. This information can serve as a basis for developing specific technical recommendations to achieve the desired level and profile of residual stresses.

On the SKAT/EPSILON diffractometer *in situ* deformation experiments have been conducted with a granite sample from the Forsmark region (Sweden) containing quartz, plagioclase and biotite. A cylindrical sample (d = 30 mm, l = 60 m) was subjected to cyclic uniaxial loading in the range from 20 to 140 MPa. The measurements were conducted at 7 load levels, for each level the sample was reloaded. Applied and internal stresses were determined from the shift of the diffraction lines in the range of up to d = 5.1 Å. In addition, the acoustic emission measurements have been carried out, the combination of which with neutron experiments is needed for better understanding of reasons for the Kaiser effect. The quartz texture in the granite sample is well developed and characterized by one maximum in the pole figure [0001] near the z-axis and 120° pole density distribution of other lattice directions around the [0001] cluster (**Fig. 14**). This gives grounds to suggest post-kinematic crystallization. In contrast, the texture of other phases is very weak (**Fig. 14**).

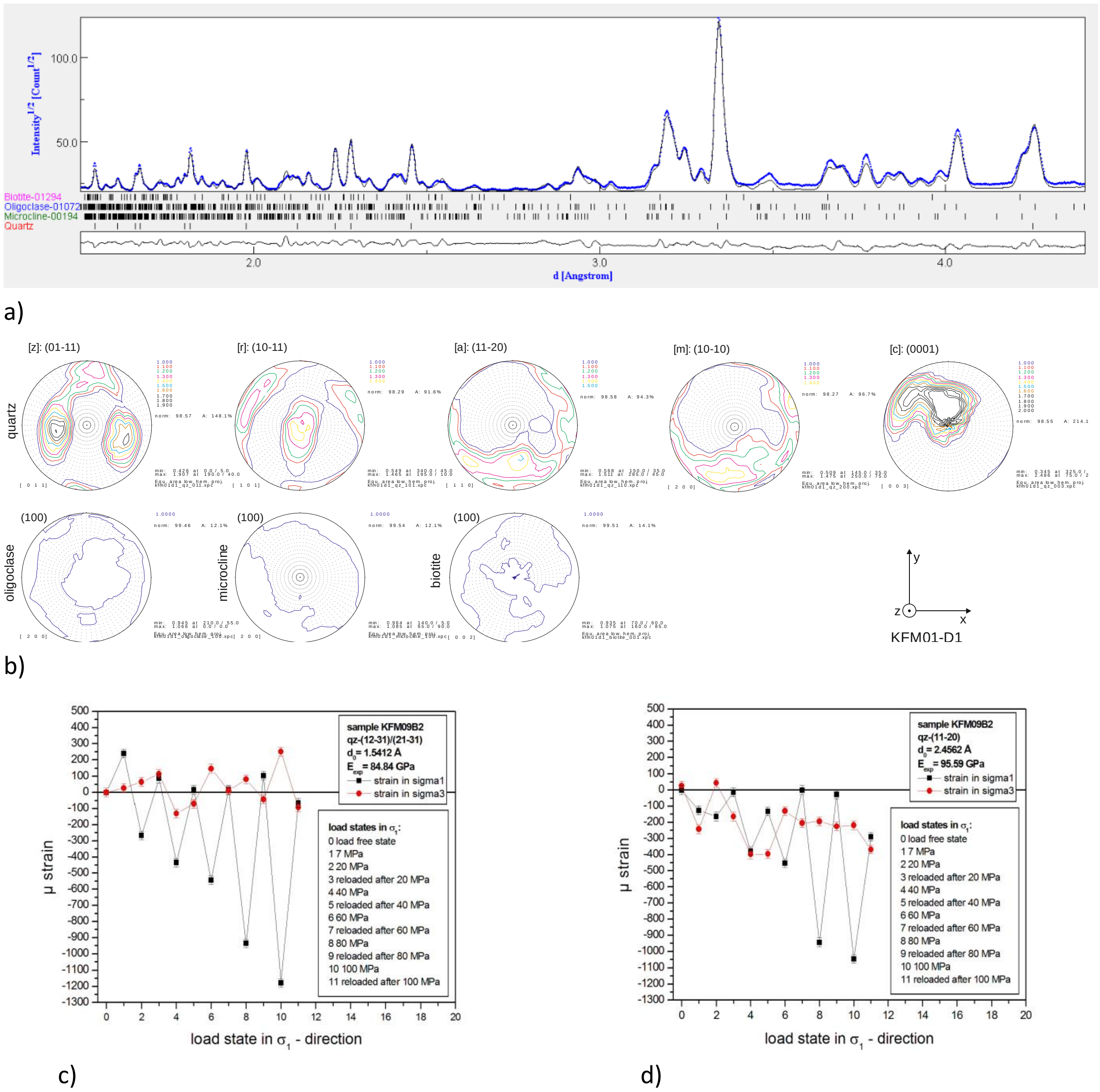

***Fig. 14**. Normalized TOF neutron diffraction spectra of granite sample obtained with the SKAT diffractometer. The Figure shows the experimental points (blue) and calculated profiles (black) as well as the positions of the diffraction peaks calculated by the MAUD program (a). Textures of quartz (top), oligoclase, microlin and biotite (bottom) (b). Applied and internal stresses of quartz (12-31) and (11-20) (c, d).*

The measured internal stresses were compared for the milled (< 62 μm) and annealed powder of the sample without stresses. During the internal stress measurements the cylindrical sample under study was rotated around the *z* axis with a step of 15° in the *xy* plane. The measured residual stresses were in the range from -1×10^{-3} to 1.2×10^{-3}.

On the EPSILON diffractometer the experiments have been conducted to determine the magnitude and distribution of internal stresses caused by tensile embrittling destruction in the course of phased "Brazilian" creep tests for a pure marble sample (>95% $CaCO_3$). A comparison of internal stresses measured before and during phases of mechanical loading has been made. The obtained data are important for studying the mechanisms of rock destruction.

The internal stresses occurring as a result of elasto-plastic deformation and residual stresses after removing the mechanical load in metal-matrix composite alloys Al/SiC$_p$ have been studied by neutron diffraction (EPSILON diffractometer) and synchrotron radiation techniques. The experimental results were compared with the elasto-plastic deformation model to determine the parameters responsible for the deformation of the Al matrix — critical allowable shear stress and hardening parameter. The analysis of data has shown that during the tensile test the Al matrix undergoes plastic deformation, and the SiC phase remains elastic. A self-consistent model allows one to correctly predict stresses in the SiC phase, but it overestimates the calculated values of the lattice strains in the Al matrix, which can be connected with the initial thermal stresses.

On the SKAT diffractometer the texture in a number of samples of high-strength vessel steels has been studied by thermal neutron diffraction (**Fig. 15**).

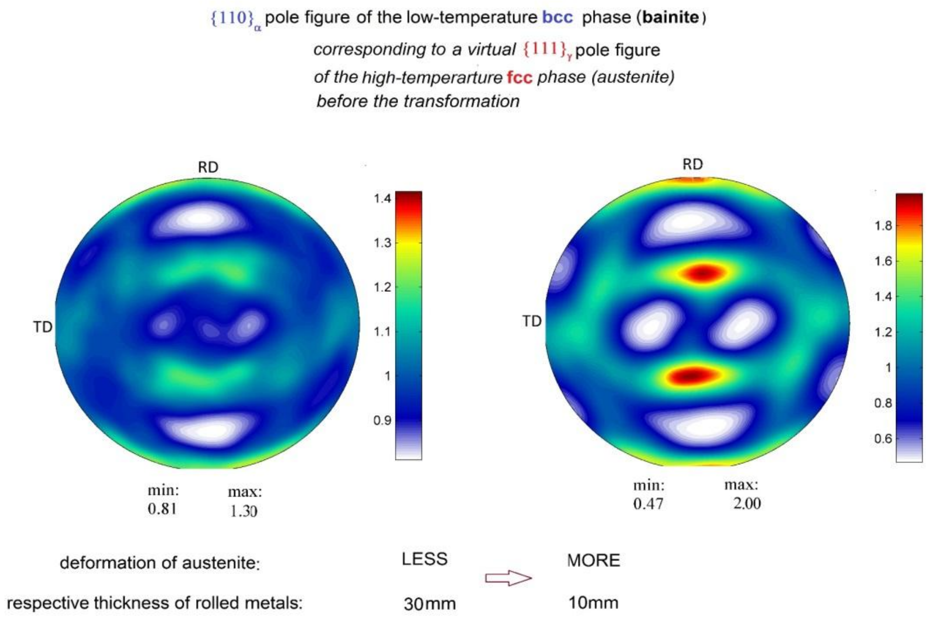

***Fig. 15**. Pole figures of low-temperature bainite phase with a bcc structure.*

The inhomogeneity of the texture across the thickness of a steel slab was investigated. Due to a large thickness (300 mm) of the slab the crystallization proceeds under various temperature conditions, therefore a strong morphological inhomogeneity can be observed across the thickness of the material. A set of 1368 (19×72) diffraction spectra was obtained from which complete direct pole figures (PF) with a grid size of 5˚×5˚ were derived. For each sample three pole figures (200) (110) (211) for α-Fe were obtained. It was revealed that the crystallographic structure changes only slightly across the thickness of the slab. From this it follows that the change in the morphological structure across the thickness of the high-strength steel slab is not related to a change in the crystallographic texture. In addition, the texture of rolled samples with different degrees of deformation has been studied as well. It has been found that the intensity of texture increases with the degree of rolling. Pole figures have been obtained for a low-temperature bainite phase with a bcc crystal lattice. The pole figure (110) for this phase corresponds to the pole figure (111) for the virtual high-temperature austenitic phase with an fcc lattice (typical texture of rolled copper). The high-temperature phase (austenite) is destroyed during quenching as a result of the phase transition. However, the revealed relationships between the pole figures of low-temperature (bainite) and high-temperature (austenite) phases provide an insight into the texture of the austenite destroyed during the phase transition.

II. Instrument development

Work to develop the final configuration of the new DN-6 diffractometer was continued. In cooperation with the SC Department a second ring detector consisting of 96 independent helium counters has been manufactured. The first successful methodological and scientific experiments with a new two-detector system have been carried out (**Fig. 16**).

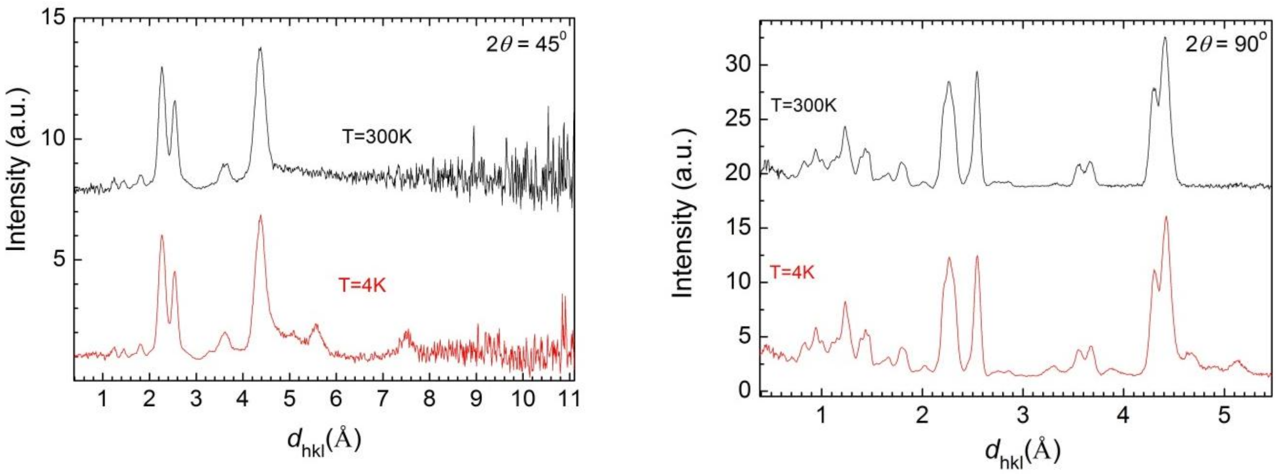

***Fig. 16**. Neutron diffraction spectra of $LiMn_2TeO_6$ obtained at scattering angles $2\theta = 45°$ (left) and $90°$ (right).*

In 2015, the user program has started to be implemented on the GRAINS reflectometer. In accordance with the list of submitted proposals for the second half of 2015, more than ten experiments on electrochemical interfaces, magnetic colloidal systems, polymer solutions and melts, lipid solutions and others have been carried out at GRAINS. Among the interested organizations are the research centers of Russia (MSU, PNPI, NRC KI), Slovakia (IEP SAS), Ukraine (KNU), Hungary (WRCP HAS), Tajikistan (IC ASRT). In particular, the possibilities of neutron reflectometry experiments for electrochemical interfaces under potential have been considered in the framework of comprehensive studies combining various complementary methods of synchrotron radiation and thermal neutrons [16]. The main emphasis was placed on the optimization of experimental conditions (substrate, electrode, solvent) to detect the formation of a transitional layer (so-called solid electrolyte interphase, SEI) on the model electrode and to obtain its characteristics (thickness and density) depending on the applied potential. To eliminate the influence of uncontrolled oxidation of metal electrodes on the results of experiments, the regulated oxidation of titanium and nickel films deposited on a glass substrate has been investidated (**Fig. 17**). The study has been carried out in collaboration with the Department of Chemistry of Moscow State University (Moscow, Russia), Petersburg Nuclear Physics Institute, NRC "Kurchatov Institute" (Gatchina, Russia) and the Faculty of Physics of the Taras Shevchenko National University of Kiev (Kiev, Ukraine).

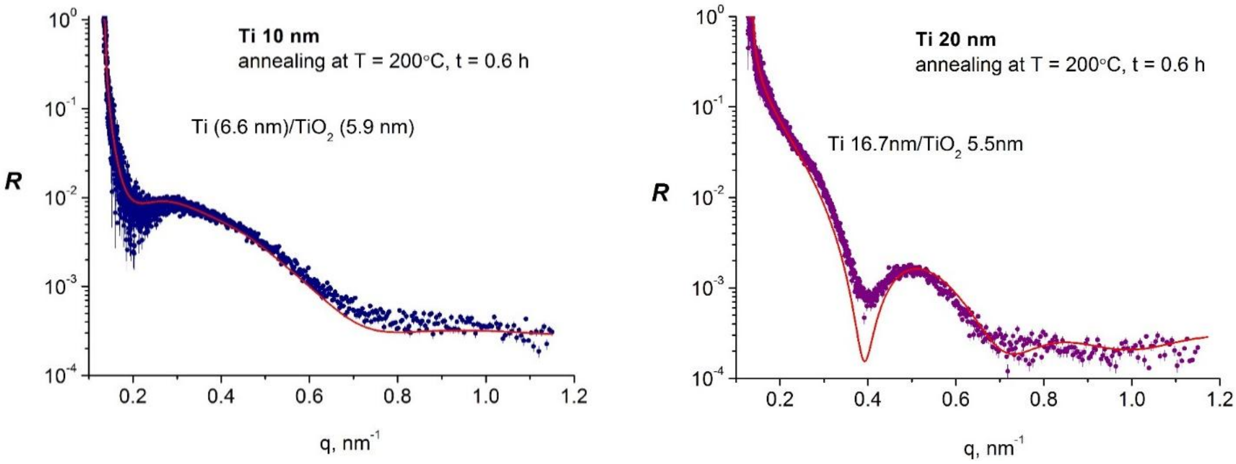

Fig. 17. *Experimental reflectivity curves (GRAINS, IBR-2) for model metal (Ti) films of different thicknesses on a glass substrate oxidized using a special procedure (PNPI, NRC KI). The solid lines show the simulation results with the indication of the obtained thicknesses for the film and the oxide layer.*

The realization of the project aimed at creating a basic configuration of the diffractometer on beamline 6a for neutron diffraction studies of transition processes in real time (RTD diffractometer - Real Time Diffractometer) has been completed. The diffractometer (**Fig. 18**) is designed to study irreversible transition processes with characteristic times ranging from fractions of a second to tens of minutes.

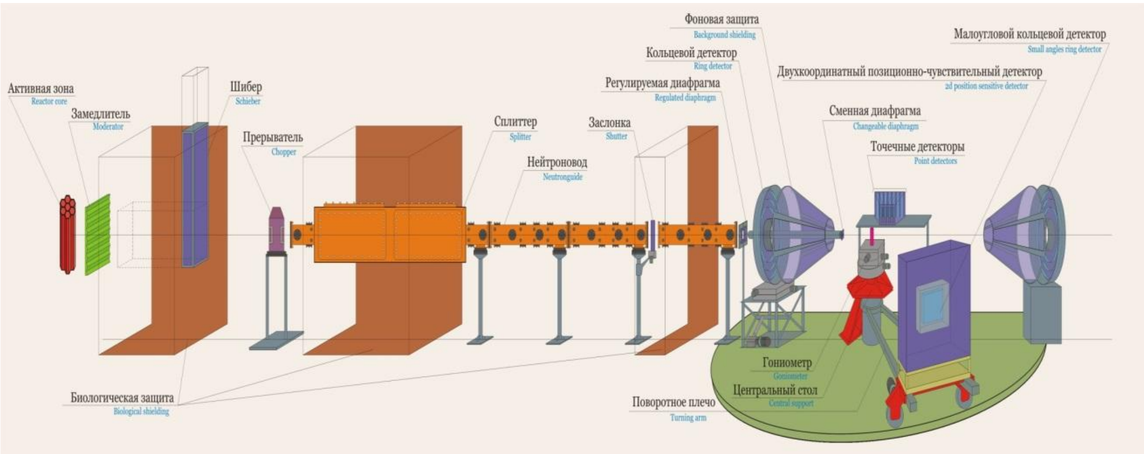

Fig. 18. *Basic components of the RTD refractometer at the IBR-2 reactor. Shown from left to right are: reactor core and moderator, biological shielding, chopper to reduce the background between the reactor pulses, splitter" to split the neutron beam into two beams, mirror neutron guide with a shutter to shut the beam, adjustable diaphragm at the exit of the neutron guide, central platform with a sample position and detectors. Four detector units are used: 2D PSD on a rotating platform, two ring detectors at small and large scattering angles and a battery of ^{3}He-counters near 2θ = 90°.*

In favorable cases, the time resolution of RTD will be fractions of a millisecond. The developed detector system (small-angle detector, detectors at medium scattering angles of 30° - 90° and a detector at large scattering angles in combination with the available wavelength range of 0.5-20 Å) makes it possible to obtain diffraction spectra over a wide range of interplanar spacings (d_{min}, d_{max}) = (0.5 - 300) Å. A triaxial goniometer and two-coordinate PSD with an active area of 225x225 mm and spatial resolution of 2x2 mm are used for investigations with single crystals and multilayer structures.

On the HRFD diffractometer the available model cell and its assembling/filling procedure have been improved. The work on the development of the cell (**Fig. 19**) based on silicon screens and multi-layer pouch-cell-type arrangement of electrode materials has been completed and first successful experiments have been conducted. The main components are: PTFE frame (white), material under study, silicon plate for incoming and scattered neutron beams, boron nitride to reduce the scattering from the cell components. The cell design allows easy assembling in an argon box, ensures good sealing and low incoherent neutron scattering from the cell screens.

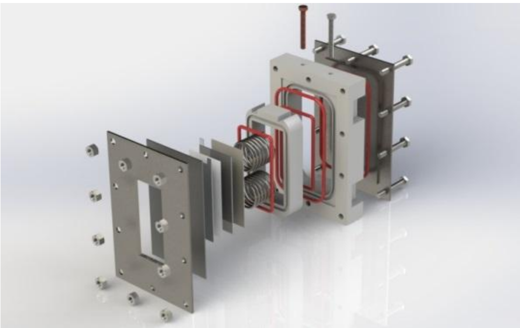

Fig. 19*. Schematic diagram of a new electrochemical cell.*

Also, on HRFD the operation of a specialized high-temperature furnace (ILL standard) designed to heat samples up to 1100°C and for a short time up to 1300°C has started. The furnace has vanadium heaters, vanadium and aluminum screens, water cooling, two K-type thermocouples, various protection mechanisms for emergency cases. An example of diffraction spectra obtained using the new furnace for Fe-27Ga alloys is shown in **Fig. 20**.

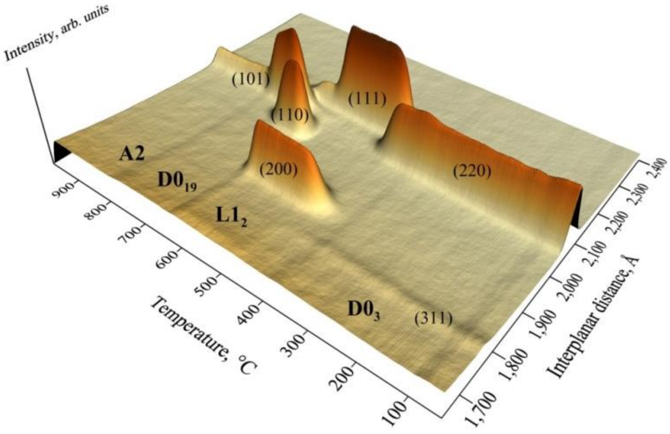

Fig. 20*. Evolution of diffraction spectra obtained during heating of Fe-27Ga alloy from room temperature to 980°C at a rate of 2.25°C/min. There can be observed a sequence of structural phase transitions: D03 → L12 → D019 → A2 (standard designations of main structural types). Shown are the Miller indices of the observed diffraction peaks.*

At FSD a uniaxial mechanical testing machine LM-20 has been installed, which significantly expands the range of possible experiments with the diffractometer. This device is intended to study samples at an external uniaxial load directly in the neutron beam. In 2015, several test neutron diffraction experiments with the application of tensile and compressive loads on austenitic and ferritic steel samples were successfully performed at FSD (**Fig. 21**). In the autumn of 2015 first experiments with a testing machine LM-20 began to be performed on the request of external users. In future, this device is planned to be used at FSD on a regular basis.

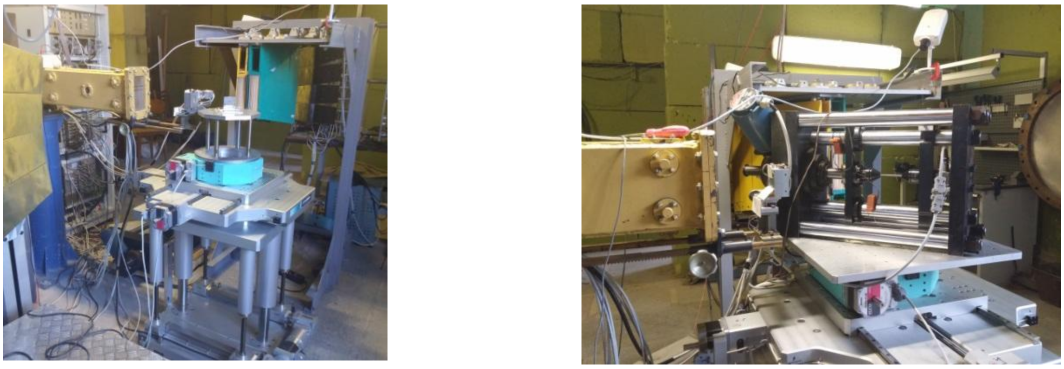

a) b)

Fig. 21. *FSD Fourier diffractometer on IBR-2 beamline 11: a) sample position on the HUBER goniometer; b) testing machine LM-20 with a steel sample.*

On IBR-2 beamline 13 the work on the development of a Fourier diffractometer FSS is in progress in cooperation with the SC Department (**Fig. 22**).

Fig. 22. *Fourier-diffractometer FSS on IBR-2 beamline 13 (from top to bottom and from left to right): operational control boxes of a shutter and beam stopper; entrance door to the bunker (beam exit location); glass mirror neutron guide sections before installation in a housing; neutron guide installed in a steel housing and control electronics of the Fourier chopper; experimenter’s control cabin mounted on the biological shielding of beamlines № 13-14.*

In 2015, operational control boxes of a shutter and beam stopper, light alarm system, power supply and control system of the Fourier chopper were installed, an experimenter's control cabin was mounted, and a mirror neutron guide in the steel casing was assembled with the participation of specialists from PNPI. In November 2015, at FSS the first trial opening of the beam was held, during which radiation conditions on the beamline were evaluated, neutron beam profiles were obtained and first diffraction spectra were collected.

A spin neutron interferometer of a new type based on the splitting of neutron waves reflected from a magnetic mirror has been studied. In the setup an initially unpolarized neutron beam passes through a system of two mirrors placed in a perpendicular magnetic field. A precession of the neutron magnetic moment as a periodic wavelength dependence for the intensity of neutrons passing through the system of two magnetic mirrors has been observed (**Fig. 23**). With increasing magnetic field up to 200 Oe the precession of the neutron beam polarization decays because of magnetic field inhomogeneities. The interferometer can be a part of a spin-echo spectrometer where the influence of magnetic field inhomogeneities and neutron beam divergence are eliminated. In particular, it can be used to study a static inhomogeneous state with a micron-size correlation length and the dynamics of media with correlation times at a microsecond level, as well as to measure the width of neutron wave packets.

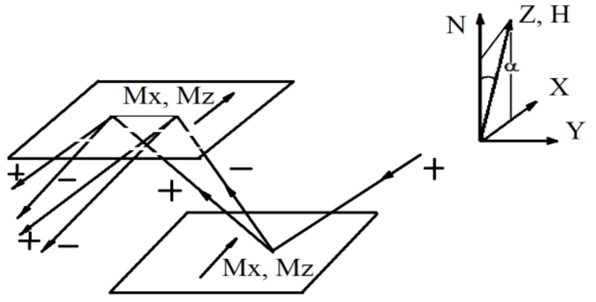

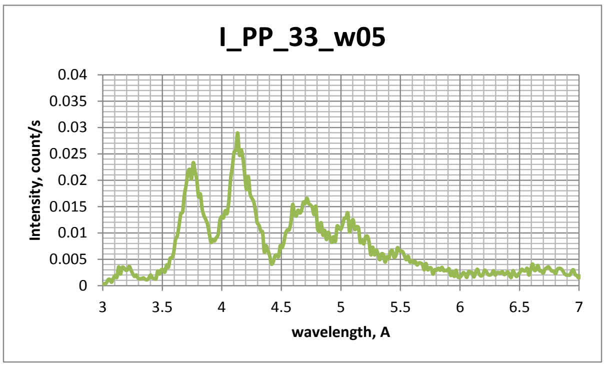

Fig. 23. *Operating principle of the neutron spin interferometer of a new type (left) and spectrum of neutrons passing through the interferometer under a magnetic field of 33 Oe (right).*

A method to study weakly magnetic films using the polarized neutron channeling has been developed (**Fig. 24**). The magnetic induction of a weakly magnetic layer has been measured. The structure Ta(3 nm) / $Ni_{0.67}Cu_{0.33}$(15 nm) / $TbCo_5$(150 nm) / $Ni_{0.67}Cu_{0.33}$(50 nm) / Si(substrate), in which the waveguide layer is made of a material ($TbCo_5$) with small saturation magnetization of about 200 G has been investigated. Such materials containing rare earth elements are widely used for the development of new methods for magnetic recording. However, because of the weak saturation magnetization these materials cannot be studied by standard reflectometry of polarized neutrons, which is used for materials with magnetization of more than 1000 G. In experiments, a polarized neutron beam falls at some grazing angle on a three-layer waveguide structure where the resonance amplification of the neutron wave in the average weakly magnetic layer occurs. The neutron wave phase in the resonance depends on the neutron spin direction, channel width and magnetic induction in a channel. Along with it, the grazing angles of the incident beam for spins (+) and (-) differ, and the difference in the squared sines of these angles directly gives the magnetic induction in the layer at its values of less than 100 mT. With increasing B, other factors start to determine the non-linear dependence. The prospects of this method for neutron measurements in research of weakly magnetic materials have been concluded to be good.

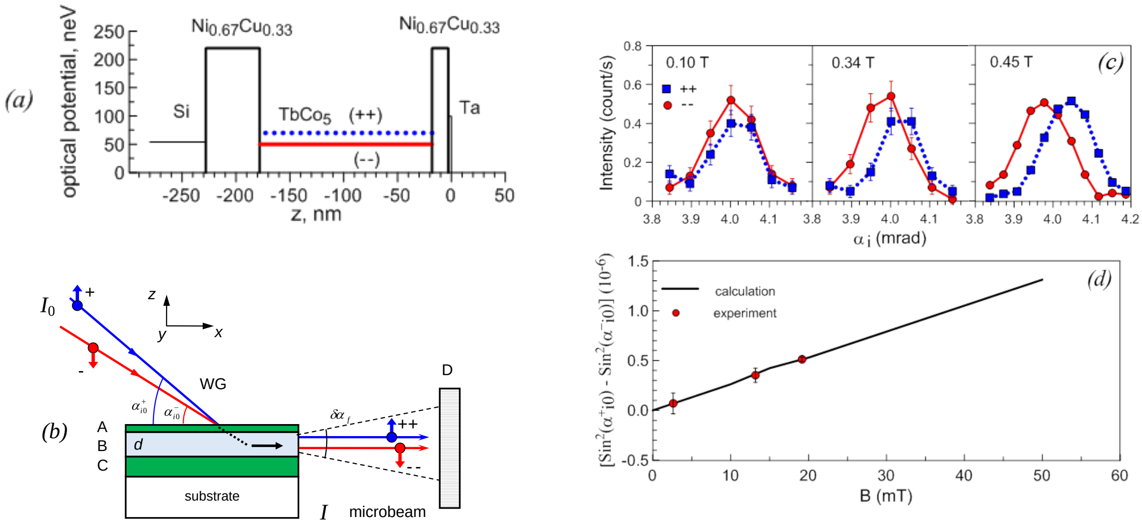

Fig. 24. *Optical potential profile for the nanostructure Ta(3 nm) / $Ni_{0.67}Cu_{0.33}$(15nm) / $TbCo_5$(150nm) / $Ni_{0.67}Cu_{0.33}$(50nm) / Si(substrate) (a), scheme of the experiment (b) parts of the spectrum of scattered neutrons at different magnetic fields (c) and difference of squared sines of grazing angles as a function of magnetic field induction (d).*

The operating modes of the spin-echo small-angle (SESANS) spectrometer with linearly increasing magnetic fields, which is under construction on the basis of the REFLEX reflectometer, have been numerically studied. Monte Carlo simulations of these modes for a virtual spectrometer have been performed in the VITESS software package. In particular, a program module simulating the main element of the SESANS spectrometer (spin rotator) has been created. The parameters of the model spectrometer have been chosen in accordance with the parameters of the prototype of the SESANS spectrometer being constructed on IBR-2 beamline 9. The purpose of the work was to determine the possible modes of the setup under constraction and its possibilities in the study of nanostructures. Basing on the IBR-2 parameters and the geometry of the spectrometer with respect to the location of its elements and their characteristics, it has been found that the measured correlation dependence *P(Z)* of the scattered beam polarization on the so-called spin-echo length is composed of separate intervals relating to specific spectral intervals of the neutron beam (**Fig. 25**).

a) b)

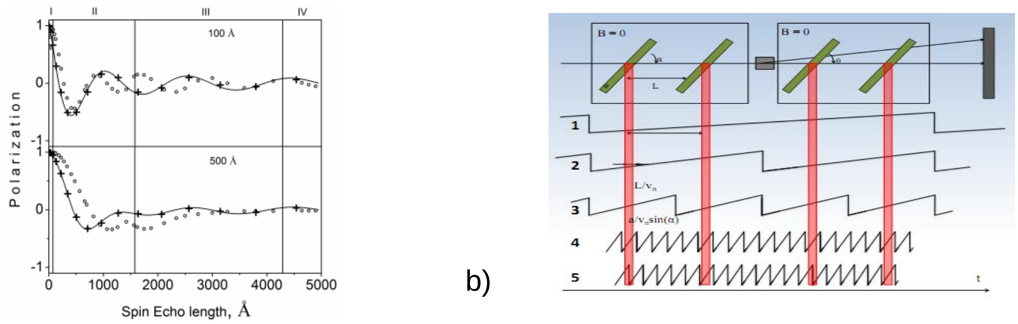

Fig. 25. *(a) SESANS signal for particles with radii of 100 Å and 500 Å. Roman numerals denote the operation modes of the instrument. The solid line and crosses designate the analytical calculations and the model scattering curve, respectively, for the ideal case of the infinite time field pulse. The circles correspond to the case of sawtooth pulses for the magnetic field realizing different modes of the spectrometer in different spectral intervals. (b) Time diagram illustrating different operating modes: one pulse of the field per passage through four (1), two (2), one (3) spin rotators; every n-th pulse per passage through one spin rotator (4).*

Each of these intervals is characterized by its own measured correlation dependence *P(Z)*, thus, the analysis of the total correlation dependence should consist of an independent analysis of its individual parts.

On the YuMO spectrometer a new data acquisition concept with respect to the software upgrade procedure has been developed. The fast task exchange option in the software has been implemented together with the scheme of the SAS software update for experimental data treatment. This software modification is a result of tight and successful collaboration with groups of A.Kirilov (SC Dpt., FLNP) and A.Soloviev (LIT), which has made it possible to prevent losses in the experimental time. The autonomous vacuum system for pumping out large (> 20 m^3) air volume from the vacuum tube of the detecting system has been implemented, which ensures reliable operation of the instrument and prompt corrections of problems during the opening/closing of the vacuum valves in both methodological experiments and experiments in the framework of the spectrometer modernization program.

On the neutron radiography and tomography spectrometer simulation energy-selective radiography experiments have been conducted [17]. In the experiments a CCD-camera-based detector was used. The frequency of the camera was synchronized with the reactor pulse frequency. Using the camera response delay relative to the start of reactor pulses and the exposure time variation, neutron images of various metal materials (aluminum, steel, lead, copper) have been obtained in the neutron wavelength ranges of 0.2-2, 2-3.7, 3.8-8 Å (**Fig. 26**).

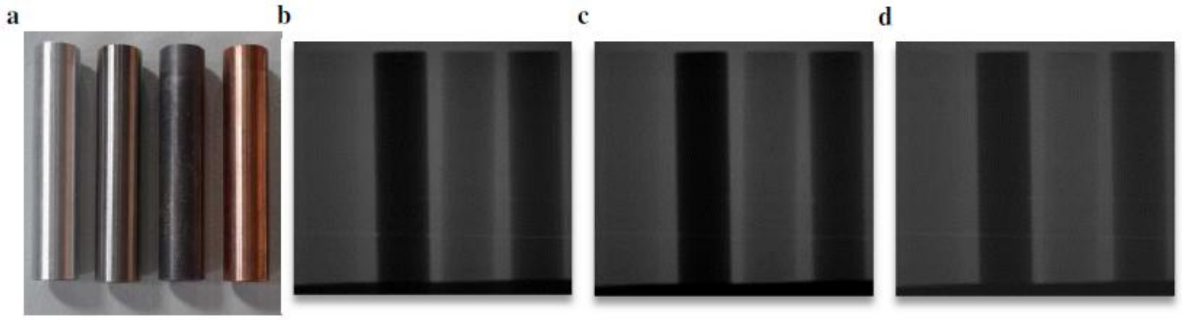

***Fig. 26**. Photo of cylindrical samples (aluminum, steel, lead, copper) (a) and their neutron images obtained in the wavelength ranges of 0.2-2 Å (b), 2-3.7 Å (c), 3.8-8 Å (d).*

A change was observed in the contrast of images of the materials in the ranges under study, which offers good prospects for further development of energy-selective radiography and tomography at the IBR-2 reactor.

References

[1] D.P.Kozlenko, N.T.Dang, S.E.Kichanov, E.V.Lukin, A.M.Pashayev, S.G.Jabarov, L.S.Dubrovinsky, H.-P.Liermann, W.Morgenroth, A.I.Mammadov, R.Z.Mekhtieva, V.G.Smotrakov, and B.N.Savenko "Competing magnetic states in multiferroic YMn_2O_5 at high pressure", Physical Review B, v. 92, p. 134409 (1-7) (2015).

[2] N.V.Kosova, I.A.Bobrikov, O.A.Podgornova, A.M.Balagurov, A.K.Gutakovskii Perculiarities of structure, morphology, and electrochemistry of the doped 5-V spinel cathode materials $LiNi_{0.5-x}Mn_{1.5-y}M_{x+y}O_4$ (M=Co, Cr, Ti; x+y = 0.05) prepared by mechanochemical way. Journal of Solid State Electrochemistry (2015) DOI: 10.1007/s10008-015-3015-4.

[3] A.I.Gusev, A.S.Kurlov, I.A.Bobrikov, A.M.Balagurov "$V_8C_{7-\delta}$ Superstructure in Nonstoichiometric Vanadium Carbide Powders" JETP Letters, 2015, Vol. 102, No. 3, pp. 154–160.

[4] A.I.Gusev, A.S.Kurlov, E.Y.Gerasimov, A.M.Balagurov, I.A.Bobrikov, A.A.Rempel "Nanocrystalline ordered vanadium carbide: Superlattice and nanostructure", Superlattices and Microstructures (2015) submitted.

[5] A.V.Trukhanov, V.O.Turchenko, I.A.Bobrikov, S.V.Trukhanov, I.S.Kazakevich, A.M.Balagurov "Crystal structure and magnetic properties of the $BaFe_{12-x}Al_xO_{19}$ (x = 0.1–1.2) solid solutions", J. Magn. Magn. Mater., v.393, pp.253-259 (2015).
[6] N.M.Belozerova, S.E.Kichanov, Z.Jírak, D.P.Kozlenko, M.Kačenka, O.Kaman, E.V.Lukin, B.N.Savenko "High pressure effects on the crystal and magnetic structure of nanostructured manganites $La_{0.63}Sr_{0.37}MnO_3$ and $La_{0.72}Sr_{0.28}MnO_3$", Journal of Alloys and Compounds, v. 646, pp. 998-1003 (2015).
[7] M.V.Avdeev, V.I.Petrenko, I.V.Gapon, L.A.Bulavin, A.A.Vorobiev, O.Soltwedel, M.Balasoiu, L.Vekas, V.Zavisova, P.Kopcansky "Comparative structure analysis of magnetic fluids at interface with silicon by neutron reflectometry", Appl. Surf. Sci., v. 352, pp. 49–53 (2015).
[8] M.Rajnak, V.I.Petrenko, M.V.Avdeev, O.I.Ivankov, A.Feoktystov, B.Dolnik, J.Kurimsky, P.Kopcansky, M.Timko "Direct observation of electric field induced pattern formation and particle aggregation in ferrofluids", Applied Physics Letters, v. 107, p. 073108 (2015).
[9] R.A.Eremin, Kh.T.Kholmurodov, V.I.Petrenko, L.Rosta, N.A.Grigoryeva, M.V.Avdeev On the microstructure of organic solutions of mono-carboxylic acids: Combined study by infrared spectroscopy, small-angle neutron scattering and molecular dynamics simulations. Chemical Physics v. 461, pp. 1-10 (2015).
[10] O.V.Tomchuk, D.S.Volkov, L.A.Bulavin, A.V.Rogachev, M.A.Proskurnin, M.V.Korobov, M.V.Avdeev "Structural characteristics of aqueous dispersions of detonation nanodiamond and their aggregate fractions by small-angle neutron scattering", Journal of Physical Chemistry C, v. 119, pp. 794-802 (2015).
[11] Yu.I.Prylutskyy, V.V.Cherepanov, M.P.Evstigneev, O.A.Kyzyma, V.I.Petrenko, V.I.Styopkin, L.A.Bulavin, N.A.Davidenko, D.Wyrzykowski, A.Woziwodzka, J.Piosik, R.Kaźmierkiewicz, U.Ritter "Structural self-organization of C60 and cisplatin in physiological solution", Phys.Chem.Chem.Phys., 2015, V. 17, P. 26084-26092.
[12] Yu.I.Prylutskyy, M.P.Evstigneev, V.V.Cherepanov, O.A.Kyzyma, L.A.Bulavin, N.A.Davidenko, P.Scharff "Structural organization of C60 fullerene, doxorubicin, and their complex in physiological solution as promising antitumor agents", J. Nanopart. Res., 2015, 17:45.
[13] N.Jargalan, T.V.Tropin, M.V.Avdeev, V.L.Aksenov "Investigation and modeling of evolution of UV-Vis spectra of C60/NMP solution", Nanosystems: physics, chemistry, mathematics, 2015, accepted.
[14] T.B.Feldman, A.I.Ivankov, T.N.Murugova, A.I.Kuklin, P.V.Shelyakin, M.A.Yakovleva, V.I.Gordeliy, A.V.Belushkin, M.A.Ostrovsky "Study of visual pigment rhodopsin supramolecular organization in photoreceptor membrane by small-angle neutron scattering method with contrast variation", Proceedings of the Russian Academy of Sciences, v. 465, № 5, pp. 1-5, 2015 (in Russian).
[15] K.Łuczyńska, K.Drużbicki, K.Łyczko, J.Cz.Dobrowolski "Experimental (X-ray, 13C CP/MAS NMR, IR, RS, INS, THz) and Solid-State DFT Study on (1:1) Co-Crystal of Bromanilic Acid and 2,6- Dimethylpyrazine", Journal of Physical Chemistry B, v. 119, p. 6852-6872 (2015).
[16] D.M.Itkis, J.J.Velasco-Velez, A.Knop-Gericke, A.Vyalikh, M.V.Avdeev, L.V.Yashina "Probing of electrochemical interfaces by photons and neutrons in operando", ChemElectroChem, v. 2, p. 1427–1445 (2015).
[17] E.V.Lukin, D.P.Kozlenko, S.E.Kichanov, A.V.Rutkauskas, G.D.Bokuchava, B.N.Savenko "First attempts on energy-selective neutron imaging at IBR-2", Physics Procedia, v. 69 (2015), p. 271 – 274.

MULTIMODAL PLATFORM FOR RAMAN AND NONLINEAR OPTICAL MICROSCOPY AND MICROSPECTROSCOPY FOR CONDENSED MATTER STUDIES

In 2015, the activities of the Sector of Raman Spectroscopy (Centre “Nanobiophotonics”) were focused on the further development and enlarging of the spectral and microscopic possibilities of the optical platform “CARS” microscope. This was done with the aim to implement the state of the art optical options for highly spectrally selective imaging and high sensitivity enhanced Raman spectroscopy:

- Polarized Coherent antiStokes Raman Scattering (P-CARS)
- Surface Enhanced Raman Scattering (SERS)
- Raman scattering using laser excitation at 532nm

All three of these options were successfully elaborated and established at the “CARS” microscope. Afterwards, the research activities were carried out on the following tasks: highly selective spectral imaging of membrane proteins; first tests of SERS with various biomolecules; photo- and up-conversion luminescence of oxyfluoride nano-glass-ceramics doped with Er^{3+}, Eu^{3+}, Tm^{3+}, and Yb^{3+}. Some other research activities for JINR labs and Member States were implemented in the frame of the “friendly user facility” as well.

1. The upgraded “CARS” microscope

Figure 1 shows the upgraded schematic of the multimodal optical platform for performing Raman, P-CARS, SERS spectroscopy and microscopy. We exploit parallel orientations of linear polarizations of the input Stokes and pump beams. Both excitation picosecond pulse trains are made coincident in time and in space utilizing an optical delay line and a series of dichroic mirrors. For CARS microscopy a water-immersion objective lens with a high numerical aperture (NA=1.2, UPLANAPO-60x, Olympus) was exploit to focus the beams tightly.

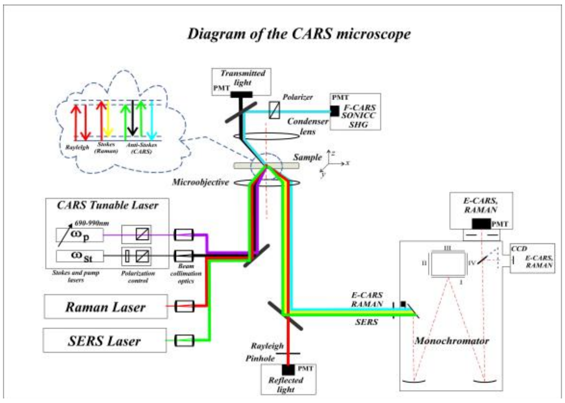

Fig. 1. Diagram of the upgraded multimodal optical platform: “CARS” microscope

Using this optical platform, a sample can be imaged by utilizing vibration frequencies in the spectral range of (1000−3580) cm^{-1}, which covers all most important vibrational modes of bio-molecules. Five detection channels allow two forward- and three backward- propagated signals to be recorded. The polarization control is adjustable with a half-wave plate in the Stokes beam. Along with the CARS signals, the system allows detection of spontaneous Raman, luminescence, including up-conversion luminescence, second and sum frequency generation signals and transmission mode as well.

In 2015 we also incorporate into the our optical system a diode-pumped green laser at 532nm with an adjustable output power of up to 20 mW and more than 50 meters coherence length (model SLM-417-20).

2. Scientific results

2.1 P-CARS imaging of membrane protein crystals

During the reporting period in cooperation with the Institute for the Physics of Complex Systems (Germany), the Institute of Structural Biology (France), Moscow Institute of Physics and Technology, and Orbeli Institute of Physiology (Armenia), research activities on membrane protein (MP) structural studies using nonlinear optical microscopy were initiated. For the first time CARS images of MP crystals with submicron resolution and high contrast were obtained. As a first step in this direction, we performed the studies with bacteriorhodopsin crystals. The C=C retinal chromophore vibrational stretch at 1529 cm-1 is chosen from the Raman spectrum of BR crystals for CARS microscopy imaging.

Figure 2 compares Raman and CARS images of a sizable BR crystal. An optical microscopy image of this crystal is shown in the figure as well (**Fig. 2a**). A Raman intensity map of the C=C stretching vibrations of the retinal chromophore in bacteriorhodopsin is shown in **Fig.2b**. Any of the small sized features is not observed in the Raman image. The analytical capabilities of the spontaneous Raman scattering microscopy are significantly limited by the difficulty in acquiring contrast image with low signals.

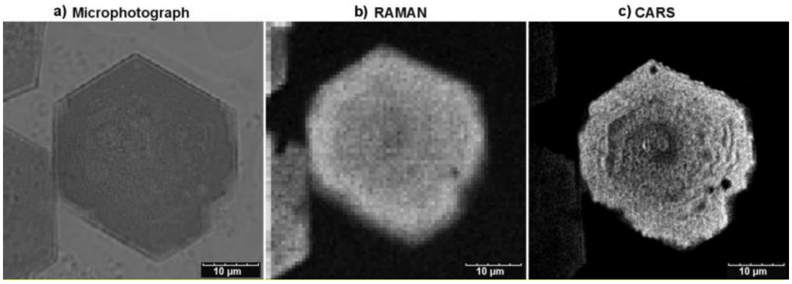

Fig. 2. *a) Microphotograph, b) Raman (λ_{ex}=785nm) and c) P-CARS (λ_p= 915.5nm, λ_{St}=1064nm), images at vibration 1529 cm-1 of bacteriorhodopsin crystal. Scan area – 48x48μ*

The CARS image is much more stronger than the spontaneous Raman signal, allowing very fast imaging acquisition of ~3s with good signal-to-noise ratio. The high spatial resolution of CARS permits visualization of detailed structures in BR crystals. Also, there were obtained P-CARS images of small crystals with submicron resolution.

A few of BR crystals consists of two roughly equal sized parts because of twinning. Twinning is one of the most common crystal-growth defects in protein crystallography. **Figure 3** demonstrated a high quality 3D-imaging of twin BR crystals.

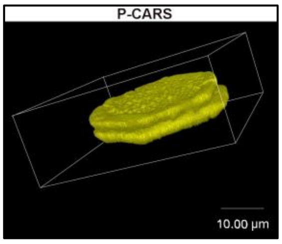

Fig. 3. *P-CARS 3D-image of twin BR crystal*

2.2 Surface Enhanced Raman Scattering (SERS): first experiments

In cooperation with partners from the Republic of Belarus (BSUIR and Scientific-Practical Materials Research Centre of NAS) the spectra of spontaneous Raman scattering and SERS for rhodamine 6G dye (R6G) and protein lysozyme were obtained using a substrate based on porous crystalline silicon. For excitation of the Raman scattering was used either He-Ne laser (632.8 nm) or diode-pump laser with a wavelength of 532nm. The power of the exciting laser exposure is selected experimentally to achieve maximal SERS - effect. The accumulation time of Raman spectrum is varied from 0.5 to 10 seconds.

In 2015 the main research directions goals on SERS were the following:

- definition of the concentration sensitivity limit on the SERS active substrates based on silver/porous silicon (Ag / PS);
- definition of the maximum enhancement factor (EF) on the SERS active substrates based on plasmonic structures Si/SiO_2/(Ag).

2.2.1. SERS - active structures on the basis of silver / porous silicon (Ag/PS) composition

Spontaneous Raman spectrum of lysozyme was obtained at a dilution of its concentration up to 10^{-3} M (control). For obtaining SERS effect was used concentration for 10^4 and 10^6 less than the control: 10^{-7} and 10^{-9} M solution of lysozyme. The power of the exciting laser (632.8 nm) was 250 µW.

Fig. 4 demonstrates enhance Raman signals from lysozyme in SERS option using substrates on the basis of silver/porous silicon (Ag/PS).

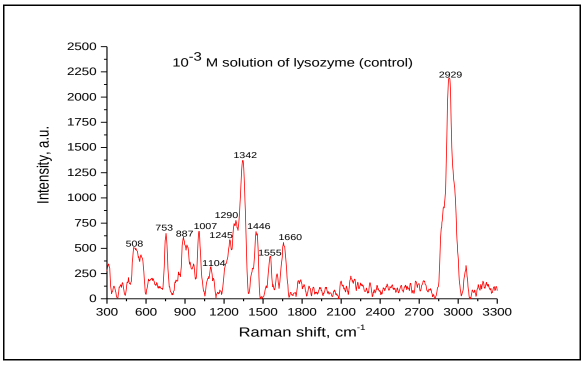

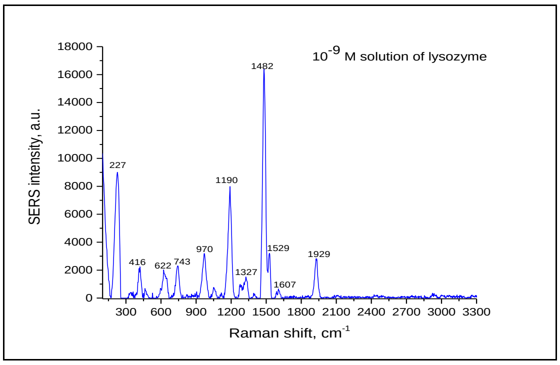

__Fig.4.__ On the left: Raman spectrum of 10^{-3}M solution of lysozyme (control), on the right: SERS spectrum of 10^{-7}M solution of lysozyme

SERS allows to identify molecules of lysozyme at the concentration of 10^{-9}M. It appears that the laser power of 250 µW was enough for this enhancement. In 2016 these activities would be proceeded.

2.2.2. Plasmonic structures of Si/SiO2/(Ag)

The second type of substrates exploited in our SERS studies were so-called plasmonic structures of Si/SiO_2(Ag) composition, produced by ion-track technology. Monocrystalline silicon plates served as a surface to develop Si/SiO_2 structures. Substrates of Si/SiO2 were exposed to the Au ions at the energy of 350 MeV. Irradiation was carried out at the normal incidence angle, leading to a random distribution of parallel oriented ion tracks in a layer of SiO_2. Plasmonic structures of Si/SiO_2(Ag) differed from each other by the time of etching in hydrofluoric acid HF (10 - 35 min), which affects the pore diameter formed in silicon oxide. The pore diameter in turn causes the dendritic morphology of silver nanoparticles when treated with a 0.02 M solution of $AgNO_3$. The obtained results are shown in **Fig. 5.**

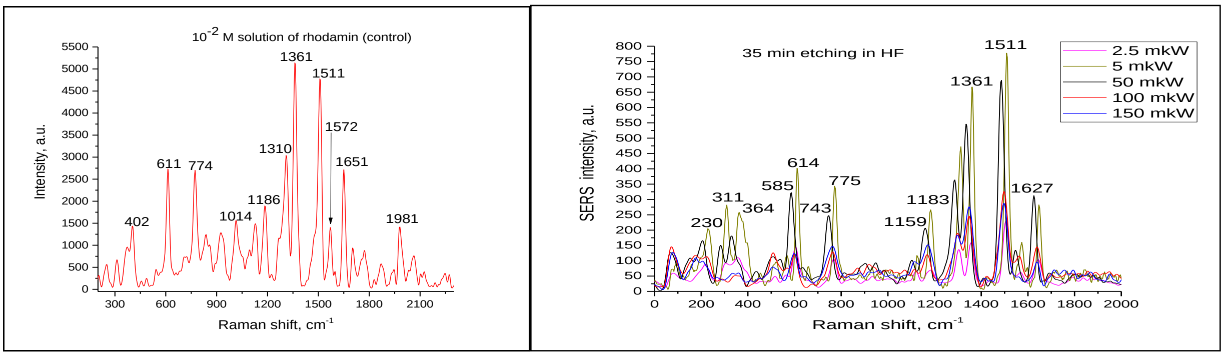

__Fig.5.__ On the left: Raman spectrum of 10-2M solution of R6G (control); on the right: SERS spectrum of 10-6 M solution of R6G on plasmonic structures of Si/SiO2/(Ag), etching time 35 min

The results indicate that the best plasmon structures are the substrates with an etching time of 35 minutes, resulting in the SERS enhancement factor of as high as 10^7-10^8 (**Fig. 5, right**). Wherein, the optimal laser power is of 5 μW.

The results obtained in 2015 on SERS studies we consider as very optimistic, thus they can be serve as a good basis for the further research activities in the Sector of Raman spectroscopy, LNP.

2.2 Photo- and up-conversion luminescence (UCL) of oxyfluoride nanoglassceramics doped with rare earth elements (REE)

In 2015, an international collaboration was established with the Institute of Solid State Physics of University of Latvia, Riga, with the Belarusian State Technological University, Minsk, and the Institute of Solid State Physics and Semiconductors, Minsk. The structural and spectral characteristics of oxyfluoride glasses co-doped by europium and ytterbium ions with different molar concentrations.

Structural studies.

The X-ray diffraction analysis (XRD) of precursors and heat-treated samples was done to identify the nanocrystalline phase of lead fluoride. The presence of diffraction peaks in the heat-treated samples indicates the formation of nanocrystalline phase, corresponding to the cubic crystal lattice of PbF_2 nanocrystals. The average size of the nanocrystals ~6,5nm was calculated using the Debye-Scherrer's equation.

Also, transmission electron microscope (TEM) «FEI Tecnai» was exploited to visualize the nanocrystalline phase (**Fig.6**.).

As it is seen from the figure, the PbF_2 nanocrystals are spherical in shape and have relatively small variations in diameter. However, the size dispersion is pronounced to be bimodal: there is a fraction of ~15nm size and a fraction of ~(2-5)nm.

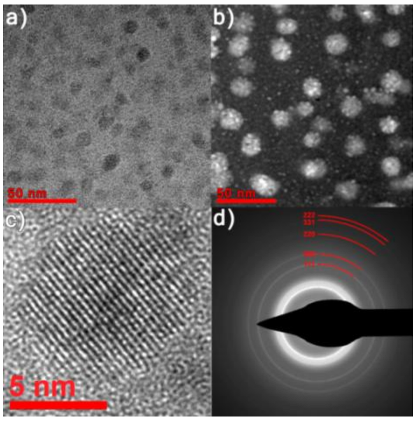

Fig. 6. TEM images of the heat-treated samples: a) bright-field image, b) dark-field image, c) the enlarged image of nanocrystals, d) electron diffraction pattern of nanocrystal.

Fig. 6(c, d) shows that nanocrystals have a face-centered cubic lattice crystal, typical for β-PbF_2.

Luminescent characteristics

Photoluminescence spectra of precursor and heat-treated samples were measured under the laser excitations of 325, 405, 456nm, and a xenon lamp at the wavelength of 440nm (**Fig.7**). At the all excitation wavelengths a pronounced red photon emission was observed, typical for *4f-4f* transition of Eu^{3+}.

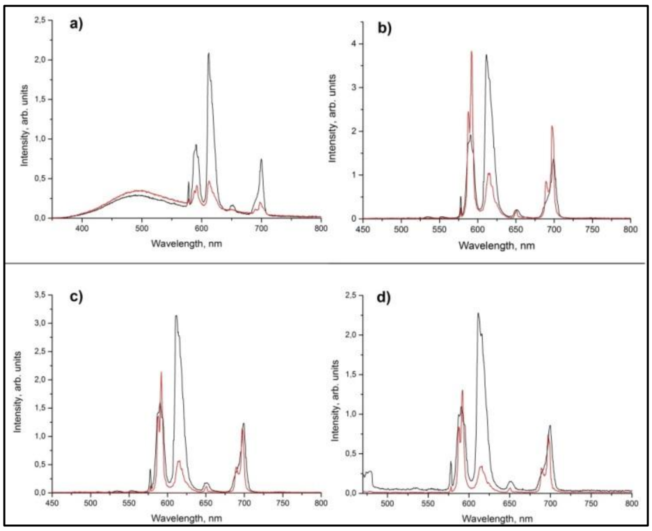

Fig.7. Photoluminescence spectra at different excitations: a) 325nm b) 405nm c) 440nm d) 457nm

The spectra of up-conversion luminescence of the precursor and heat-treatment samples were detected at the «CARS» microscope using laser excitation at 976nm corresponding to the maximal value of absorption coefficient of ion Yb^{3+} (**Fig.8**).

As can be seen from **Fig. 5**, in addition to the luminescence bands typical for the europium ions, additional bands are observed at 510, 525, and 550 nm, related, with a high probability, to the erbium ions in the sample as an impurity. Subsequently conducted energy dispersive analysis (EDS) confirmed this assumption. It should be also noted the increase of the erbium peaks in heat-treated samples are due to the inter-ion interaction processes described in details in our previous studies.

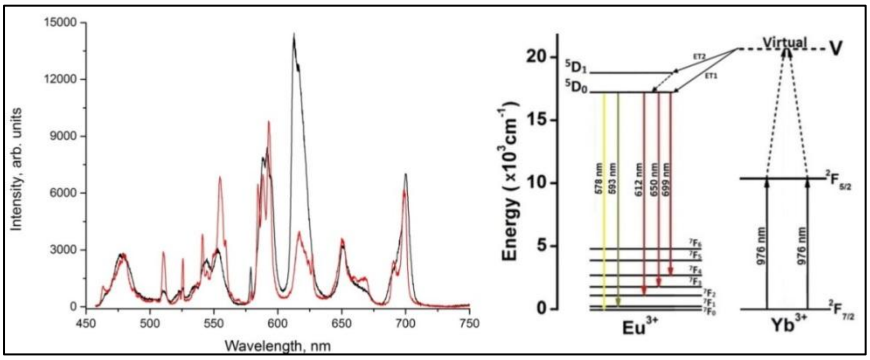

Fig.8. *UCL spectra of precursor and heat-treated sample, excitation 976nm. On right – energy transition diagram for* Eu^{3+} *ion.*

Presently, the above mentioned results on photo- and UC luminescence are being in preparation for publication in a peer-reviewed journal in this field.

REFERENCES

[1] A. Zumbusch, G.R. Holtom, and X.S. Xie, “Three-Dimensional Vibrational Imaging by Coherent Anti-Stokes Raman Scattering,” Phys. Rev. Lett. **82,** 4142-4145 (1999).

[2] J.-X. Cheng, Y. K. Jia, G. Zheng, X.S. Xie, “Laser-Scanning Coherent Anti-Stokes Raman Scattering Microscopy and Applications to Cell Biology”, Biophysical Journal **83,** 502-509 (2002).

[3] Andreas Volkmer, “Vibrational imaging and microspectroscopies based on coherent anti-Stokes Raman scattering microscopy”, J. Phys. D: Appl. Phys. **38,** R59–R81 (2005).

[4] D.J. Kissick, D. Wanapun, G.J. Simpson, “Second-Order Nonlinear Optical Imaging of Chiral Crystals”, Annu. Rev. Anal. Chem. **4,** 419–437 (2011).

[5] Ji-Xin Cheng, Lewis D. Book, and X. Sunnie Xie, “Polarization coherent anti-Stokes Raman scattering microscopy”, Opt. Letters, **26**, 1341-1343 (2001).

[6] A. Barhoumi, D. Zhang, F. Tam, N.J. Halas, “Surface-enhanced raman spectroscopy of DNA”, J. AM. CHEM. SOC, **130**, 5523-5529, (2008).

[7] T.-W. Koo, S. Chan, A. A. Berlin, “Single-molecule detection of biomolecules by surface-enhanced coherent anti-Stokes Raman scattering”, Optics letters, **30 (9)**, 1024-1026, (2005).

[8] J.B. Jackson, S.L. Westcott, L.R. Hirsch, J.L. West, N.J. Halas, “Controlling the surface enhanced Raman”, Applied Phys. Lett., **82 (2)**, 257-259, (2001).

[9] G.M. Arzumanyan, V. Vartic, et all “CARS microscope: “Possibilities, the first results, problems and prospects”, Communication of JINR, P13-2013-108, Dubna, (2013).

[10] G. Arzumanyan, V.Vartic, A. Kuklin, D. Soloviov, G. Rachkovskaya, et al. “Upconversion Luminescence of Er3+ and Co-Doped Er3+/Yb3+ Novel Transperent Oxyfluoride Glasses and Glass Ceramics: Spectral and Structural Properties” Journal of Physical Science and Application 4, 150-158 (2014).

[11] J. Zhou, Q. Liu, W. Feng, Y. Sun, F. Li “Upconversion Luminescent Materials: Advances and Applications” Chem. Rev., 115(1), 395-465 (2015).

[12] Y.Dwivedi, S.C. Zilio, “Infrared cascade and cooperative multicolor upconversion emission in $Y_8V_2O_{17}$:Eu:Yb nanophosphors” Optical Express, 21, 4717-4177, (2013).

NEUTRON NUCLEAR PHYSICS

In 2015, in FLNP the scientific activity in the field of neutron nuclear physics was carried out in the following traditional directions: investigations of time and space parity violation processes in neutron-nuclear interactions; studies of the fission process; experimental and theoretical investigations of fundamental properties of the neutron; gamma-spectroscopy of neutron-nuclear interactions; atomic nuclear structure, obtaining of new data for reactor applications and for nuclear astrophysics; experiments with ultracold neutrons, applied research using NAA. The scientific program to study the inelastic scattering of fast neutrons made into a separate project "TANGRA" was successfully implemented. A number of investigations in the field of fundamental physics and ultracold neutron physics were performed on the neutron beams of nuclear research centers in Germany, China, USA, France, Switzerland.

Of particular note is the accurate implementation of the planned activities on the modernization of the IREN facility aimed to ensure that in 2016 two accelerating sections of the accelerator will operate.

Experimental and methodological investigations

Investigations of prompt fission neutrons

In 2015, the first stage of works on the development of a facility for studying prompt neutrons from fission induced by low-energy neutrons was completed, which resulted in the construction of a setup consisting of a double ionization chamber (DIC) with Frisch grids (see **Fig. 1**). DIC is designed to measure masses, kinetic energies of correlated fission fragments and angles between the fission axis and the normal to the target plane.

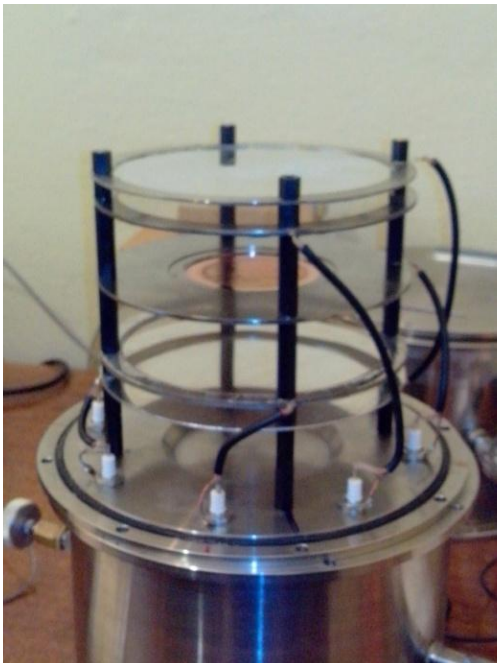

Fig. 1. *Double ionization chamber with Frisch grids with a target mounted on a common cathode.*

A fast neutron detector (FND) on the basis of liquid scintillator BS-501A from Saint-Gobain is located at a distance of ~0.7 m from the target along the normal to its center and allows one to determine the angle between the direction of motion of prompt fission neutrons and fission fragments.

The determination of energy of prompt fission neutrons is realized by measuring the time of flight using a cathode signal as a "T-zero" signal and an FND signal as a "Stop" signal. A schematic of electronic equipment and acquisition system is shown in **Fig. 2**.

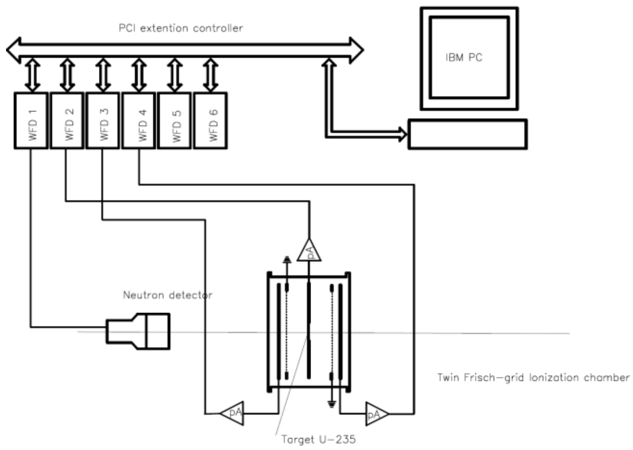

***Fig. 2**. Schematic of a setup for studying prompt fission neutrons.*

It consists of current amplifiers with cathode and two anode circuits. Signals from the outputs of amplifiers and fast neutron detector arrive to the inputs of digitizers from "SPECTRUM-INSTRUMENTATION". The digitizers are mounted on an autonomous bus PCI-Express, which is connected to a PC via a fiber-optic communication line SONET.

The detector signals are digitized simultaneously in six channels at a rate of 250 MHz and amplitude resolution of 12 bits. The start of ***digitization*** is given during the registration of a fission fragment using the signal from the DIC common cathode. The setup was tested on thermal neutron beamline 11B of the IBR-2 reactor. Some preliminary results of the measurements are shown in **Figures 3, 4**.

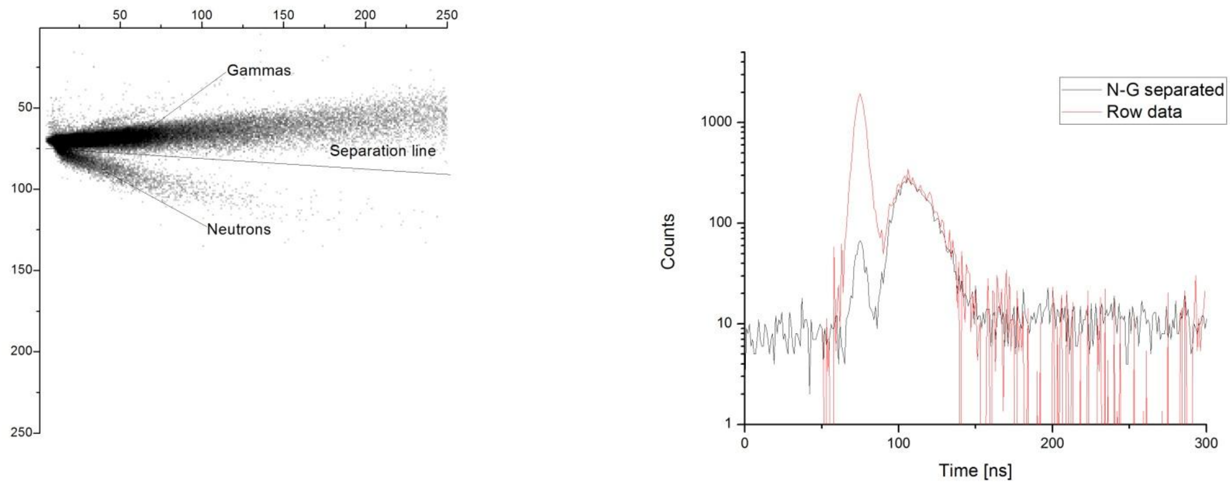

***Fig. 3.** Separation of events of registration of neutrons and γ-rays using the two integral method (left). TOF spectra of prompt fission neutrons (right): initial data (red line) and after separation of neutrons and γ-rays (black line).*

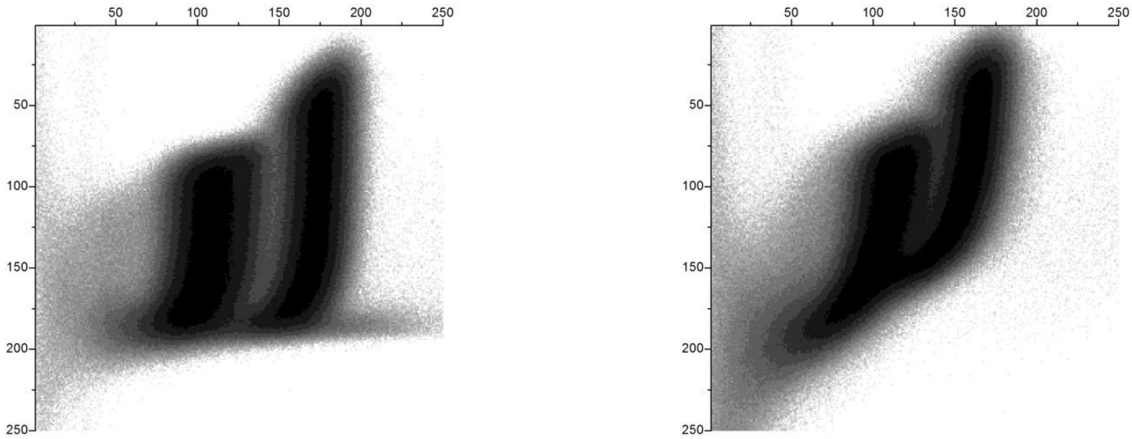

***Fig. 4**. Two-dimensional distributions of fission fragments in the coordinates of amplitude-time of charge collection on the anodes of DIC: for the anode from the side of the target layer (left) and for the anode from the side of the substrate (right).*

Monte-Carlo calculations of angles between directions of motion of two light charged particles in "pseudo"-quaternary fission

A lot of experiments have been devoted to the study of charged particles from ternary and quaternary fission, in which in addition to two heavy fragments, one or two lighter charged particles are emitted. If the emitted particle is unstable, it may in turn decay during its travel. The use of position-sensitive detectors makes it possible to identify such events by finding two particles detected simultaneously in different parts of one or two detectors. Timepix detectors are convenient for detecting such events. We have developed two ΔE-E telescopes to study light unstable charged particles from the spontaneous decay of ^{252}Cf. Of particular interest is the study of the emission of two unstable particles: ^{8}Be and ^{7}Li. In the decay of ^{8}Be two alpha-particles should be detected, and in the decay of ^{7}Li — an alpha-particle and tritium nucleus. The decay of ^{8}Be has three channels, which can be separated. These channels are the decay of ^{8}Be in the ground state, and two variants of decay when ^{8}Be is in the first excited state and the second excited state. In the case of ^{7}Li it makes sense to consider three variants of decay: when ^{7}Li is in the first, second and third excitation levels. Decay channels of particles under study are separated by the registration of the distance between two charged particles simultaneously detected by position-sensitive detectors. Knowing the energy of flying particles and the positions and sizes of telescopes, one can calculate the distances. Monte Carlo calculations of three variants of ^{8}Be decay and three variants of ^{7}Li decay have been performed. As a result of the calculations it has been found that in a real experiment in the case of ^{8}Be the events from two decay channels can be obtained: from decay of ^{8}Be in the ground and first excited states. In the case of ^{7}Li it has been revealed that three decay channels cannot be separated using the developed setup, and one can only study the total contribution of these channels.

Measurement of T-odd effects in ^{235}U fission on a hot source of polarized neutrons

In the framework of the FLNP-ITEP collaboration a series of experiments have been conducted to measure the ROT-effect for studying prompt γ-rays and neutrons in binary fission of ^{235}U and ^{233}U induced by polarized cold neutrons. In 2015, at the facility POLI (FRM-2, Garching) beam time (11 days) was allocated to conduct an experiment to measure the effect of rotation of the fissioning nucleus in the resonance region of ^{235}U at an energy of 0.3 eV on the beam of polarized resonance neutrons being constructed (hot source of neutrons). In July of 2015 the first experiment to measure the ROT-effect in the resonance region was carried out. The experimental setup is shown in **Fig. 5**.

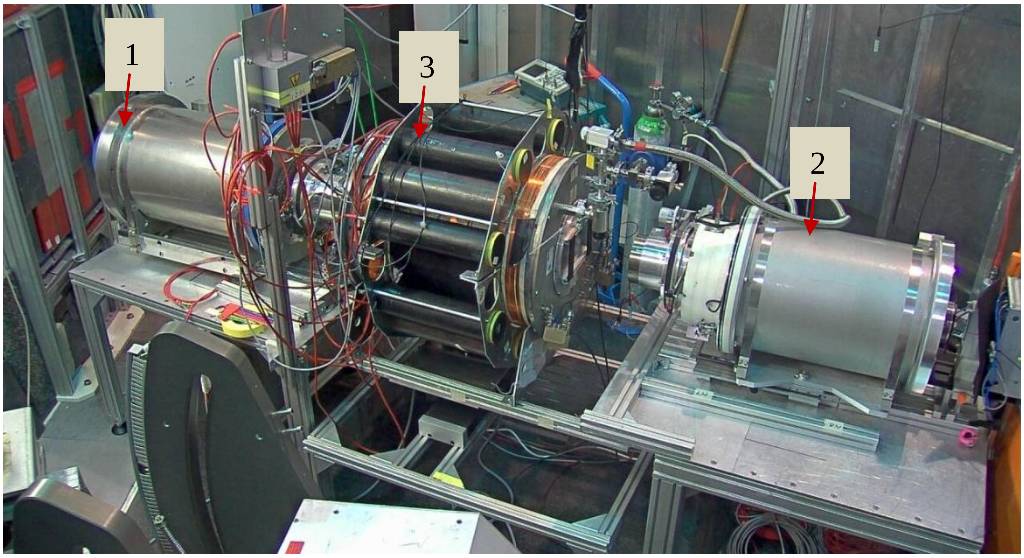

***Fig. 5**. A setup for measuring the ROT-effect on the POLI instrument (FRM-2, Garching). 1 – neutron polarizer, 2 – analyzer, 3 – fission chamber surrounded by detectors of gamma-rays and neutrons.*

The neutron beam with an energy of 0.3 MeV was cut using a mosaic single crystal diffractometer and focused on the target. A neutron polarizer on the basis of a polarized ^{3}He cell with an average polarization of ~70% was placed between the diffractometer and the target. The polarized neutron flux density at the target was ~5x10^6 n/cm^2/s. The polarization was controlled by a similar analyzer and measured using the readings of neutron counters.

Since the neutron beam should be longitudinally polarized at the target and a ^{3}He polarizer produces a vertically polarized beam, additional magnetic coils have been installed, thus providing an adiabatic spin rotation by 90° in the target. The direction of the magnetic field in the coils changed once per second, which created an analogue of a spin-flip and allowed us to measure the difference effect.

A schematic of the fission chamber is shown in **Fig. 6**.

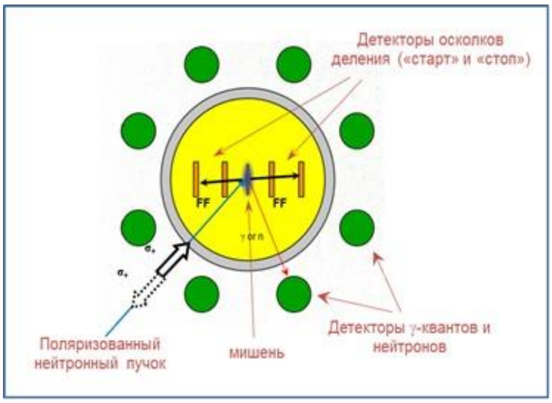

***Fig. 6**. Fission chamber with a ^{235}U target.*

Fragments were detected using fast multiwire detectors and separated into light and heavy ones by the time of flight. Gamma-rays and neutrons were detected by scintillation counters (plastic, NaI(Tl)) positioned at specific angles to the direction of emission of the fragments. We measured the so-called TRI-effect (up-down emission asymmetry) and the ROT-effect (rotation of the fissioning system in or against the direction of the angular momentum transferred by a polarized neutron).

The search for the effect was conducted during 48 hours with a polarized beam and 12 hours with a non-polarized beam (measurements of zero-effect). The statistical accuracy achieved was of the order of 2-5x10^{-3} (depending on the detector), which was not enough to observe the desired effect. Nevertheless, the experiment has demonstrated a principal possibility to measure such an effect with the POLI instrument with the required accuracy of better than 10^{-3}. The adjustment of the equipment, as well as the check of the background conditions and the rate of statistics collection have been carried out. On the basis of the results of this experiment, a new proposal to the POLI instrument for a longer beam time has been submitted and approved by the Program Committee. In 2016, a new experiment is planned, in which we expect to observe the effect or determine its upper limit with the accuracy comparable to that obtained on the cold neutron beam.

Measurement of the angular distribution of γ-rays with an energy of 4.43 MeV produced in the inelastic scattering of neutrons with an energy of 14.1 MeV by carbon

One of the first experiments planned in the framework of the project «TANGRA» (TAgged Neutrons and Gamma RAys), is the measurement of angular correlations of γ-rays and neutrons produced in the reaction of inelastic scattering of neutrons with an energy of 14.1 MeV by carbon nuclei:

$$^{12}C(n,n')^{12}C^{*}\xrightarrow{\gamma}{}^{12}C$$

The result of this experiment will make it possible not only to make a correct comparison with the experimental data obtained earlier in the experiments studying the characteristics of the reaction and significantly differing among themselves, but also to obtain information on the mechanism of inelastic scattering of fast neutrons by carbon nuclei. It should be noted that in the framework of the project «TANGRA» it is planned to carry out a series of experiments for a detailed study of the inelastic scattering of fast neutrons by ^{12}C, ^{14}N, ^{16}O, ^{27}Al, ^{56}Fe, ^{37}Cl, ^{32}P and other nuclei using the tagged neutron method (TNM).

In addition, the interest in the study of these reactions is dictated by the need to address many applied problems basing on the use of TNM and connected with mineralogy and geology of the Earth, determination of the elemental composition of rocks, as well as with the creation of algorithms and devices for detection of hidden dangerous substances (explosives, narcotic and highly toxic substances).

A schematic of the experimental setup is presented in **Fig. 7a**, and its general view is given in **Fig. 7b**.

As a source of neutrons with an energy of 14.1 MeV, we used a portable neutron generator ING-27 developed and manufactured at the *N.L.Dukhov* All-Russia Research Institute of Automatics (VNIIA). To form a tagged neutron flux, the generator comprises a built-in silicon double-sided strip detector that consists of 8 mutually perpendicular strips on each side forming an 8x8 matrix of 4x4 mm^2 pixels. The total active area of the 64-element α-detector is 32x32 mm^2. The alpha-detector is located 62 mm away from the tritium target of the neutron generator and intended to detect α-particles with an energy of 3.5 MeV produced in the reaction $d+t\rightarrow\alpha(3.5\,\text{МэВ})+n(14.1\,\text{МэВ})$.

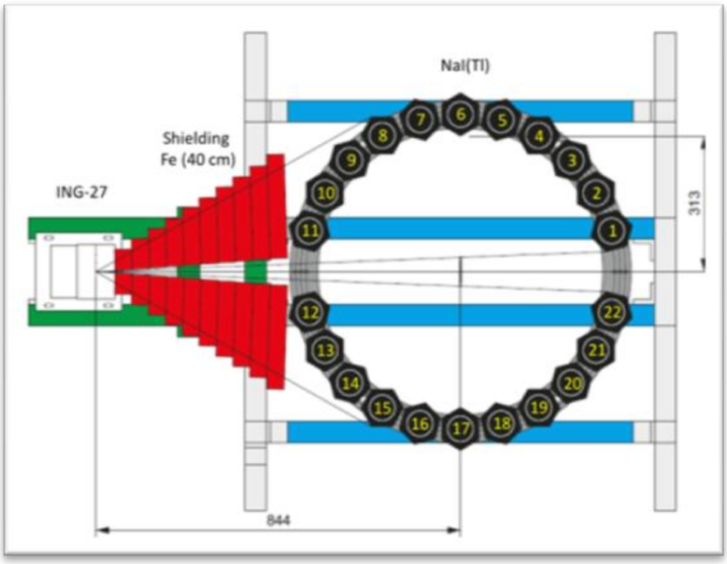

a) b)

***Fig. 7. a)**. A schematic of the experimental setup; **b)** A general view of the setup.*

Twenty two detectors of γ-rays on the basis of NaI(Tl) crystals shaped as hexahedrons (distance between the crystal faces – 85 mm, the crystal height – 200 mm) were used as detectors of characteristic nuclear γ-radiation with an energy of 4.43 MeV from carbon. The γ-ray detectors were arranged perpendicularly to the horizontal plane in a circle of radius of 370 mm with a carbon target placed in its center. The angle between the axes of two adjacent NaI(Tl) crystals in the horizontal plane was 15º.

In the experiment, for each detector the number of detected events corresponding to the total absorption peaks for gamma-rays with an energy of 4.43 MeV (detected in coincidence with the central pixel of alpha-detector) was determined. Then, the obtained number of events was averaged for each pair of γ-detectors located symmetrically at a specified polar angle relative to the axis of the central tagged neutron beam.

To describe quantitatively the anisotropy of the angular distribution for γ-rays generated in the inelastic scattering reaction, the anisotropy parameter W is used. It is defined as the ratio of the number of events detected by the detector positioned at an angle θ to the number of events detected by the detector positioned at an angle of 90º:

$$W(\theta) = 1 + a\cos^2\theta - b\cos^4\theta .$$

Figure 8 shows the anisotropy parameter for γ-rays generated in the course of the reaction of inelastic neutron scattering from carbon as a function of the polar angle obtained from the experimental data processing. The errors in the angle (angular resolution of the detector) were obtained by the Monte Carlo simulations using the Geant4 package. The obtained angular dependence can be described using the above formula with the parameters $a = 2.47 \pm 0.10$ and $b = 2.04 \pm 0.12$. The Figure also shows a comparison with the experimental data obtained in other studies and a theoretical curve from the ENDF/B-VII.1 library.

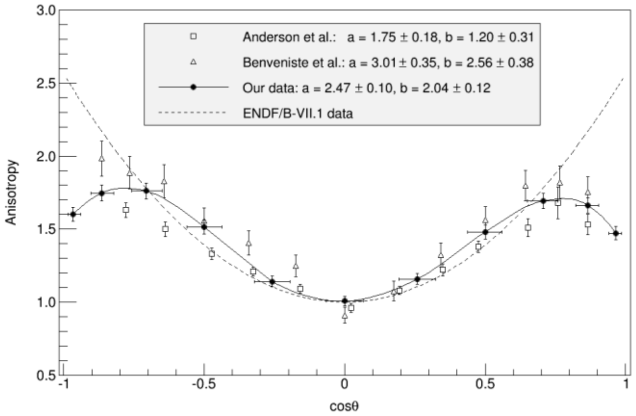

***Fig. 8**. Angular dependence obtained from the experimental data in comparison with the evaluated and other experimental data.*

Investigations of (n,p), (n,α) reactions

The experimental and theoretical investigations of the (neutron, charged particle) reactions induced by fast neutrons have been conducted. The experiments were carried out at the Van de Graaf accelerators EG-5 in FLNP JINR and EG-4.5 of the ***Institute of Heavy Ion*** Physics of Peking ***University***. Data on the neutron reactions with the emission of charged particles induced by fast neutrons are of much interest for studying the mechanisms of nuclear reactions and atomic nuclear structure as well as in choosing engineering materials and in performing calculations in the development of new facilities for nuclear power engineering.

In 2015, the data treatment for the measurements of the $^{40}Ca(n,\alpha)^{37}Ar$ and $^{54,56,nat}Fe(n,\alpha)$ reactions was completed; the results were published [1,2]. Taking into account the results of the previous study on ^{57}Fe, a full cycle of measurements for this element in the neutron energy range of 4-6.5 MeV has been completed.

Cross sections of the $^{56}Fe(n,\alpha)^{53}Cr$ and Fe54(n,α)Cr51 reactions were measured in several experiments at E_n = 5.5 и 6.5 MeV and E_n = 4.0, 4.5, 5.5, и 6.5 MeV, respectively (**Fig. 9** and **10**). The results are in agreement with the calculations using the TALYS-1.6 code.

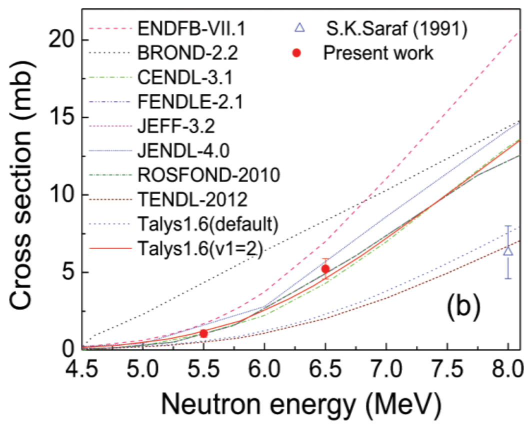

***Fig. 9**. Cross sections of the $^{56}Fe(n,\alpha)^{53}Cr$ reaction in comparison with those from the existing experiments and estimations for neutron energies from 4.5 to 8.0 MeV.*

For the $^{56}Fe(n,\alpha)^{53}Cr$ reaction, there are only two measurements with large uncertainties, which are in significant disagreement with the estimates of the libraries. These experimental data are supported by such libraries as JENDL-4.0, JEFF-3.2, FENDLE-2.1 and CENDL-3.1. The obtained results are useful both for revision of nuclear data libraries and testing nuclear models and practical applications. Measurements of these reactions are planned to be performed at neutron energies above 7 MeV.

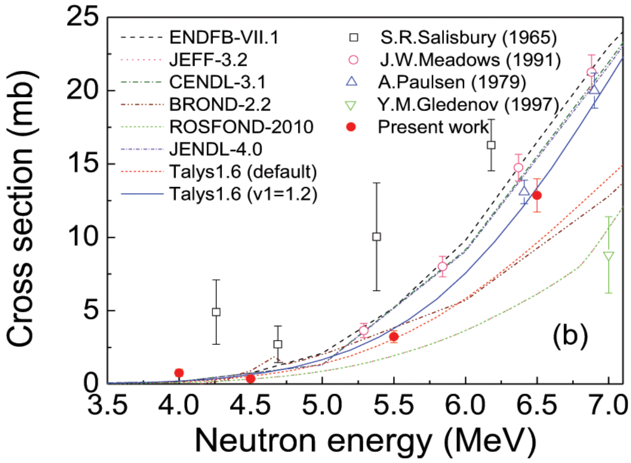

***Fig. 10**. Cross sections of the $^{54}Fe(n,\alpha)^{51}Cr$ reaction in comparison with those from the existing experiments and estimations for neutron energies from 3.5 to 7.0 MeV.*

The measurements of the (n,α) reaction on ^{144}Nd and ^{91}Zr isotopes at an energy of 5.0 - 6.5 MeV have been conducted, the data treatment is in progress.

The cross sections and angular distributions of the (n,α) reaction for the nuclei of medium atomic weights have been analyzed. Calculations using the TALYS-1.6 computer code have been done and compared with our data, other existing experimental data and estimates of various libraries for 11 isotopes from ^{39}K to ^{95}Mo.

The development of a PIXIE-4-based electronic system of acquisition and storage of multidimensional data from an alpha-spectrometer has been completed and tests have been carried out on a fast neutron beam.

Investigations of nuclear structure

An experimental study of the dynamics of the superfluid state of nuclear matter in excited nuclei requires the simultaneous determination of both the density levels and the partial widths of the emission of nuclear reaction products [3] in the entire range of excitation energies. In practice, this condition can be realized only in the measurement of the intensities of two-step cascades between compound states and several low-lying levels. The data are represented as the convolution of energy dependencies of the level density $\rho(E_{ex})$ and radiation widths $\Gamma(E_\gamma)$ (E_{ex} is the excitation energy, E_γ is the gamma-ray energy). In practice, ρ and T should be specified as functional dependencies with a minimum number of free parameters.

The intensities $I_{\gamma\gamma}(E_1)$ of two-step cascades were measured for 43 nuclei of different parities: even-odd nuclei ^{71}Ge, ^{125}Te, ^{137}Ba, ^{139}Ba, ^{163}Dy, ^{165}Dy, ^{181}Hf, ^{183}W, ^{185}W, ^{187}W, ^{191}Os, ^{193}Os, even-even nuclei ^{74}Ge, ^{114}Cd, ^{118}Sn, ^{124}Te, ^{138}Ba, ^{150}Sm, ^{156}Gd, ^{158}Gd, ^{164}Dy, ^{168}Er, ^{174}Yb, ^{184}W, ^{188}Os, ^{190}Os, ^{196}Pt, ^{200}Hg and odd-odd nuclei ^{28}Al, ^{40}K, ^{52}V, ^{60}Co, ^{64}Cu, ^{128}I, ^{140}La, ^{160}Tb, ^{166}Ho, ^{170}Tm, ^{176}Lu, ^{177}Lu, ^{182}Ta, ^{192}Ir, и ^{198}Au.

Figure 11 shows the relationships U_l/Δ_0 (l = 2, 3) and B_n/Δ_0. It can be seen that the points in the mass region 150<A<190 (region of deformed nuclei) are significantly lower than the others. The model parameters U_l are determined with an accuracy allowing one to notice the difference for nuclei with different parities of neutrons and protons. As can be seen from the figure, the threshold for the breaking of the third Cooper pairs of nucleons outside the specified mass range approximately corresponds to the neutron binding energy (for spherical nuclei it is the lower bound estimate of the U_3 parameter), and for deformed nuclei the U_3 parameter is half as much. Thus, the main result of the analysis is the statement that the thresholds for the breaking of Cooper pairs have larger values for spherical nuclei than for deformed ones.

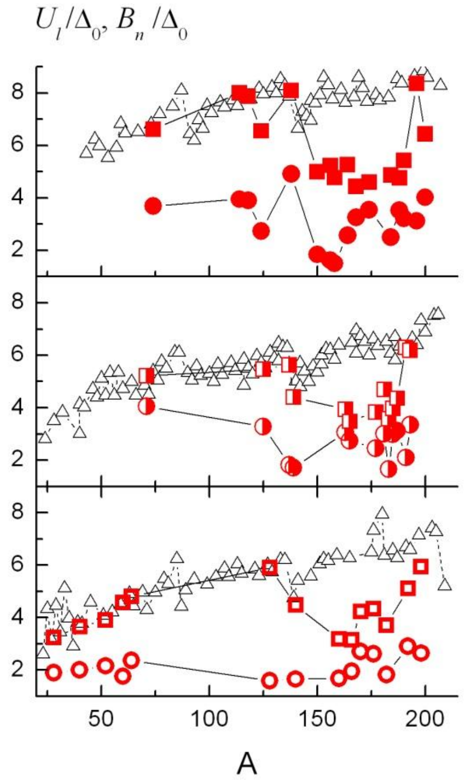

***Fig. 11**. The dependence of the threshold for the breaking of the second (circles) and third (squares) Cooper pairs U on the mass number A. Solid circles are even-even compound nuclei, half-open circles indicate even-odd ones and open circles represent odd-odd compound nuclei. Triangles stand for the mass dependence of the ratio B_n/Δ_0 of the neutron binding energy to the average value of the coupling energy of the last neutron in the nucleus with the same nucleon parity.*

Calibration of the "DEMON" neutron detector on a beam of the Nuclotron accelerator

A large neutron detector "Demon" based on liquid scintillator NE-213 (diameter – 16 cm, length – 20 cm) was used in the measurements of leakage neutron spectra on the "Quinta" setup in the framework of the "Energy+Transmutation" collaboration. The main feature of this detector is its ability to separate signals from neutrons (recoil protons produced as a result of the elastic scattering of neutrons by protons) and γ-rays by a pulse shape. In the experiments with "Quinta" instrumental spectra of leakage neutrons have been obtained, but to obtain the energy spectra, the calibration of the detector response function at different neutron energies is required. Experiments at the Nuclotron allow one to determine the response function with reasonable accuracy using the time-of-flight method to select neutrons of required energies. For this purpose it is necessary to have a start detector in the direct beam of the Nuclotron capable of detecting single signals from the beam particles, a neutron-producing target installed immediately after the start detector, "Demon" installed on the flight path which is sufficient to determine the neutron energy with reasonable accuracy (5-10 m) and a veto detector placed in front of it to eliminate charged particle events. **Figure 12** presents a schematic of the experimental setup.

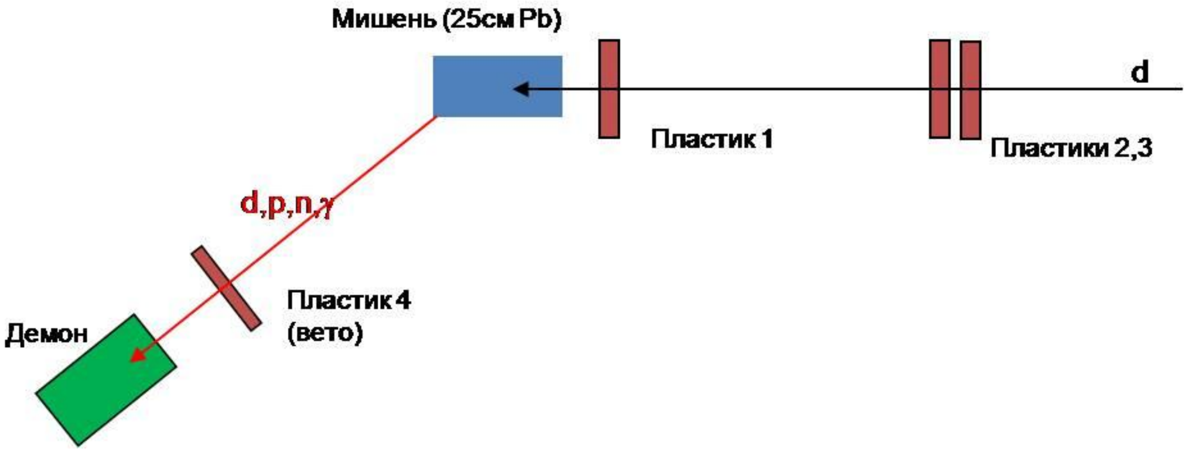

Fig. 12. A schematic of the experimental setup.

Plastic-1 served as the main start detector installed directly in front of the target (25-cm-thick lead). Plastics-2,3 were included in the coincedence circuit and served to eliminate background events in plastic-1. Plastic-4 was included in the anti-coincidence circuit as a veto detector. The distance from the target to the front wall of the "Demon"detector was 520 cm.

The signals in the "Demon" detector were separated by the time of release into two groups: light group containing mainly gamma-rays and light particles (electrons, muons) and heavy group containing signals from neutrons (recoil protons), as well as heavy charged particles (protons, deuterons) from the target. **Figure 13** shows the TOF spectra for these two components, as well as the second (neutron) component from the veto detector rejecting charged particles.

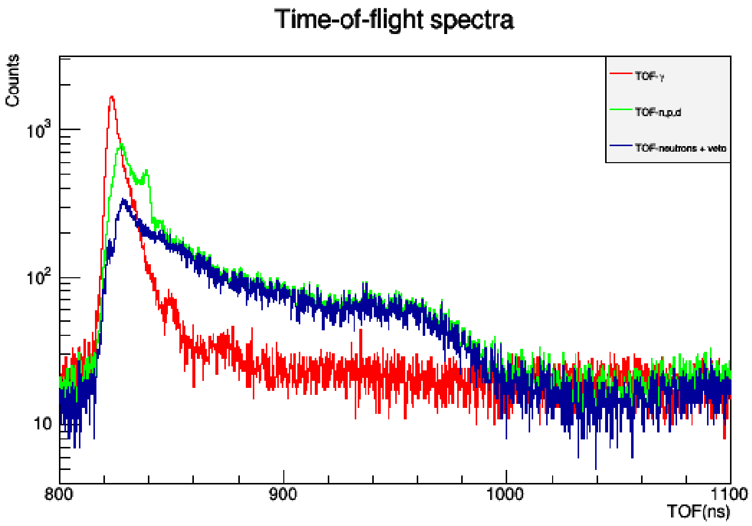

Fig. 13. TOF spectra of gamma-rays (red), neutrons and charged particles (green) and neutrons (blue). The zero (start) time corresponds to channel 806 ns.

To obtain the response functions for neutrons of various energies, the TOF neutron spectrum (blue curve in **Fig. 14**) was divided into intervals corresponding to specified average neutron energies (see **Fig. 14**).

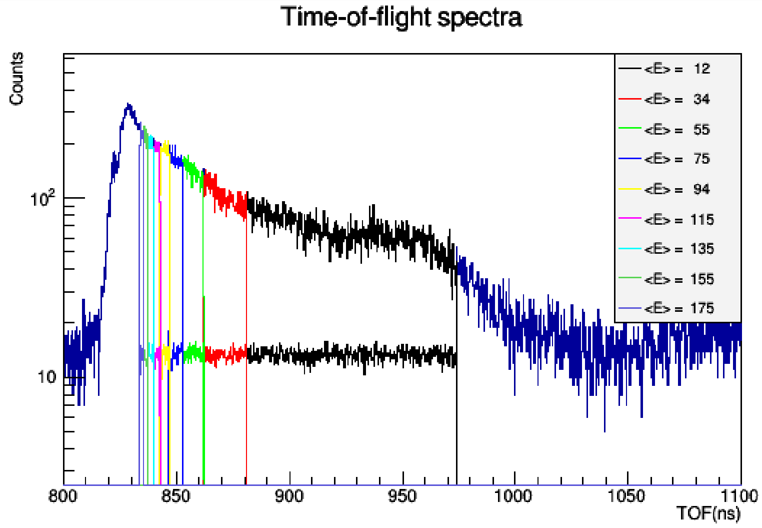

***Fig. 14**. Partition of the TOF neutron spectrum into energy intervals. Horizontal spectra below show the background level found to be at the level of random coincidences.*

For these intervals the obtained instrumental spectra of the "Demon" detector approximate to a certain degree the detector response functions for the neutrons of corresponding energies. A correction for the background of random coincidences was made by subtracting a "random" detector response function normalized to the contribution of the background of random coincidences in each energy interval. The resulting response functions for the indicated medium-energy neutrons are given in **Fig. 15**.

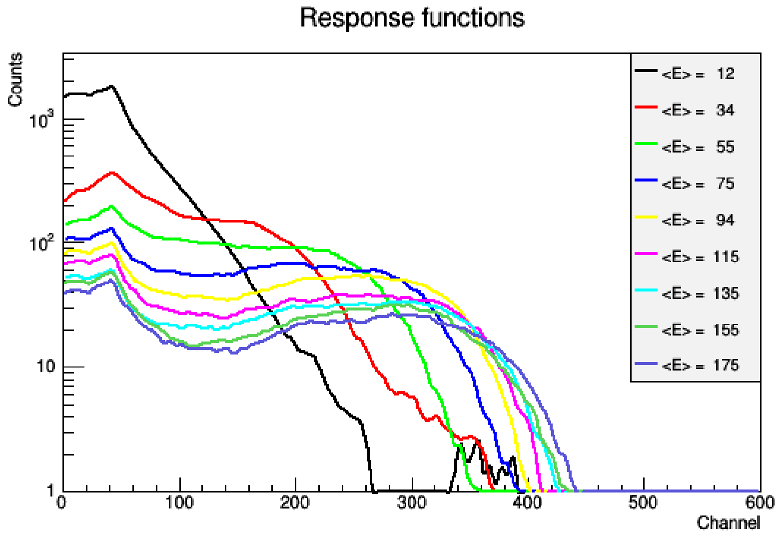

***Fig. 15**. Response functions of the "DEMON" detector for different neutron energies.*

On the whole, the experiment has shown a principal possibility for this type of calibration to be carried out on the Nuclotron beam. Despite the presence of overlaps in the start plastic detector they could be eliminated with a sufficiently high degree of reliability by analyzing the digitized signals from the plastic detector. The obtained response functions have poor statistical accuracy, yet they appear to be sufficient for qualitative analysis of the data obtained by "Quinta".

Measurement of P-odd asymmetry in the emission of α-particles in the reaction $^{10}B(n,\alpha)^7Li$ with cold polarized neutrons

An experiment to measure P-odd correlations of the ($\sigma_n p_\alpha$) type, where σ_n is the neutron spin, p_α is the momentum of the emitted α-particle in the $^{10}B(n,\alpha)^7Li$ reaction, has been started on a cold polarized neutron beam of the PF1B instrument at the ILL reactor (Grenoble, France). The experiment is carried out in the framework of the search for neutral currents in electroweak hadron interactions conserving strangeness. A 48-section ionization chamber is used as a neutron detector (**Fig. 16**). The events are detected using the current method with the compensation of reactor power fluctuations and false effects [4]. According to the theoretical estimates [5] the expected effect does not exceed several units of 10^{-8}. For 7.5 days of the experiment the value of $A_\alpha = (-4.0 \pm 5.6)\times10^{-8}$ has been obtained (**Fig. 17**) basing on the raw data treatment (without corrections for the background, degree of polarization and the average value of the cosine of the detection solid angle). The experiment will be continued in 2016.

Fig. 16. Multisection ionization chamber before final assembly and installation on the beam (left).

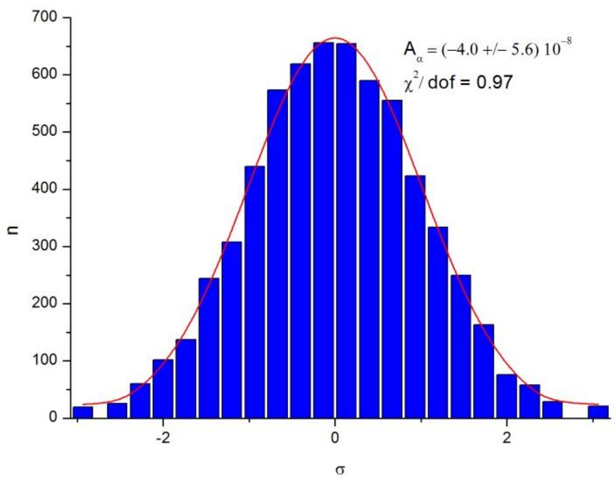

Fig. 17. Histogram of experimental values and a comparison with the normal distribution (right).

Investigations of UCN interaction with the surface of Fomblin oil

The interaction of UCN with the surface of hydrogen-free Fomblin oil has been experimentally studied. The experiments have been carried out on the GRANIT spectrometer, which allows simultaneous measurements of the UCN loss factor during the interaction with the surface of a substance (η), and the probability of quasi-elastic scattering of UCN (P_{VUCN}) at various temperatures. Measurements were carried out for three types of Fomblin oil with different molecular weights of 6500, 3300, 2800 amu. The results of the measurements are presented in **Fig. 18**.

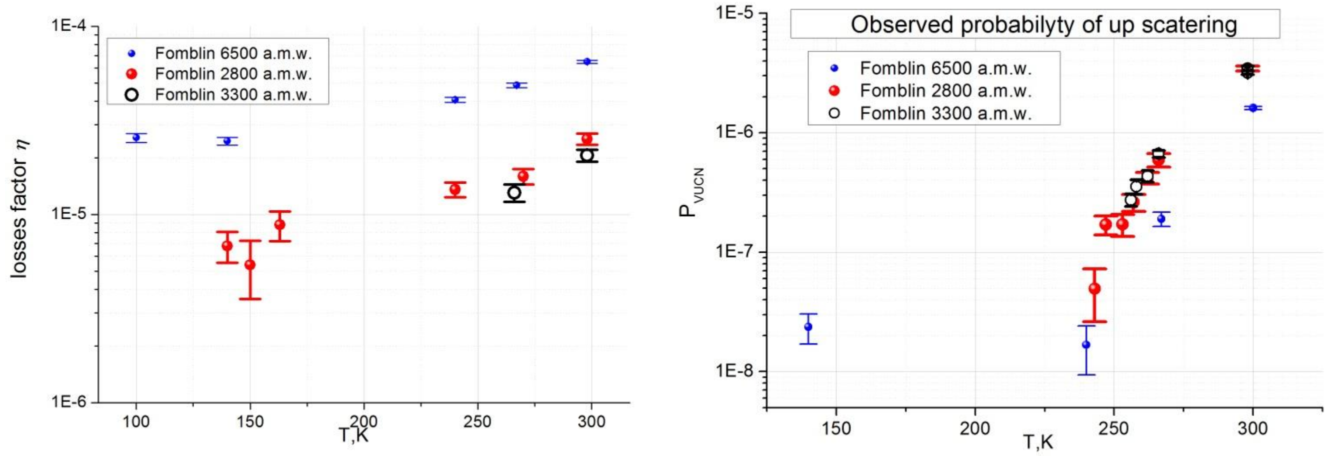

***Fig. 18**. Results of the measurements of the UCN loss factor (η) during the interaction with the surface of the substance, and the probability of quasi-elastic scattering of UCN (P_{VUCN}).*

These measurements had two objectives. One was to study the process of quasi-elastic scattering of UCN from the surface of hydrogen-free Fomblin oil. The results suggest that from the two existing hypotheses about the nature of quasi-elastic scattering of UCN — scattering from nanoparticles (nanodroplets) on the surface and scattering from surface capillary waves — the second hypothesis is apparently most reliable.

Another objective concerned the choice of material for the walls of the UCN storage volume in the framework of the preparation for an experiment on measuring the neutron lifetime. The required material should have the lowest η and P_{VUCN}.

The measurements have shown that for all the samples under study the probability of quasi-elastic scattering becomes less than the spectrometer sensitivity (10^{-8}) with decreasing temperature below the freezing point of the oil. At the same time, when the temperature is lowered below 150 K, there is a slight increase in P_{VUCN}, which is apparently due to the cracking of the hardened oil. Therefore, the optimum temperature of the UCN storage volume with the walls covered with Fomblin oil will be in the range of 150 - 200 K.

The smallest loss factor was obtained for the oil with a molecular weight of 3300 amu; therefore this oil is the best candidate for covering walls of the UCN storage volume.

Calculations of a UCN source of a new type at an external beam of thermal neutrons

A detailed calculation of the parameters of a UCN source of a new type has been conducted, which is based on a new method for production of ultracold neutrons in a helium source. The principal idea of the method presented for the first time in [6] consists in installing a helium UCN source into a thermal neutron beam and in surrounding it with a moderator/reflector, which is a source of cold neutrons needed to produce UCN. At the same time, the flux of cold neutrons in the source could be several times greater than the flux of incident neutrons due to their numerous reflections from the moderator/reflector.

The source of this type should be installed close to the reactor biological shielding. **Figure 19** presents the layout of the source on one of the beamlines of the PIK reactor.

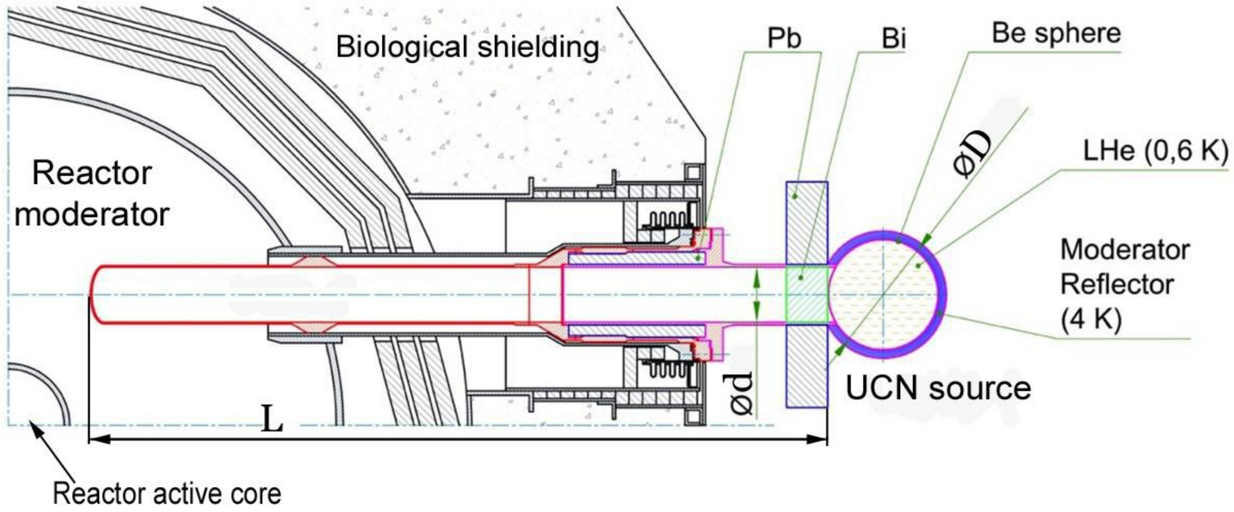

***Fig. 19**. A possible layout of the UCN source on one of the thermal neutron beamlines of the PIK reactor.*

Calculations of the parameters of the source with a moderator/reflector of solid methane and liquid deuterium have been performed.

These calculations have shown that the installation of such a UCN source with a methane moderator on a thermal neutron beamline of the PIK reactor allows achieving the UCN density of $\sim 1 \cdot 10^5$ cm^{-3} in the source with the production rate of $\sim 2 \cdot 10^7$ s^{-1}, which is, respectively, a factor of 1000 and 20 higher than those that can be provided by the most intensive UCN source available today. At the same time the UCN density in the source with a deuterium moderator can be $\sim 2 \cdot 10^5$ cm^{-3} with the production rate of the source of $\sim 8 \cdot 10^7$ s^{-1}.

Calculations of the heat release in the UCN source have also been performed demonstrating that with achieving the above parameters, the heat release power will be in the range of 1-2 W, which makes it possible to realize the proposed concept of the source in practice.

Neutron diffraction from a moving grating

The results obtained in the experiment in 2014 (November-December) have been analyzed. In that experiment time-of-flight spectra of UCN that passed through a rotating phase diffraction grating were obtained using the Fourier spectroscopy method (**Fig. 20**). The method for the first time made it possible to carry out measurements for a wide range of the resulting neutron energy, 60÷250 neV, which allowed us to simultaneously observe the lines corresponding to five diffraction orders. The spectra were obtained for three velocities of the grating. The profile of the grating was analyzed using an atomic force microscope (**Fig. 21**).

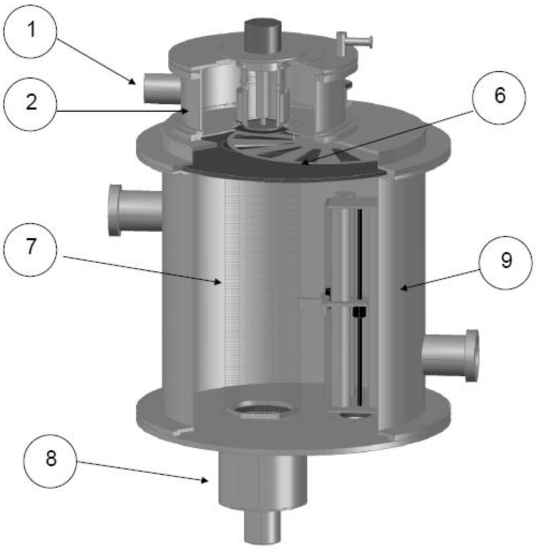

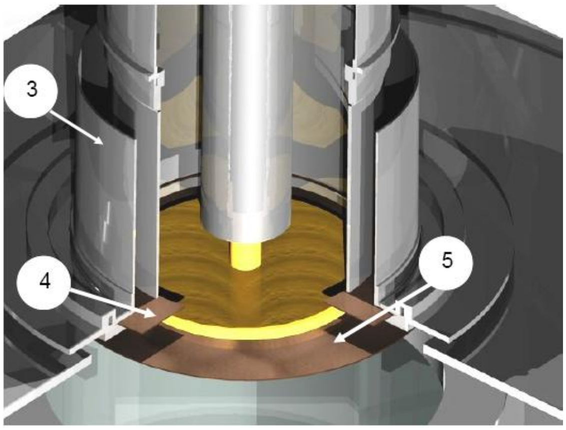

Fig. 20. *TOF Fourier spectrometer: general view (left) and its upper part (right): 1 – inlet neutron guide, 2 – inlet chamber, 3 – annular corridor, 4 – filter-monochromator, 5 – grating, 6 – rotor of Fourier chopper 7 – vertical glass neutron guide, 8 – detector, 9 – vacuum chamber.*

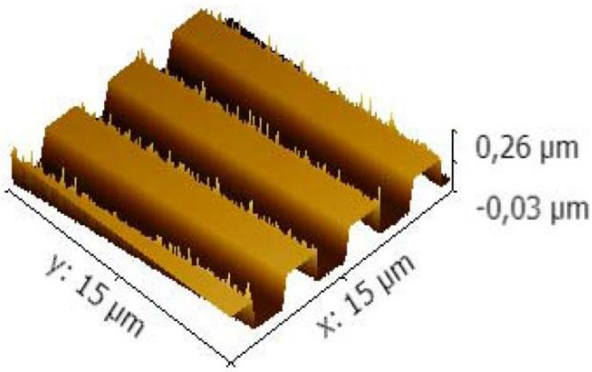

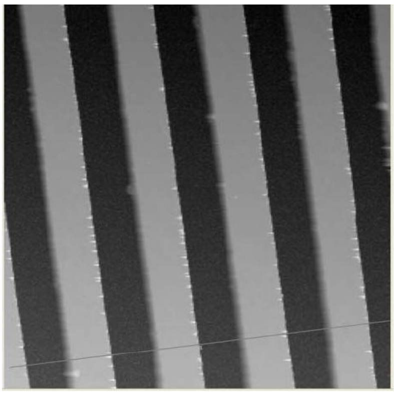

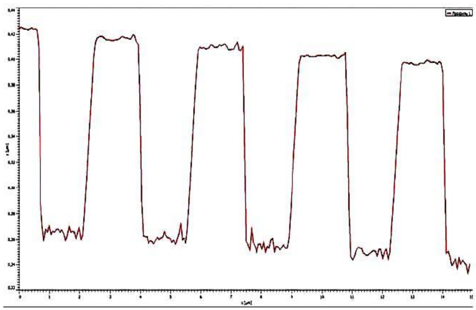

Fig. 21. *3D image of a fragment of the grating obtained using an atomic force microscope (top left), 2D image of a fragment of the grating (top right) and its profile (bottom).*

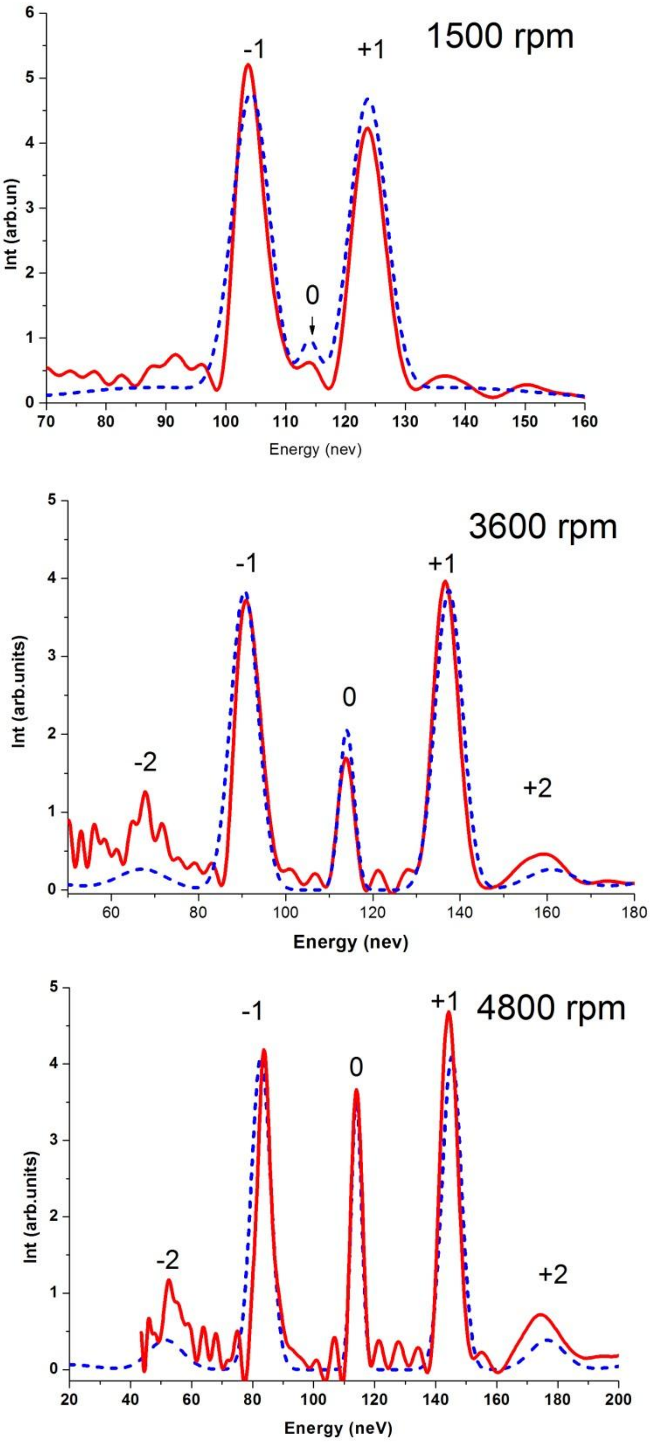

Fig. 22. *Experimental (red solid line) and theoretical (blue dotted line) spectra of neutrons resulting from the diffraction by a moving grating for three rotation frequencies of the latter.*

The theoretical calculation of the diffraction pattern for a specified initial neutron energy distribution, velocity of the grating and its measured profile was performed by numerically solving the system of equations obtained in the framework of the multi-wave theory of dynamical diffraction in the approximation of slowly varying amplitudes. The experimental TOF spectra were compared with the theory after conversion to the energy scale taking into account the transformation of the spectrum due to the Earth's gravity. The experimental and theoretical results are presented in **Fig. 22**. It can be seen that the data are in good agreement with the theoretical predictions.

Improvement of the TOF Fourier spectrometer of UCN

To increase the luminosity of the Fourier spectrometer, a search for other possibilities of forming the initial spectrum of UCN free of the very cold neutron background has been undertaken. As an alternative to the flow-type UCN storage chamber used previously, a system of two total reflection mirrors has been proposed. A preliminary study of the properties of this system was carried out by the MC simulation using the Geant4-UCN package. On the basis of the results of the calculation a full-scale prototype of a spectrum formation unit (**Fig. 23**) has been produced. Its efficiency was checked in a test experiment on a UCN beam at ILL in October 2015.

Fig. 23. *Sectional view of a spectrum formation unit of the spectrometer (left) and a frame with mirrors (right). 1 – vacuum chamber, 2 – frame with mirrors, 3 – mirrors 1 and 2.*

Measurements were performed with silicon, glass, and sapphire mirrors. The best results were obtained with glass mirrors. It has been shown that the use of the specified inlet chamber makes it possible to achieve a gain in the counting rate by a factor of 6-7 with a satisfactory effect/background ratio.

Preparation of an experiment on the observation of interaction of UCN with an oscillating barrier at giant accelerations

The purpose of the planned experiment is the verification of the validity of the effective potential model at giant accelerations of the sample. An important stage in the preparation of the experiment is a quantum calculation of the interaction of a neutron wave packet with a potential structure oscillating in the space for different values of the maximum acceleration of the object $w_{max} = A(2\pi f)^2$, where A and f are the amplitude and frequency of vibration, respectively. In the case of the oscillating potential barrier, the calculations have shown that for the values of interest $w_{max} \approx 10^8$ cm/s^2 the observed non-stationary effects are rather small. In the case of the vibrating resonant structure defined as two barriers and a well in between, the calculations have shown that there is a noticeable oscillation in the count rate for a wide range of amplitudes and frequencies in the transmitted state. This geometry has been selected as the main one for further research. Possible approaches to carry out the experiment to test the effective potential model at giant accelerations of a sample have been considered.

A new approach to the experiment to test the weak equivalence principle for the neutron

A new approach to the experiment testing the weak equivalence principle for the neutron has been proposed. It is suggested that in an experiment on the observation of the neutron free fall a fall time is measured for several lines of the spectrum obtained by diffraction from a moving grating. This approach requires only the knowledge of the value for the quantum splitting of the spectrum $\Delta E = 2\pi\hbar\left(V/d\right)$, where V and d are the velocity and period of the grating, respectively. The knowledge of the absolute energy or geometric parameters of the setup is not necessary.

Theoretical investigations

Quantum mechanics

As a result of theoretical research in the field of quantum mechanics, it has been discovered that a continuous spectrum of singular bound states of electrons can exist in atoms. In these states, with a probability of ~ 10^{-6} the screening of the Coulomb field is possible at distances of the order of the nuclear radius. In case of hydrogen or deuterium, such screening leads to the formation of a neutral particle that can participate in nuclear fusion reactions with other nuclei at moderate temperatures. In particular, this allows one to explain the star ignition mechanism with increasing density due to the gravity. Another achievement is the formulation of a new Bell inequality in the field of the EPR paradox. New inequality makes it possible to check out the particle states in one measurement. Namely, the question is, if a source radiates a pair of similar particles, then whether individual particles are emitted or the particles are emitted in a mixed state, which transforms into individual particles only after measurements. Previous approaches to answer this question required minimum four measurements, and no indisputable result has yet been obtained.

Electroweak interactions

The effective lagrangian describing electroweak hadron transitions has been investigated [7]. On the basis of the general principles of global and local symmetries the effective pion-nucleon lagrangian, essentially non-linear in a pion field, has been developed to describe the low-energy electroweak hadron interactions with strangeness conservation. We encounter no divergence summarizing properly all the infinite power series in a pion field which occur in the course of the treatment. The used consistent approach can be applied to consider the pion-nucleon interactions with the spatial parity violation.

3. Methodological and applied research

Methodological investigations at the IREN facility

Since one of the possibilities to increase the neutron yield at the IREN facility is the replacement of a tungsten neutron production target with a target of natural uranium, measurements with a uranium target prototype and comparison of yields have been performed. The comparison has been made using the yield of the (n,γ) reaction in resonances of Ta in the energy range of ~ 4-1200 eV. The events have been detected by a large 6-section liquid scintillation detector [8] at a 60-m flight path. The detection mode for the multiplicity of γ-rays in the neutron capture (simultaneous response of the sections) was $m \geq 2$. The sample was a Ta-foil (thickness 0.11 mm, size 12.2 x 15.4 cm and weight 34.06 g). The results of the measurements and analysis are shown in **Fig. 24**. The spectra in the top figure are normalized to the acquisition time of 8 h 50 min (acquisition time for the tungsten target). The accelerator parameters were about the same for both measurements: electron current in a pulse – 1.2-1.5 A; repetition frequency – 20 Hz. The experimental data have also been normalized to the average values of the electron current. The bottom figure demonstrates the yield ratios in the resonances compared with the yields calculated using the GEANT and FLUKA programs. The experimental and calculated values are R_{exp} = 2.57 ± 0.12; R_{GEANT} = 3.05; R_{FLUKA} = 1.39.

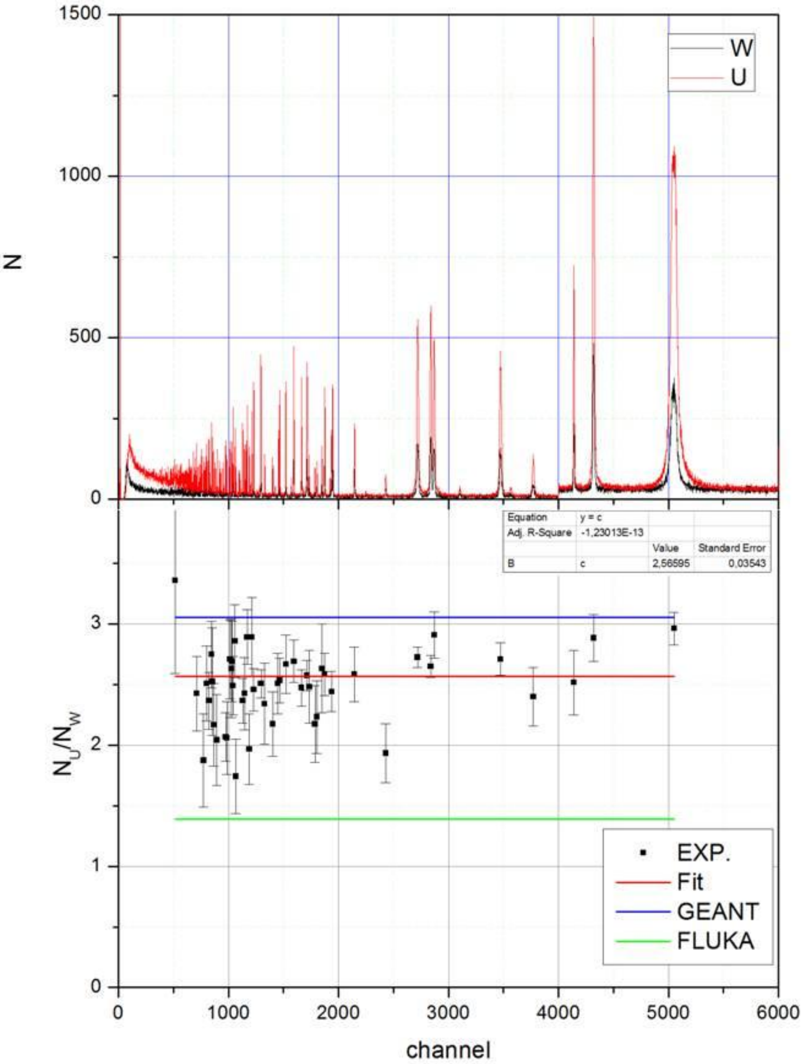

Fig. 24. At the top - TOF spectra of the Ta(n,γ) reaction normalized to the same acquisition time for tungsten (black line) and uranium (red line) targets. At the bottom – yield ratios: points – experimental data; red line – the average over the experimental data; blue line – calculations by GEANT; green line – calculations by FLUKA.

Analytical investigations on charged particle beams of the EG-5 accelerator

Experiments with the beams of charged particles employing analytical techniques of the Rutherford back scattering and recoil detection analysis were regularly carried out throughout the year. The elemental depth profiles in the samples used to study structural characteristics of epitaxial films have been measured. The effect of neutron and Xe-ion irradiation on the properties of SiC films synthesized by different technologies of the plasma-chemical vapor deposition has been investigated.

Also, the temperature-induced growth of oxide films on a steel surface and the effect of annealing on the structure and optical properties of TiO_2 films deposited on silicon substrates have been studied.

Using the recoil detection method the accumulation/redistribution of hydrogen and deuterium in an assembly of two (Ni, Ti and Zr) high-purity foils after exposure to pulsed fluxes of high-temperature deuterium plasma at the "Plasma Focus" (PF-4) setup has been studied. It has been found that when exposed to pulsed fluxes of high-temperature plasma the assemblies of the studied foils show the redistribution of the implanted deuterium and gas impurities of hydrogen to great depths far exceeding deuterium ion flight paths.

As a result of the studies of the effect of proton irradiation (energy 2.5 MeV) on the critical current and critical temperature of 2-G composite HTSC tapes, the radiation resistance values: $2x10^{16}$ rad/cm^2 for YBCO (123) and $6x10^{16}$ rad/cm^2 for GdBCO (123) have been obtained. These values have been determined from the analysis of the critical current degradation, which is accompanied only by slight decrease in the critical temperature. A strong influence of proton irradiation on the critical current at a temperature of 770 K in its own field has been revealed for conductive tapes of these two compositions.

In 2015, the EG-5 accelerator was in operation for experiments for 510 h.

Analytical investigations at the IBR-2 reactor

In 2015, at the REGATA facility a multielement instrumental neutron activation analysis of ~ 2600 ecological samples (vegetation, soil, air filters), as well as a number of technological, biological and archaeological specimens and samples of extraterrestrial origin has been performed in the framework of the programs and grants of JINR Member States and Protocols of Cooperation with JINR Non-Member States. Investigations of test samples have been conducted for an interlaboratory comparison of the results under the IAEA program.

Development of the NAA&AR Sector experimental base

In the reporting period in the NAA&AR Sector the development of a software package for complex automation of multielement neutron activation analysis (NAA) at the IBR-2 reactor [9] was continued; three automatic sample changers (SC) were installed and successfully operated to automate mass measurements of spectra of irradiated samples on three detectors. Two HPGe detectors (new and upgraded) have been put into operation. Work has started on the automation of sample irradiation procedure (replacement of sensors, electronics and software development). The activities on automation of NAA were conducted in the framework of the IAEA Coordinated Research Project «Development of an Integrated Approach to Routine Automation of Neutron Activation Analysis” (F1.20.25/CRP1888, Contract No. 17363).

A radiation monitoring system has been installed and put into service in the rooms of the REGATA facility.

The specialists from Intertech Corporation have completed the start-up and commissioning work on the iCE3500 atomic absorption spectrometer by Thermo Scientific and conducted personnel training.

Biomonitoring of air pollution

In 2015, the summing-up of the activities conducted in 2010-2011 in the framework of the international program "Heavy metal atmospheric deposition in Europe – estimations based on moss analysis" was done [10]. The long-term cooperation with the Slovak specialists in the field of biomonitoring atmospheric deposition of trace elements has found its reflection in the chapter of a book "Air Pollution" [11] as well as in the ISINN Proceedings [12, 13]. The analysis of moss-biomonitors from Belarus collected in 2014 on the territory of Minsk, Mogilev, Gomel and Vitebsk regions has been completed [14]. In the reporting period, two studies on data analysis of atmospheric deposition of heavy metals and other elements in Albania have been performed [15, 16]. In the framework of the Serbia-JINR Cooperation Program a comparative analysis of air pollution in the so-called "street canyons" in Moscow and Belgrade has been performed. The paper was submitted to the journal «*Environmental Monitoring and Assessment*». The NAA has been used to study the samples of mosses collected by teachers and pupils in the national parks of Poland in the framework of the Poland-JINR Cooperation Program. The preparation of a joint publication is in progress.

The study on the determination of concentrations of elements in mosses-biomonitors and soils collected in the area of the lead-zinc plant in Kardzhali (one of the most environmentally contaminated places in Bulgaria) has been completed [17, 18].

Biotechnologies

In 2014-2015, in collaboration with the biophysicists from the E.Andronikashvili Institute of Physics, I.Javakhishvili Tbilisi State University and I.Chavchavadze State ***University*** (***Tbilisi*****,** ***Georgia***) the studies were conducted on the development of methods for synthesis of silver and gold nanoparticles by new species of microorganisms – Archaea. The strain of thermo-acidophilic crenarchaeon *Sulfolobus islandicus* LAL14/1 provided by the Pasteur Institute (Paris, France) was used to obtain silver and gold nanoparticles at high temperatures (75 °C). In combination with a number of optical and analytical methods the neutron activation analysis at the IBR-2 reactor was used to characterize the processes of synthesis of gold and silver nanoparticles by the Archaea strain [19]. The interest in the ongoing studies is connected with both unique technological application possibilities of Archaea and almost complete lack of studies in this research area.

In collaboration with the A.N.Frumkin Institute of Physical Chemistry and Electrochemistry of RAS in the framework of the projects supported by RFBR (15-05-08919 and 15-33-20069) work has started to study the processes of accumulation and biosorption of metals (vanadium, chromium, uranium, lanthanum) from mono- and multicomponent systems by microalgae *Spirulina platensis* and bacteria *Pseudomonas putida*.

In cooperation with the University of Oulu, Finland, the application of NAA for analysis of pine sawdust used in wastewater treatment as a sorbent of metals has been studied [20].

In cooperation with the Institute of Microbiology and Biotechnology of ASM studies of biochemical changes in the main components of *Spirulina* biomass (proteins, carbohydrates, etc.) during the synthesis of silver nanoparticles by microalgae were conducted [21]. Work has started on the biosynthesis of selenium nanoparticles using *Spirulina platensis* and *Nostoc linckia* microalgae as a matrix. To understand the mechanisms of synthesis of metal nanoparticles and to determine their localization in the biomass, experiments have been performed to obtain silver nanoparticles on the fractions of proteins and polysaccharides extracted from the biomass of microalgae.

In 2015, the joint investigation carried out in cooperation with the biochemists from the Institute of Microbiology and Biotechnology of ASM was continued to study the process of removing toxic metals (chromium, nickel) from wastewater using microalgae *Spirulina platensis* [22].

Environmental assessment

In 2015, the NAA analysis of soils and bottom sediments from various regions of the Nile delta, along its riverbed and artificial canals performed in the framework of the joint JINR-Egypt project «Assessment of the environmental situation in the delta of the Nile River using nuclear and related analytical techniques» was completed. The obtained results have shown that the element composition of these samples is determined mainly by geochemical features of the region under study and is not affected by the anthropogenic load [23]. For the first time the NAA was applied to study the composition of the soil and sediment samples from the Siwa oasis in the Western Sahara desert, the obtained results have provided new information about this unique oasis [24].

In collaboration with the University in Stellenbosch, South Africa, complex investigations of air pollution using mosses and lichens were continued. In the framework of the project "Mollusks as Biomonitors of Water Ecosystems in the Republic of South Africa" the stage of the work on the analysis of soft tissues and shells of the Saldanha and Danger bays in the Atlantic Ocean, West Coast of South Africa has been completed [25].

In order to assess the state of the Crimea coastal ecosystem, the analysis of the samples of macroalgae-biomonitors (red, green and brown) collected in the coastal zone of the Black Sea has been completed in collaboration with the A.O.Kovalevsky Institute of Marine Biological Research (Sevastopol). The algae-concentrators of specific groups of elements including halogens were revealed and the cleanest water areas of the coastal zone of the Crimea were found [26]. The study of the seasonal variation of concentrations of 46 elements in the phytoplankton of the Black Sea has been completed. The effect of the elemental composition on the biophysical parameters of the functional activity of phytoplankton communities in the coastal areas has been assessed. The results have shown that phytoplankton can be successfully used as a biomonitor of water ecosystems [27].

In 2015, in cooperation with Moscow State University (Faculty of Biology) the investigation on the determination of the elemental composition of soil, bottom sediments, terrestrial and aquatic vegetation to assess the transport of pollutants in the strategically important areas of the Black Sea (coastal zone of Anapa, Novorossiysk and Tuapse) was completed [28] .

On the basis of the analysis of mosses-biomonitors and lichens, an important study has been performed on the impacts of an oil refinery and oil pipeline on the natural environment of the Yamal Peninsula. The assessment of the atmospheric deposition of toxic elements associated with the oil industry has shown no excess of the maximum allowable concentration of these elements [29].

Analysis of food products

The studies have been completed and a joint paper (in cooperation with the analytical center of the Geological Institute of RAS) on the application of nuclear-physical analytical methods for studying the intake of Cl, Br, I and Se in the human body with food, has been published in the leading American academic journal *Food and Nutrition Sciences* [30]. The results of a complex study using NAA, ICP-MS, AAS on the assessment of mercury content in diagnostic biomaterials of different population groups of urban areas in the Moscow region have been analyzed in cooperation with the analytical center of the Geological Institute of RAS and I.M.Sechenov First Moscow State Medical University [31].

Geology

The study performed in 2015 in the framework of the joint JINR-Romania project (University of Bucharest) on the geochemistry of loess samples of the Quaternary Period collected in the Dobrogea region (Romania) made it possible to obtain information about the climate of the Quaternary Period [32].

In cooperation with the Western Cape University (South Africa) the NAA study of new samples of coal fly ash from the Matla coal power station in the Mpumalanga province in South Africa was conducted. The data treatment is in progress.

Analysis of materials of extraterrestrial origin

In 2015, a study aimed at searching for cosmic dust in peat columns collected in Siberia in the area of the Tunguska meteorite fall was performed in cooperation with the Adam Mickiewicz University in Poznan, Poland. The age determination of peat column layers was carried out in Poland.

The data treatment has been completed; a paper is being prepared for publication. Using scanning electron microscopy and energy-dispersive X-ray spectroscopy (EDAX) moss samples collected in the Arctic (Northern Norway) and Antarctic (King George Island) have been analyzed. The particles detected by means of electron microscopy along with the results of the neutron activation analysis of samples allow us to make a conclusion about their origin, which will contribute to the development of criteria for identification of particles of extraterrestrial origin. A multielement analysis of meteorites of unknown nature received from Italy has been performed. The NAA results and the use of statistical methods of multielement analysis for their processing have made it possible to determine the type of the meteorite material: ferrous chondrites and carbonaceous chondrites. The results of the research were presented and discussed at the International Conference organized by LRB JINR "Modern Trends in Radiobiology and Astrobiology", October 28-30, 2015. Dubna [33].

Medicinal plants

In 2015, we continued investigations in a new promising line of research – determination of the elemental composition of plants used in medicine. These studies are conducted in cooperation with the specialists from Mongolia, Bulgaria, Poland [34] and starting from 2015 from China [35].

Materials science

In 2015, in the framework of the BRFBR-JINR joint grant and in cooperation with the Scientific and Practical ***Materials Research Center*** of the National Academy of Sciences of Belarus, the investigations of the crystallization processes and the characterization of artificial diamonds in the C-Mn-Ni-Fe system were conducted. In the course of the experiment diamond crystals were obtained in the Fe-Ni-C and Mn-Ni-C systems at a pressure of 5 GPa and a temperature of 1700 K. The use of NAA allowed us to study the impurity composition of the diamonds. Using electron microscopy the size and shape of the obtained crystals were determined. The results of the research were published [36, 37]. In 2014, a part of the experimental material was sent to the University of Galaţi, Romania, to perform X-ray diffraction and scanning electron microscopy analyses [38]. A joint project was continued aimed at studying phase formation processes and physical characteristics of the compounds in the Cu-Fe-S system at high pressures and temperatures. The NAA of 12 samples was performed and the results were forwarded to Minsk.

REFERENCES

[1] Han Jinhua, Liu Jiaming, Liu Xiang, Fan Xiao, Wang Zhiming, Chen Jinxiang, Zhang Guohui, Gledenov Yu.M., Sedysheva M.V., Krupa L., Khuukhenkhuu G., Szalanski P.J., Differential and angle-integrated cross sections for the ^{40}Ca(n,α)^{37}Ar reaction from 4.0 to 6.5 MeV". European Physical Journal, 2015, vol. 51:12, pp. 1-10.

[2] Wang Zhimin, Fan Xiao, Zhang Luyu, Bai Huaiyong, Chen Jinxiang, Zhang Guohui, Gledenov Yu. M., Sedysheva M. V., Krupa L., and Khuukhenkhuu G. Cross sections of the ^{56}Fe(n,α)^{53}Cr and ^{54}Fe(n,α)^{51}Cr reactions in the MeV region. Phys.Rev. C92, 044601, 1-7 (2015)

[3] Суховой А.М., Новая практическая модель каскадного гамма-распада нейтронного резонанса. Основные положения и достижимая точность ЯФ 2015, т. 78, 3-4, стр. 256-271.

[4] V. A. Vesna, et al. Phys. Rev C77 (2008) 035501

[5] Г. А. Лобов, Г. В. Данилян. Изв. АН СССР. Сер. Физ. 41 (1977) 1548

[6] E. V. Lychagin, A. Yu. Muzychka, G. V. Nekhaev, V. V. Nesvizhevsky, E. I. Sharapov, and A. V. Strelkov. http://www.hindawi.com/journals/ahep/2015/547620/. 2015.

[7] <arXiv:1511.04279>

[8] Малэцки Х., Пикельнер Л. Б., Родионов К. Г., Саламатин И. М., Шарапов Э. И., Детектор нейтронов и гамма-лучей для работ в области нейтронной спектроскопии. Сообщение ОИЯИ. 13-6609. Дубна, 1972.

[9] Pavlov S.S., Frontasyeva M.V., Dmitriev A.Yu.. Automation of reactor neutron activation analysis. The International Atomic Energy Agency's third Research Coordination Meeting on Development of an Integrated Approach to Routine Automation of NAA (CRP 1888), June 22-26, 2015, Vienna, Austria.

[10] Harmens H., Mills G., Hayes F., Sharps K., Frontasyeva M., Aboal J.R., Aherne J., Alber R., Alekseev A., Alonso R., Aleksiayenak Y., Anicic M., Balint A., Barandovski L., Baggard M., Bassin S., Batic F., Bender, T. Berg, V. Bermejo, O. Bethenod, O. Blum, S. Boltersdorf, K. Borowiak, S. Braun, A. Briolat, P. Büker, V. Calatayud, H. Cambridge J., Carballeira Ocaña A., Castell J.-F., Chaligava O., Chursin A., Cieslik S., Cinderby S., Cooper D., Coskun M., Cotrozzi L., Cucu-Man S. M., Dam M., Danielsson H., Davies B., Dott D., Dunaev A.M., Eler K., Emberson L., Ene A., Fares S., Fernández I.G., Fernández Escribano J. Á., Finco A., Fränzle S., Frolova M., Fuhrer J., Fumagalli I., Fusaro L., Galsomiès L., Garrec J.-P., Gerosa G., Gluschenko V., Godzik B., Goltsova N., Grünhage L., Hall J., Hoydal K., Ibrahimov Z., Infante Olarte M., Izquieta S., Jančík P., Jeran Z., Jones L., Kalabegeshvili T., Kapusta P., Karlsson G. P., Karlsson P. E., Kirkesali E., Koroleva Y., Kosior G., Krmar M., Krüger G., Kvietkus K., Kubin E.,. Las Heras R. T, Lazo P., Lebedeva N. A., Leblond S., Liiv S., Magnússon S., Mammadov E., Manes F., Manninen S., Maňkovská B., Martínez-Abaigar J., de Marco A., Marzuoli R., Mastrorilli M., Maxhuni A., Mehrabova M., Melece I., Meyer M., Milanovic I., Minkova-Gecheva G., Marinova S., Nali C., Nickel S., Norris D., Núñez-Olivera E., Omarova N., Paoletti E., Pavlikova I., Piispanen J., Pihl Karlson G., Pleijel H., Poikolainen J., Popescu I. V., Purvis W., Qarri F., Rana G., Radnovich D., Radulescu C., Repellin A., Ruttens A., Saitanis C., Salvatori E., Santamaría J., Schaab M., Schaub M., Schlabach M., Schröder W., Shetekauri S., Sicard P. L., Skudnik M., Sogo H.C., Soja G., Solodukhin V., Spiric Z., Stafilov T., Steinnes E., Stihi C., Suchara I., Sucharová J., Szarek-Łukaszewska G., le Thiec D., Thöni L., Tibor K., Todoran R., Turk B., Uggerud H., Urbaniak J., Vandermeiren K., Velissariou D., Vergel K. N., Vikhrova I. V., Vitale M., Volk M., Waegeneers N., Werner W., Zechmeister H. G., Zeiko G., Zlobin V., Air Pollution and Vegetation, ICP Vegetation, Annual Report 2014/2015, H. Harmens, G. Mills, F. Hayes, K. Sharps, M. Frontasyeva, (Eds.), ICP Vegetation Programme Coordination Centre, Centre for Ecology and Hydrology, Environment Centre Wales, Bangor, Gwynedd, UK, Moss Survey Coordination Centre, Frank Laboratory of Neutron Physics, Joint Institute for Nuclear Research, Dubna, Moscow Region, Russian Federation, September, 2015.

[11] Maňkovská B., Frontasyeva M. V. and Ostrovnaya T.M. Temporal and spatial trends (1990−2010) of trace element atmospheric deposition in Slovakia − assessment based on moss analysis. Chapter of a book "Air Pollution", INTECH, Open Access Publisher, 2015.

[12] Florek M., Holý K., Kovačik A., Sýkora I., Melicherová T., Frontasyeva M.V., Pavlov S.S.: Concentrations of Elements in the Atmosphere in Bratislava, Slovakia. Book of Abstracts, ISINN-23, Dubna, Russia, May 2015.

[13] Maňkovská B., Oszlányi J., Izakovičová Z., Florek M., Holý K., Frontasyeva M.V., Ostrovnaya T. M.. Biomonitoring of trace elements in Slovak mining country, and control sites experiencing environmental stress. Book of Abstracts, ISINN-23, Dubna, Russia, May 2015.

[14] Aleksiayenak Yu.V., Frontasyeva M.V., Ostrovnaya T.M., Okin O.I. Moss biomonitoring echnique, NAA and AAC for air pollution in Belarus. Problems of Reginal Ecology. No. 4, 2015 (Алексеенок Ю.В., Фронтасьева М.В., Островная Т.М., Окина О.И.. Метод мхов-биомониторов, НАА и ААС в исследовании воздушных загрязнений Беларуси. *Проблемы региональной экологии*, № 4, 2015).

[15] Qarri F., Lazo P., Bekteshi L., Stafilov T., Frontasyeva M., Harmens H., The effect of sampling scheme in the survey of atmospheric deposition of heavy metals in Albania by using moss biomonitoring, *Environmental Science and Pollution Research*, Vol. 22, No. 3, 2015, p. 2258-2271.

[16] Allajbeu Sh., Yushin N.S., Qarri F., Lazo P., Duliu O.G., Frontasyeva M.V.. Atmospheric deposition of rare earth elements in Albania studied by the moss biomonitoring technique, neutron activation analysis and GIS technology. *JINR Preprint*, E-18-2015-64, Dubna, 2015, pp. 18. Submitted to *Env Sci Poll Research.*

[17] Hristozova G., Marinova S., Strelkova L.P., Goryainova Z., Frontasyeva M.V., Stafilov T.. Milti-element atmospheric deposition study in the area of lead-zinc plant in Kardzhali, Bulgaria. *American Journal of Analytical Chemistry*, USA, Vol. 5, 2015, p. 920-931

[18] Marinova S., Zaprianova P., Hristozova G., Frontasyeva M.V., Assessment of soil contamination with zinc in the area of Kardzhali lead-zinc plant, XXIII International Seminar on Interaction of Neutrons with Nuclei dedicated to the centenary of the birth of Fyodor L. Shapiro (1915-1973), Dubna, Russia, May 25-29, 2015, Abstracts,. ISBN 978-5-9530-0409-1, Dubna: JINR, 2015, 60 p.

[19] Kalabegishvili T.L., Murusidze I.G., Kirkesali E.I., Rcheulishvili A.N., Ginturi E.N., Gelagutashvili E.S., Kuchava N.E., Bagdavadze N.V., Janjalia M.V., Pataraya D.T., Gurielidze M.A., Frontasyeva M.V., Zinicovscaia

I.I., Pavlov S.S., Tsertsvadze G.I., Gabunia V.N., Possibilities of physical methods in development of microbial nanotechnology. *European Chemical Bulletin*, Vol. 4, No. 1, 2015, p. 43-49.
[20] Keränen A., Leiviskä T., Zinicovscaia I., Frontasyeva M.V., Hormi O., Tanskanen J., Quaternized pine sawdust in the treatment of mining wastewater. *Environmental Technology,* 2015 Nov 20, 1-23.
[21] Cepoi L., Rudi L., Chiriac T., Valuta A., Zinicovscaia I., Duca Gh., Kirkesali E., Frontasyeva M.V., Culicov O., Pavlov S.S., Bobrikov I., Biochemical changes in cyanobacteria during the synthesis of silver nanoparticles. *Canadian Journal of Microbiology*; Jan 2015, Vol. 61 No. 1, 2015, pp. 13.
[22] Zinicovscaia I., Cepoi L., Chiriac T., Culicov O. A., Frontasyeva M. V., Pavlov S.S., Kirkesali E., Akshintsev A., Rodlovskaya E. *Spirulina platensis* as biosorbent of chromium and nickel from wastewaters. *Desalination and Water Treatment*, 2015, DOI:10.1080/19443994.2015.1042061.
[23] Arafa W.M., Badawy W.M., Fahmi N.M., Ali K., Gad M.S., Duliu O.G., Frontasyeva M.V., Steinnes E.. Geochemistry of sediments and surface soils from the Nile delta and lower Nile valley studied by epithermal neutron activation analysis. *Journal of African Earth Sciences*, No. 107, 2015, p. 57-64. Elsevier.
[24] Badawy W.M., Ali K., El-Samman H.M., Frontasyeva M.V., Gundorina S.F., Duliu O.G., Instrumental Neutron Activation Analysis of Soil and Sediment Samples from Siwa Oasis, Egypt. *Physics of Particles and Nuclei*. Vol. 12, No. 4, p. 637-644.. ISSN 1547-4771. Pleiades Publishing, 2015.
[25] Pavlov D., Frontasyeva M.V., Bezuidenhout J., Goryainova Z.. Monitoring of trace elements in marine ecosystems: “Mussel Watch” approach. The 4th south Africa - JINR symposium “Few to Many Body Systems: Models and Methods and Applications” September 21-25, 2015, Dubna, Russia. Book of Abstracts.
[26] Kravtsova A.V., Milchakova N.A., Frontasyeva M. V.. Levels, spatial variation and compartmentalization of trace elements in brown algae *Cystoseira* from marine protected areas of Crimea (Black Sea). *Marine Pollution Bulletin*. No. 3, 2015, p. 97-99.
[27] Nekhoroshkov P.S., Frontasyeva M.V., Tokarev Yu.N., Biophysical parameters and muli-element content of phytoplankton communities of the Black Sea in the coastline zone of Crimea. *Water: chemistry and ecology*. (www.watchemec.ru) 2015) (Нехорошков П.С., Фронтасьева М.В., Токарев Ю.Н.. Биофизические параметры и многоэлементный состав фитопланктонных сообществ Черного моря в прибрежной зоне Крыма. *Вода: химия и экология* (www.watchemec.ru), № 8, 2015. с. 10-17б 2015).
[28] Kamnev A.N., Frontasyeva M.V., Kravtsova A.V., Nekhoroshov Pavel S., Zinicovscaia I.I., Yushin N.S.. Assessment of elemental composition of vegetation, soil and bottom sediments along a ”transect Anapa – the Black Sea”, studied by neutron activation analysis. PAC, January 2015, Dubna.
[29] Gorbunov A.V., Lyapunov S. M., Okina O.I., Chamov N.P., Frontasyeva M. V., Pavlov S. S., Avdoseva M. V., Assessing biomonitoring opportunities in the study of technogenic pollution of the environment of the Yamal Peninsula. *Ecology of Urbanized Territoriers*, No.1, 2015, p. XX (Горбунов А.В., Ляпунов С.М., Окина О.И., Чамов Н.П., Фронтасьева М.В., Павлов С.С., Авдосьева М.В., Оценка возможностей биомониторинга при изучении техногенного загрязнения природной среды п-ова Ямал. *Экология урбанизированных территорий*, № 1, 2015, p. 253-270).
[30] Gorbunov A.V., Lyapunov S.M., Frontasyeva M.V., Pavlov S.S., Intake of Cl, Br, I, Se in human body with food in Central Regions of the European Part of Russia. *Food and Nutrition Sciences*, No. 6, 2015, p. 168-178. Published Online January 2015 in Sci Res. http://www.scirp.org/journal/fns; http://dx.doi.org/10.4236/fns.2015.61018.
[31] Gorbunov A.V., Granovskaya G.A., Ermolaev B.V., Lyapunov S.M., Ilchenko I., Frontasyeva M.V., Pavlov S., Assessment of mercury in diagnostic biomaterials of different population groups of urban areas of Moscow Region. Ecology of Urbanized Territoriers, No. 2, 2015, p. 16-24 (Горбунов А.В., Грановская Г.А., Ермолаев Б.В., Ильченко И.Н., Ляпунов С.М., Фронтасьева М.В., Павлов С.С., Авдосьева М.В.. Оценка содержания ртути в диагностических биоматериалах различных групп населения урбанизированных территорий Московского региона. *Экология урбанизированных территорий.* № 2, 2015, с. 16-24).
[32] Tugulan C., Duliu O.G., Voica Bojar A., Dumitras D., Zincovskaya I., Culicov O.A., Frontasyeva M.V. Late Quaternary climatic conditions in Dobrogea (Romania) as reflected by loess geochemistry. Quaternary International, 08/2015; DOI: 10.1016/j.quaint.2015.06.062.
[33] Frontasyeva M.V. Neutron activation analysis and microscopy of extraterrestrial materials. International conference “Modern Trends in Radiobiology and Astriobiology”. Dubna, 28-30 October, 2015.
[34] Kosior G., Prell M., Samecka-Cymerman A., Stankiewicz A., Kolon K., Kryza R., Brudzińska-Kosior A., Frontasyeva M., Kempers A. J., Metals in *Tortula muralis* from sandstone buildings in anurban agglomeration. *Ecological Indicators,* No. 58, 2015, p. 122-131.

[35] Xuesong Li, Hristozova G., Nekhoroshkov P.S., Frontasyeva M.V., Neutron activation analysis of constituent elements of edible and medicinal plant of iron stick yam (Dioscorea opposita Thunb). Accepted by *International Research Journal of Public and Environmental Health*, 2 November, 2015.
[36] Ignatenko O.V., Konovalova A.V., Komar V.A., Leonchik S. V., Shempel N. A., Aleksiayenak Yu. V., Frontasyeva M.V., Shvetsov V.N., Ene A., Cantaragiu A., Comparative characteristics of synthetic diamond powder obtained in systems Fe-Ni-C and Mn-Ni-C, Proceedings of the 2nd International Conference on Modern Applications of Nanotechnology, 6-8 May 2015, Minsk, Belarus, 3 pp
[37] Игнатенко О.В., Коновалова А.В., Комар В.А, Леончик С.В., Шемпель Н.А., Алексеенок Ю.В., Фронтасьева М.В., Швецов В.Н., Ене А., Cantaragiu A., Влияние состава ростовой системы на характеристики синтетических алмазных порошков. Сборник материалов международного симпозиума «*Перспективные материалы и технологии*», 27-29 мая 2015 г., г. Витебск, Беларусь.
[38] Ene A., Frontasyeva M.V., Ignatenko O.V., Cantaragiu A., Investigation of synthesized diamonds, lithium and boron nitrides using SEM-EDX and XRD techniques, 15th International Balkan Workshop on Applied Physics (IBWAP 2015), Constanta, Romania, 2-4 July 2015, Poster S5_P33, Section 5-Engineering and Industrial Physics, Book of Abstracts, pp. 188-189

NOVEL DEVELOPMENT AND CONSTRUCTION OF EQUIPMENT FOR THE SPECTROMETER COMPLEX OF THE IBR-2 FACILITY

.

Cryogenic moderators

In 2015, work and research continued on a special stand of a cryogenic pelletized moderator with an inclined section at an angle of elevation of 40° in the direction of experimental beamlines № 4,5,6. Hardware and software of the stand have demonstrated stable and trouble-free operation during all experiments and in the future will be used in a real moderator CM201.

The trial operation of the CM202 moderator was conducted in February and March 2015. The moderator operated during two reactor cycles for 9.5 days in each round; in 2014 its continuous operation was 10.5 days. During its operation there were no accidents or emergency situations.

In the framework of the development of the CM202 moderator a device was proposed for nitrogen-free charging of frozen pellets into a dosing machine; its computer model is shown in **Fig. 1**.

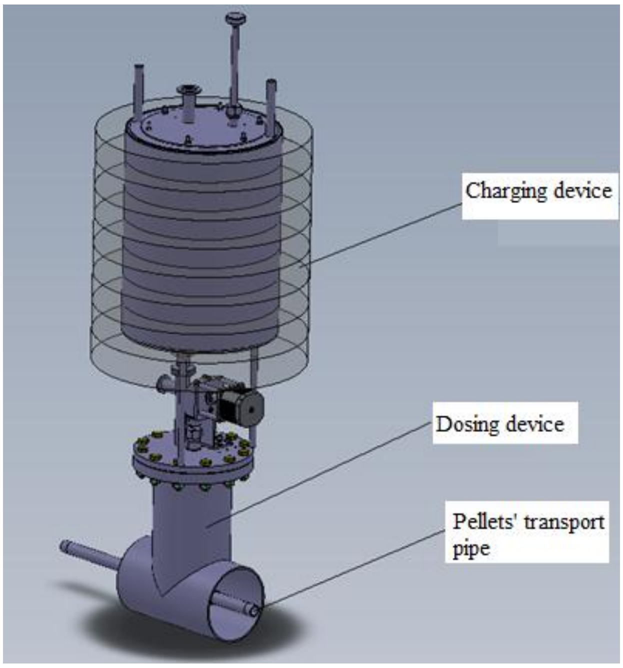

Fig. 1*. A device for nitrogen-free charging of frozen pellets into a dosing machine of the pelletized moderator of IBR-2.*

The main advantage of this device is that in the process of loading of frozen pellets into the dosing machine, liquid nitrogen will not leak into the pneumatic pipeline. This will make it possible to avoid problems related with the freezing of liquid nitrogen in the pipeline, namely, in the heat exchanger of the cold moderator.

The modernization of the system of sensors for monitoring the passage of mesitylene pellets in moderators CM202 and CM201 has been carried out.

During the two cycles of operation of the cold moderator, experiments have been performed to obtain a neutron microbeam using a waveguide and beam spatial splitting from a non-collinear magnetic system (reflectometer REMUR) as well as texture analysis of olivine (rock) has been done (spectrometer SKAT). The results have shown a gain in the neutron flux by a factor of 3-10 when using the cold moderator for these experiments.

The main problem with using a pelletized cold moderator on metaxylene and mesitylene is a limited time of its continuous operation for physics experiments. At present, it amounts to 10.5 days, which is actually equal to the duration of a standard reactor cycle with a warm-water moderator (11 days). At the same time, after irradiation for 10.5 days the viscosity of a metaxylene and mesitylene mixture is observed to increase (more than 20 times higher, see **Fig. 2**), which may become an obstacle for safe and reliable operation of the moderator. This requires further study. In the near future the development and improvement of the pelletized moderator will be focused, first of all, on looking for opportunities to prolong its continuous operation.

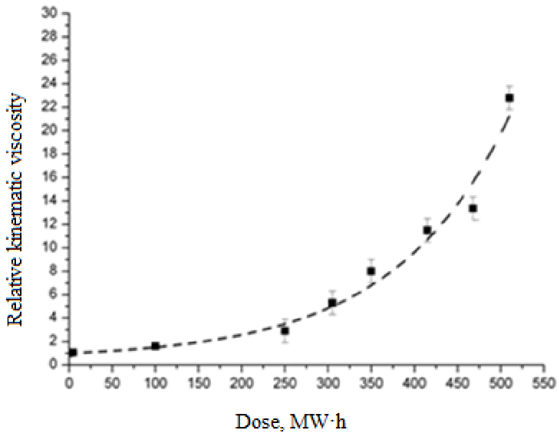

***Fig. 2**. Relative kinematic viscosity for different doses of irradiation of a mixture of mesitylene and metaxylene (points - experimental viscosity values, dashed line - approximation).*

There are several ways to prolong the non-stop operation of the cold moderator:

1) Creation of a system of continuous loading/unloading of pellets. This system makes it possible to unload the frozen pellets with high radiation load, and to load new unexposed ones, thereby providing an optimum viscosity of the mixture. The creation of this system at the IBR-2 reactor is a challenging engineering task. At the present time the development of a full-scale prototype of a device for loading/unloading pellets has started for conducting tests on the stand of the pelletized moderator.

2) Introduction of different additives to the initial working mixture. When using additives, two mechanisms of viscosity reduction of a mixture under irradiation are possible. The first one is based on the replacement of some of mesitylene molecules with more radiation-resistant aromatic hydrocarbons. These may be naphthalene and anthracene molecules consisting of benzene rings. By using these additives, radiation resistance of the mixture may increase up to 1.5 times with a slight decrease in the cold neutron flux. The second mechanism is based on the addition of substances with heavy nuclei by which a certain part of recoil protons occurring as a result of neutron moderation will be slowed down. Thus, a small spatial replacement of mesitylene molecules with homogeneously distributed microparticles will be inessential for neutron moderation. These additives may be neutron nonabsorbing materials: nanopowders of diamond, zirconium, lead.

3) Prolongation of operation time of the pelletized moderator by replacing the working mixture of mesitylene and metaxylene with another substance with better radiation resistance and equivalent neutron-physical properties (yield of cold neutrons, etc.). This substance may be triphenylmethane.

Using triphenylmethane as a potential pelletized cold moderator for IBR-2, an important point is the possibility of manufacturing pellets of the right shape, required size, with good hardness and strength, which is essential for ensuring their transportation to the cold moderator chamber. In 2015, we carried out research work that proved the possibility of producing solid pellets of triphenylmethane with the desired properties (photo of pellets is shown in **Fig. 3**).

Fig. 3. *Pellets of triphenylmethane.*

Radiation Research Facility

In 2015, the following research activities were performed on the facility:

• measurement of low neutron fluences (10^{11} - 10^{15} n/cm^2) using various neutron detectors in a curved tube of the irradiation facility located on beamline 3 of the IBR-2 reactor;

• test irradiation of specimens of silicon photomultipliers from Hamamatsu (in cooperation with ITEP, MEPhI, VBLHEP and CERN);

• studies of radiation resistance of promising detector materials (single crystals of diamond) for CERN (ATLAS project) and Nanjing University (China);

• investigation of radiation resistance of magnetic sensors (3D-Hall sensors) in the framework of the international project ITER (**Fig. 4**);

• irradiation of Iridium-193 isotope for obtaining isotopes of promising materials for medicine (in cooperation with FLNR).

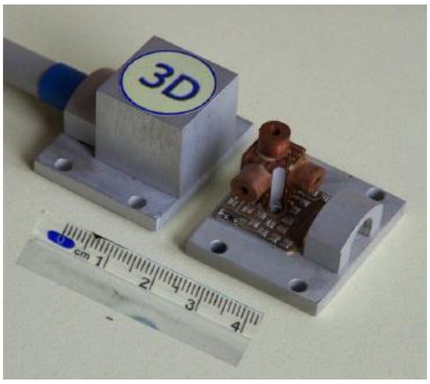

Fig. 4*. Magnetic sensors (3D-Hall sensors).*

Technical specifications for modernization of the radiation research facility (installation of biological shielding, modernization of facility motion control unit) have been prepared. The implementation of these tasks is scheduled for 2016.

Calculations and simulation of spectrometers

The development of new modules and improvement of old ones of the VITESS software package for simulation of neutron instruments continued. Particular emphasis was placed on VITESS modules that simulate spectrometers with polarized neutrons. In the first half of 2015 studies on the simulation of a spin-echo small-angle spectrometer (SESANS) were carried out in cooperation with the NICM Department. The simulation was performed with a set of model spheres with a fixed radius, thus bringing the simulation closer to a real experiment. For this purpose we had to make laborious adjustment of the VITESS modules responsible for simulation of spectrometer components including the module of a pulsed magnetic field (t_dependent_magnetic_field) and the module for simulating a small-angle sample (sample_sans). A general scheme of the spectrometer is shown in **Fig. 5**.

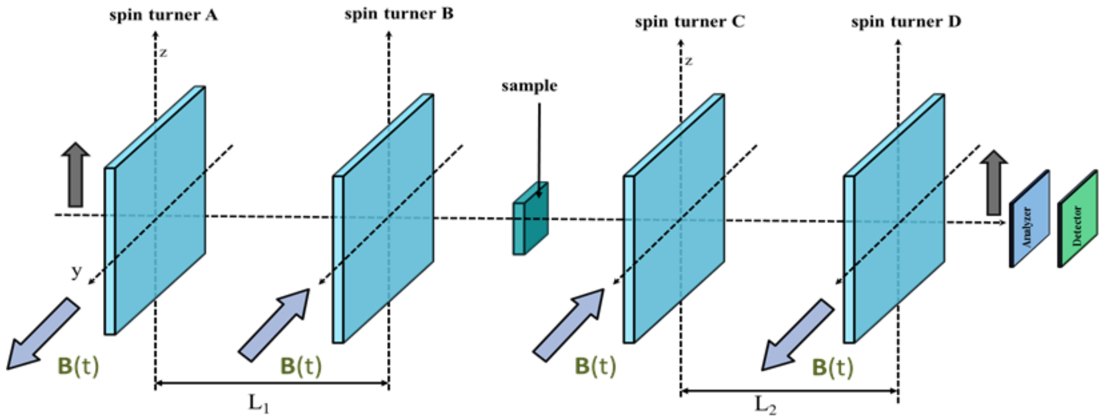

***Fig. 5**. General scheme of a spin-echo spectrometer with 4 flippers with pulsed gradient magnetic fields B(t).*

To verify the correctness of the obtained results of the Monte Carlo simulation of a spin-echo spectrometer, an analytical evaluation has been performed as well. It should be noted that an analytical evaluation is possible only for a simple ideal spectrometer. As a rule, for a real instrument even with a model sample the Monte Carlo simulation is the only tool to evaluate the parameters of a spectrometer. For the simulation the following parameters were chosen: field frequency – 100 kHz, amplitude — 5200 Gs, radius of the sphere in the sample — 10 nm. **Figure 6** shows the results of the Monte Carlo simulation in comparison with the analytical evaluation. The obtained simulation results testify the adequacy and correctness of the used Monte Carlo mathematical model.

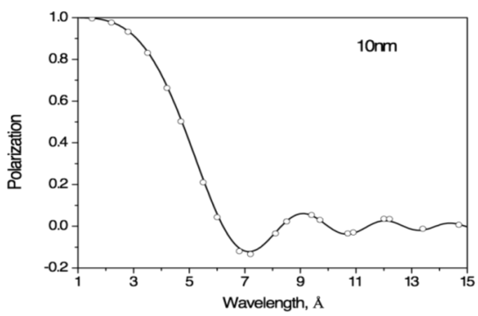

***Fig. 6**. The results of the Monte Carlo simulation (points) and analytical evaluation (solid line).*

The development of special mathematical models and corresponding programs for the simulation of neutron scattering (including magnetic scattering) from samples (including rough multilayer samples) was continued. The studies were carried out with reflectometric multilayer samples with a regular surface structure using the Parratt's method and kinematic approximation. Using the developed programs we performed virtual GISANS experiments in the kinematic approximation with thin-film samples and a regular surface structure to obtain diffraction. A provision was made for simulation of surface roughness and interfaces. The developed programs have an input and output data format which is compatible with DWBA BornAgain. Below (**Fig. 7,8**) are the results of GISANS simulation of two virtual experiments in the kinematic approximation:

1. Diffraction from columns of ^{58}Ni isotope on a silicon substrate (column height – 200 Å, column width – 50x50 Å, periods – 100x100 Å in the horizontal plane).
2. Diffraction from columns on a rough surface of ^{58}Ni isotope (column height – 200 Å, column width – 50x50 Å, periods – 100x100 Å in the horizontal plane). The parameters describing the roughness were chosen as follows: σ = 23 Å, ξ = 200 Å, which to a greater extent corresponds to a real sample.

The simulation results show that the diffraction is detectable and this will allow us to determine lattice parameters from a diffraction pattern in a real experiment.

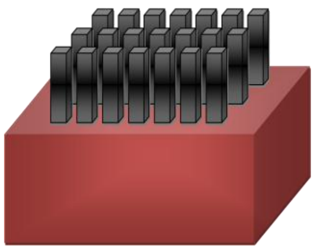

Fig. 7*. An example of a sample for a GISANS experiment.*

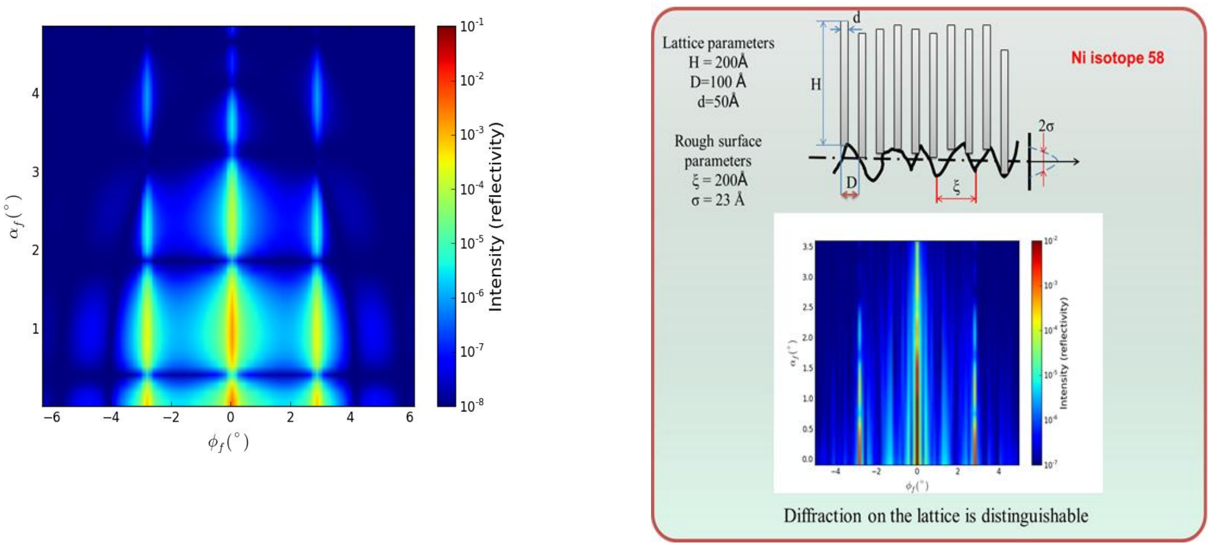

a) b)

Fig. 8*. Simulation of a GISANS experiment: diffraction from* ^{58}*Ni isotope columns: a) on a smooth silicon substrate, b) on a rough surface.*

FSS spectrometer

Work was continued on the construction of a new high-resolution Fourier diffractometer on IBR-2 beamline 13 on the basis of the units of the FSS spectrometer from the GKSS research center (Geesthacht, Germany). In cooperation with PNPI (Gatchina) and the NICM Department neutron guide sections were assembled (**Fig. 9**), alignment of optical sections was done, vacuum equipment was installed and vacuum sealing of the neutron guide was conducted.

Fig. 9*. The exit section of the neutron guide on IBR-2 beamline 13.*

At present, activities are carried out to measure beam characteristics at the exit of the neutron guide and to improve the background conditions at the diffractometer. **Figure 10** shows the distribution of beam intensity along the x-axis at the exit of the neutron guide. The distribution width corresponds to the geometric aperture of the neutron guide, which is 15 mm.

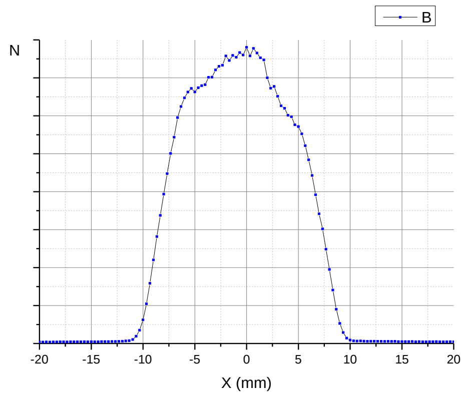

Fig. 10*. Distribution of beam intensity along the x-axis at the exit of the neutron guide.*

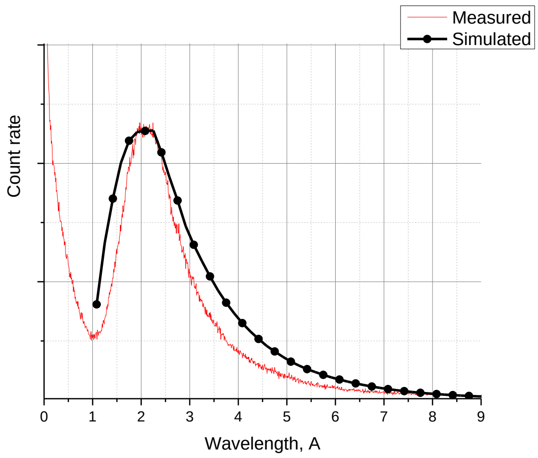

Fig. 11*. Calculated and measured distributions of the neutron beam intensity at the exit of the mirror neutron guide.*

Figure 11 illustrates a comparison between the output beam intensity distribution calculated by the Monte Carlo method (reflection coefficient used in the calculations was R = 0.99) and the spectrum obtained for a vanadium sample placed at the exit of the mirror neutron guide used in GKSS. Positions of the maxima of the measured and calculated spectra coincide. The narrowing of the measured spectrum can be explained by the low quality of the coating of the mirror neutron guide. The measured maximum flux density across the beam is about 1.3 x 10^6 n/(s·cm^2).

Cryogenics

Major activities in the area were carried out in accordance with the project on the development of a cryostat for temperature and magnetic investigations of condensed matter at the DN-12 spectrometer. The project is being implemented in cooperation with the National Institute of Research and Development in Electrical Engineering ICPE-CA, Bucharest, Romania. In 2015, a detailed design was developed and 3D-simulation was performed for a horizontal cryostat with a superconducting magnet producing a magnetic field of 4 T, and a cryostat with a high-pressure cell for the magnet, which are cooled by closed-cycle cryocoolers. The design documentation for the cryostats was prepared. The drawings were forwarded to SPA "Atom" to manufacture all mechanical components of the cryostats. Tests of the cryocoolers were conducted. It has been established that their characteristics meet the specifications. **Figures 12** and **13** present the computer models of the cryostat and magnet.

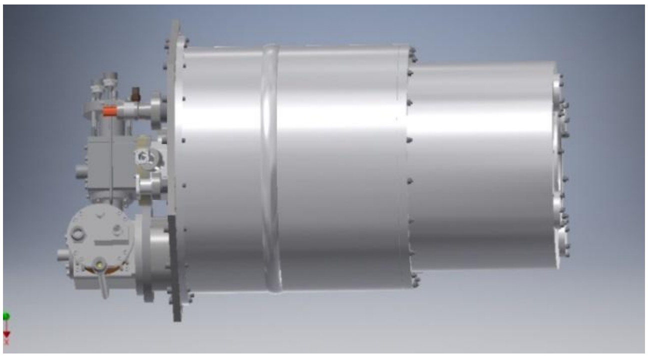

__Fig. 12__. A horizontal cryostat for the DN-12 spectrometer. A general view (left).

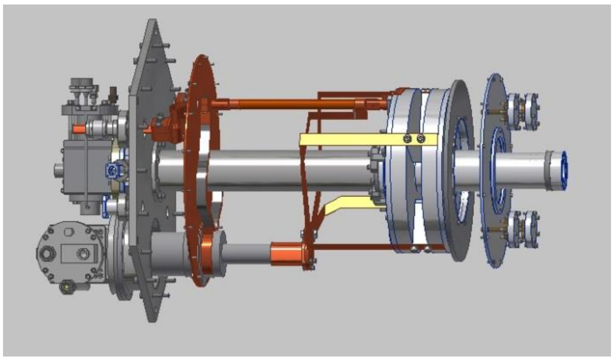

Fig. 13. *The magnet of the cryostat and its horizontal shaft for loading the cryostat with a high-pressure cell (right).*

The magnet is a Helmholtz pair of magnets made of a high-temperature superconducting tape of the second generation YBCuO (manufactured by "SuperOx", Russia). The magnet is cooled by a closed-cycle cryocooler to a temperature of (10 - 20) K. The cryostat with a high pressure cell, which in its turn is cooled by another closed-cycle cryocooler, is inserted into the center of the magnet through a horizontal shaft. The temperature of the cell is regulated by a controller in the range of (4 - 300) K.

The cryostat with a closed-cycle cryocooler was tested and prepared for installation on the DIN-2PI spectrometer. **Figures 14, 15** present a photo showing a cold head of the cryocooler in the shaft of the spectrometer and time dependences of the temperature of the sample chamber and the cryocooler second stage in the process of temperature regulation.

Fig. 14. Photo of a cryocooler cold head (1) in the shaft of the DIN-2PI spectrometer (right).

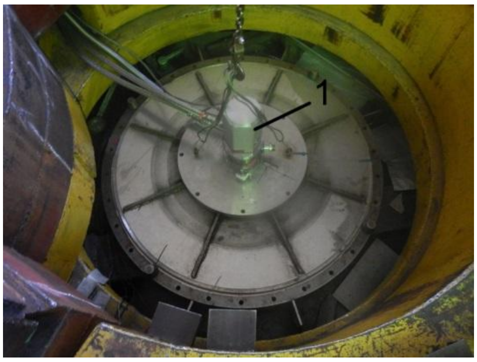

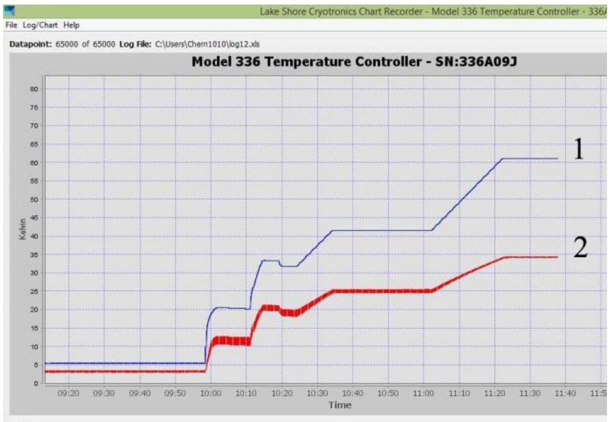

Fig. 15. Time dependence of the temperature of the sample chamber in the process of temperature regulation: 1 - temperature of the sample chamber, 2 - temperature of the cryocooler second stage (left).

Detectors and electronics

A 2D gas position-sensitive detector (PSD) for the REMUR spectrometer has been manufactured and tested with a neutron source. It has been designed to replace the available outdated PSD of the spectrometer. Also, all scintillation counters and electronic components of the fourth section of the ASTRA detector for the FSD diffractometer have been manufactured, adjusted and tested. Both detector systems are ready to be put into operation in the coming IBR-2 cycles. In the process of manufacturing of scintillation counters we have developed a new design and layout of the counters in the ASTRA detector, making it possible to provide as high accuracy of positioning of scintillation surfaces as need be, which is important for detectors using a space-time focusing principle. In addition, the new design allows us to significantly reduce the material resources required for manufacturing of the detector. A 3D-model (**Fig. 16**) and a technical design of the new detector system, which is planned to be manufactured in 2016-2017 and installed in place of the existing sections of the detector ASTRA at FSD, have been developed.

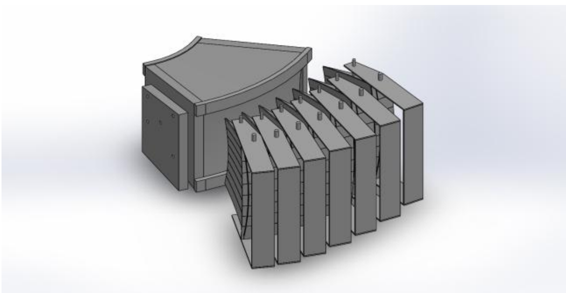

Fig. 16. New layout of the modules of the detector ASTRA.

A prototype of a ring small-angle detector has been developed for the DN-2 diffractometer (**Fig. 17**). The prototype consists of one ring with the cathode divided into 16 independent sectors. Signals can be picked up by both the anode wire and each individual sector of the cathodes, thereby determining the angles φ and θ. We have tested the prototype and obtained amplitude spectra from the anode and individual cathodes.

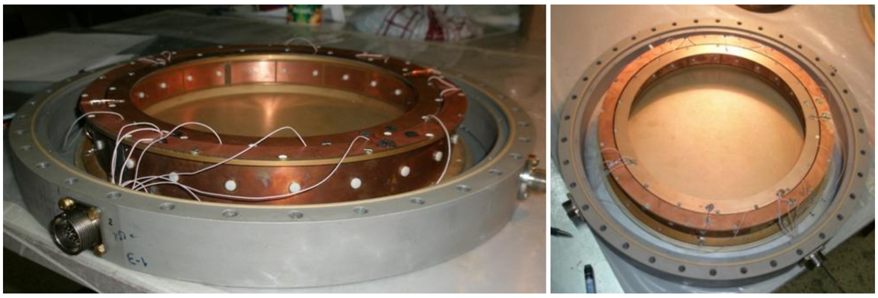

***Fig. 17**. Prototype of a ring small-angle detector for the DN-2 diffractometer.*

On the DN-6 diffractometer a new ring neutron detector for obtaining neutron spectra at a scattering angle of 90° has been put into operation. The detector consists of 16 sections with 6 independent detector elements each (helium proportional counters) with background shielding and collimation. Charge-sensitive preamplifiers (96 channels), three modules of 32-channel amplitude discriminators and a 192-channel digital data acquisition and accumulation module (MPD) were developed and manufactured specially for this detector. The electronics was adjusted and all the equipment with the software of the diffractometer was tested. The available multi-section ring detector relocated to the scattering angle of 45° and the new one was integrated into a single measurement system (**Fig. 18**).

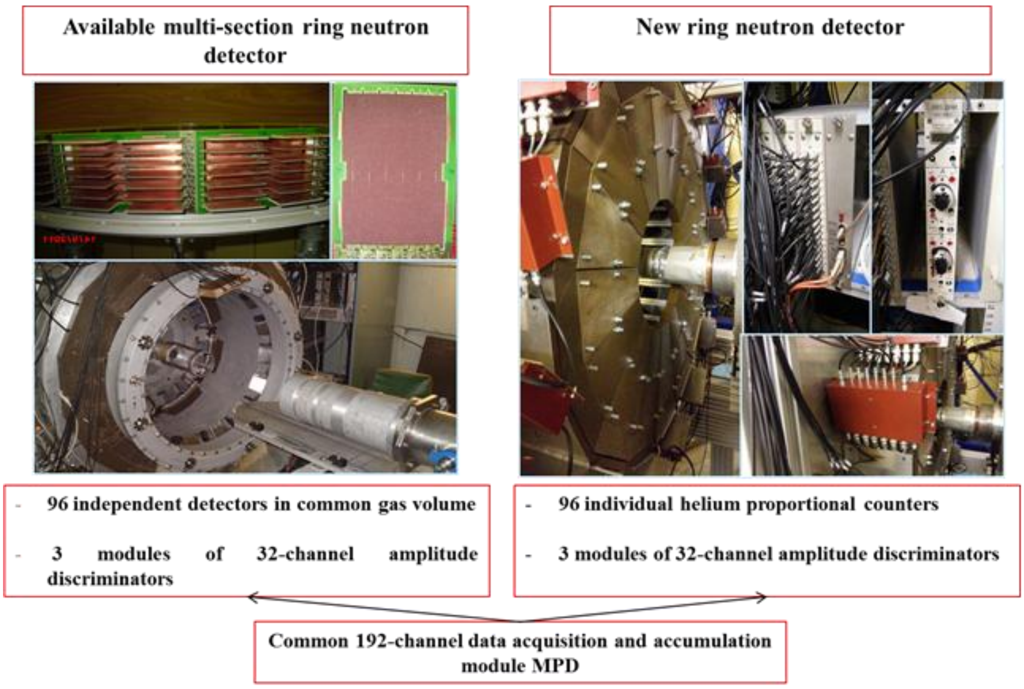

***Fig. 18**. New detector system of the DN-6 diffractometer.*

For experimental studies with fast neutrons a new spectrometer based on a proton telescope (PT), in which the measurement of energy distributions of neutron fluxes is performed by measuring the kinetic energy of recoil protons elastically scattered at small angles as a result of (n, p) interaction in a gas hydrogen-containing medium, has been designed, manufactured and tested (detailed description of PT can be found in the Annual Report 2012 and JINR Patent http://www.freepatent.ru/images/patents/13/2445649/patent-2445649.pdf). New versions of PT, electronics and software have been designed in accordance with protocol №4519-4-15/17 of 15.06.2015 between JINR and the National Fusion Research Institute (Daejeon, Republic of Korea), where the spectrometer is planned to be used for the diagnostics of a nuclear fusion reactor (KSTAR). In FLNP it will be used to obtain spectra of fast and resonance neutrons of neutron-producing targets of IREN and EG-5. **Figures 19, 20** show the electrode system of PT and beam spectrum from a neutron generator ING-07.

__Fig. 19__. Electrode system of the new proton telescope (left).

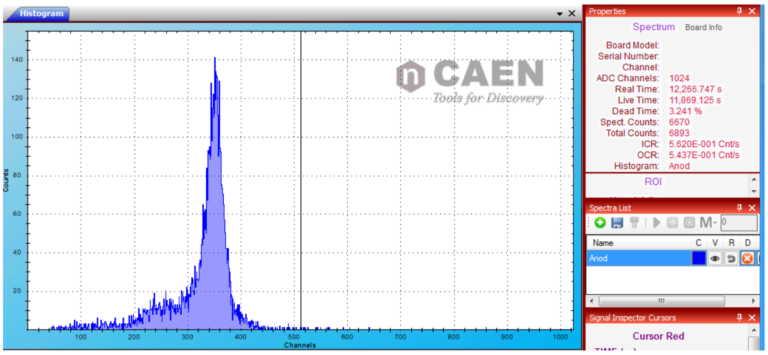

__Fig. 20__. Beam spectrum from a neutron generator ING-07 obtained using PT (neutron energy 2.5 MeV, gas mixture composition: 500 mbar CH_4 (right)).

Because of a large amount of unplanned work on electronics and software for the ring detector of DN-6 and proton telescope, only a schematic circuit diagram was designed and hardware components were selected for a USB-3.0 interface unit, and a part of the work (design of a printed circuit board and manufacture of a prototype) had to be postponed until 2016.

Modernization of control systems and actuators of the IBR-2 spectrometers

On the YuMO spectrometer a control system for sample changing (**Fig. 21**) was put into operation. The number of samples in the cassette was increased from 14 to 25 and the time required for automatic sample change was reduced.

__Fig. 21__. Device for horizontal positioning of samples at the YuMO spectrometer (left).

__Fig. 22__. New control system for monitoring the instrument operation on the basis of interface converters (right).

On the REMUR spectrometer the number of control channels has been increased from 34 to 36. On two devices absolute linear displacement wire-type (0-2 m) sensors on the basis of absolute angular multiturn sensors have been mounted. On the GRAINS spectrometer the control system of actuators has also been expanded to 28 channels. On IBR-2 beamline 14 a control system of the equipment of the spectrometer for neutron radiography and tomography has been put into operation. The modernization of control systems of the experimental facilities on IBR-2 beamlines 5, 6 and 7a has been carried out. They have become more technologically advanced and easy to operate. Interface converters have been replaced as well. **Figure 22** shows a new control system for monitoring the instrument operation on the basis of interface converters AC4 (USB-RS485) and AC3-M (RS485-RS232).

On the IBR-2 spectrometers the modernization of choppers and their control systems has been continued. In particular, a new drum-type chopper on the basis of 2.2 kW asynchronous motor with a standardized variable frequency drive VFAS1-4022 (**Fig. 23**) has been put into service on the REFLEX spectrometer. A chopper opening sensor on the basis of a magnet and reed switch MKA-10110, which makes it possible to use it in the IBR-2 ring corridor, has been developed and installed. The accuracy of chopper phasing is +/– 150 μs.

***Fig. 23**. New drum-type chopper on the REFLEX spectrometer.*

The control system of the Fourier chopper on HRFD has been upgraded. The frequency drive of the Fourier chopper has been connected to the host PC via a USB fiber optic extender, which has significantly increased the noise immunity of the control system of the chopper.

On a number of spectrometers the modernization of temperature controllers LakeShore has been carried out to connect a larger number of different types of sensors and for communication with a computer via a USB-interface.

Software and computer infrastructure

In 2015, the development of the software package Sonix+ was continued, in which a number of components were added at the request of users or further improved following the operating experience. Among the most important activities were the following:

- development of new components for controlling equipment of a number of spectrometers (RTD HRFD, REMUR, GRAINS);
- supplementation and improvement of programs of graphical user interface (GUI);
- development of a new version of the command library for reflectometers, in which preliminary data processing is conducted simultaneously with the continuation of exposure;

- continuation of development of software tools for testing and debugging of electronics of data acquisition systems.

Eight spectrometers have been connected to the WebSonix service (YuMO, HRFD, FSD, SKAT, NERA-PR, EPSILON, DIN-2PI, REFLEX) making it possible to remotely control the course of an experiment.

In the FLNP local area network the number of WiFi access points in buildings 42 and 117 has been increased. The creation of access points in the IBR-2 reactor premises is technically difficult and has been temporarily postponed. The routers in the reactor control building and experimental hall №1 (building 117) have been upgraded to provide a data rate of 10 Gbit/s.

Due to the change-over to the List-mode in the accumulation of raw data on a number of spectrometers (for example, it is the main mode on Fourier-diffractometers HRFD and FSD) the question arose of providing storage and preliminary processing of large amount of data.

Accumulation and storage of data

Until recently, physicists accumulated and stored experimental data on control computers of spectrometers. Data transmission to the central server of the Laboratory was performed by each user manually when required. At the same time there was always a risk of accidental erasure of data, network failure, losses in case of disk drive failure, etc. To eliminate these problems, in 2014, a centralized network storage was organized on the basis of a file-server Supermicro with two CPU Intel Xeon, 16 GB RAM and 72 TB disk memory (characteristics and description of the software of the server are given in the Annual Report 2014). This storage system provides an automatic transfer of data from the control computer to the file-server during the experiment. The storage capacity is quite sufficient for recording and storing data from all IBR-2 spectrometers.

Preliminary processing of raw data

If the accumulation is conducted in the List-mode, the amount of data can reach several terabytes and their preliminary processing (for example, neutron time focusing, calculation of the cross-correlation function between the intensity of neutrons recorded by a detector and the sequence of delayed functions of modulation of the neutron flux from the pulsed reactor and chopper and reconstruction of high-resolution spectra from initial diffraction data collected on Fourier diffractometers) may take a long time (several hours).

To accelerate the process of data treatment, specialists of the NICM Department have developed a fast algorithm for calculating the cross-correlation function and programs for parallelizing calculations on several processors allowing a several-fold reduction of processing time. Another method to speed up the computation is the application of computing nodes with graphics processors (for example, graphics accelerator GPU NVIDIA can provide a 10-fold acceleration). Such parallel data processing can be organized within individual physics groups or on the central computing servers of FLNP, but we cannot provide their normal load, therefore it is reasonable to use the available computing resources of LIT: heterogeneous cluster "HybriLIT" (http://hybrilit.jinr.ru/) and cloud services (https://cloud.jinr.ru/).

Both of these resources can also be used for calculations and simulation, specifically using the Monte Carlo method. The efficiency of their application will depend on whether it will be possible to parallelize calculations.

THE IBR-2 PULSED REACTOR

Information on the operation of the IBR-2 research nuclear facility

The IBR-2 research nuclear facility is operated under Rostekhnadzor license № GN-03-108-2614 of 27.04.2012 and Rostekhnadzor license № GN-03-108-2871 of 30.04.2014.

Since January 2015 regular IBR-2 cycles of scientific experiments have been carried out at a power of 2 MW with the CM-202 moderator operating either in the water or cryogenic mode in accordance with the schedule of the physical start-up of the cold moderator.

Table 1 presents data on the IBR-2 operation for physics experiments.

№ cycle	Period	Reactor operation at power, hr	Reactor operation for physics experiments, hr	Moderator type
1	19.01-02.02	331	326	water
2	11.02-21.02	237	230	cryogenic
3	11.03-21.03	264	240	cryogenic
4	30.03-16.04	350	330	water
5	13.05-27.05	342	336	water
6	28.09-09.10	271	264	water
7	19.10-02.11	275	267	water
8	09.11-23.11	331	326	water
9	07.12-21.12	333	327	water
TOTAL		**2734**	**2646**	

Information on the activities under the project "Complex of cryogenic moderators of the IBR-2 reactor"

1. The cryogenic moderator CM-202 operated at power during the 2nd and 3rd cycle (February and March). In the 2nd cycle – for 9.4 days (470 MW/h), in the 3rd cycle – for 10.4 days (510 MW/h), after which the operation of CM was suspended for carrying out construction and assembly work on the preparation of the premises for installation of the cryogenic facility "Linde". The cryogenic facilities KGU-500 and KGU-600 manufactured in 1972 and 1986, respectively, and being well beyond their expected service life were dismantled.
2. In October 2014 an agreement on the installation of KGU-1200/10 "Linde" in bldg 117 of the IBR-2 reactor was concluded with GSPI. Works on the preparation of the premises for the assembly of the facility units are in progress in accordance with the GSPI project.
3. A contract was signed with NIKIET on the development of a detailed design of an inclined channel moderator CM201 (neutron beamlines 4-8). The completion of the project is scheduled for the middle of 2016, after which the moderator will be manufactured at a specialized plant (SPA "Atom" or NIKIET) until the middle of 2017.
4. On November 3, 2015 the equipment of the facility "Linde" was delivered. The assembly, installation and commissioning of the facility will be started immediately after the completion of construction works and scheduled to be completed by July 2016.
5. Upon completion of the adjustment of the facility it is planned to carry out tests: a) on the stand; b) simultaneously on the stand and with the moderator to determine the cooling capacity of the facility "Linde" and the working temperature range.
6. In the 2nd half of 2016 it is planned to continue bench testing of promising versions of cryogenic moderators, such as a moderator with triphenylmethane, moderator with replaceable substance, etc.

7. In accordance with the plans for 2016 it is projected to finalize the design of CM-203 (beamline 2).

IREN FACILITY

In 2015, the IREN facility operated for experiments for 237 hours. In April-May 2015, at the IREN facility a group of staff members of VBLHEP and FLNP together with the specialists from «Dawonsys» (Republic of Korea) carried out the final stage of assembling and adjustment of two sets of new modulators to power pulsed klystrons — SHF sources of power of the LUE-200 accelerating system, which is a driver of the pulsed source of resonance neutrons. Commissioning of the modulators capable of generating electrical load pulses with a pulse power of up to 180 MW and an average power of 180 kW will allow doubling the average energy of accelerated electrons and providing operation of the accelerating system with a cycle frequency of up to 120 Hz, which will increase the power of the accelerated beam by more than one order and correspondingly the neutron yield from the irradiated target of the IREN source.


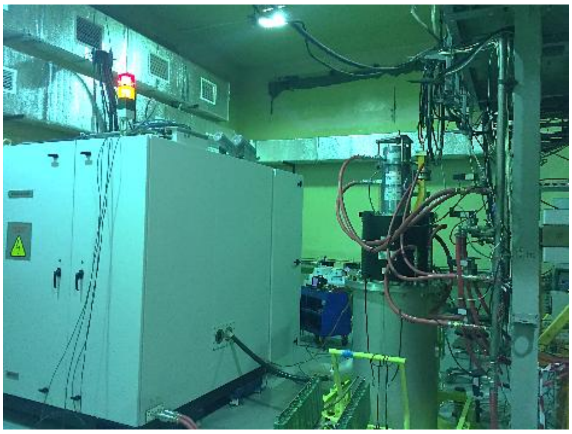

Fig. 1*. Assembling of modulators and klystrons; the modulator during tests.*

Experiments have been conducted to compare the neutron yield from tungsten and uranium nonmultiplying targets. The accelerator operated with one accelerating section, DAWONSYS modulator and TH2129 Thomson klystron of 17 MW. At the same operating modes of the accelerator the gain in the case of the uranium-238 target was 2.6.

At present, the second section of the accelerator has been installed; the work on its connection is in progress.

EG-5 ACCELERATOR

In 2015, the EG-5 accelerator operated for experiments for 510 hours. Experimental studies on charged particle beams using nuclear analytical methods of Rutherford backscattering (RBS) and elastic recoil detection (ERD) were conducted in cooperation with representatives of various institutes of the JINR Member States (Institute of Applied Physics of NAS, Sumy, Ukraine; Institute of Electrical Engineering of SAS, Bratislava, Slovakia; Maria Curie-Skłodowska-University, Lublin, Poland), Russian institutes (A.M.Prokhorov General Physics Institute of RAS, Moscow; B.P.Konstantinov Petersburg Nuclear Physics Institute, Gatchina; Voronezh State University), as well as of the JINR laboratories (DLNP, FLNR). Samples of different elemental composition and various preparation technologies were analyzed. The structure and properties of silicon and oxide films, the processes of accumulation and distribution of hydrogen and deuterium in the samples, the effect of proton irradiation on the characteristics of composite HTSC materials were investigated.

PUBLISHED PAPERS

DEPARTMENT OF NEUTRON INVESTIGATION OF CONDENSED MATTER

Atomic and magnetic structures (diffraction)

1. Аскеров Э.Б., Д.Н. Тоан, А.И. Бескровный, А.И. Мададзада, Д.И. Исмаилов, Р.Н. Мехдиева, С.Г. Джабаров Э.М. Керимова, “Магнитная структура в халькогенидах $TlFeS_2$ и $TlFeSe_2$ Физика и техника полупроводников” т. 49, № 7 (2015), с. 899-903. (E.B Asgerov, N.T Dang, A.I Beskrovnyy, A.I Madadzada, D. I. Ismayilov, R. N. Mehdiyeva , S. H. Jabarov, E. M. Karimova, Semiconductors, Volume 49, Issue 7, July 2015,pp 879-882.
2. Балагуров А.М., А.И. Бескровный, В.В. Журавлев, Г.М. Миронова, И.А. Бобриков, Д. Неов, С.Г. Шеверёв, Дифрактометр для исследований переходных процессов в реальном времени на импульсном источнике нейтронов ИБР-2. Поверхность. Рентгеновские, синхротронные и нейтронные исследования. Принята в печать (2015). (Journal of Surface Investigation. X-ray, Synchrotron and Neutron Techniques, (2015), accepted.
3. Гусев А.И., Курлов А.С., Бобриков И.А., Балагуров А.М., “Сверхструктура $V_8C_{7-\delta}$ в порошках нестехиометрического карбида ванадия”, Письма в ЖЭТФ, т. 102, № 3 (2015), с. 179-185. Gusev A.I., Kurlov A.S., Bobrikov I.A., Balagurov A.M., “$V_8C_{7-\delta}$ superstructure in nonstoichiometric vanadium carbide powders”, JETP Letters, 2015, Vol. 102, Issue 3, pp. 154-160.
4. Джабаров С.Г., Мамедов Т.Г., Мамедов А.И., Кичанов С.Е., Алиева В.Б., Лукин Е.В. “Структурный фазовый переход в TlGaSe2 при высоком давлении”, Поверхность. Рентгеновские, синхротронные и нейтронные исследования, № 1 (2015), с. 40-45. Jabarov S.H., Mammadov T.G., Mammadov A.I., Kichanov S.E., Aliyeva V.B., Lukin E.V. “Structural phase transition in $TlGaSe_2$ under high pressure” Journal of Surface Investigation. X-ray, Synchrotron and Neutron Techniques, v. 9, 1 (2015), p. 35-40.
5. Руткаускас А.В., Д.П.Козленко, И.О.Троянчук, С.Е.Кичанов, Е.В.Лукин, Б.Н.Савенко “Подавление антиферромагнитного состояния в кобальтите $La_{0.82}Ba_{0.18}CoO_3$ при высоком давлении” Письма в ЖЭТФ, т. 101, №.12 (2015), с.919–924. Rutkauskas A.V., Kozlenko D.P., Troyanchuk I.O., Kichanov S.E., Lukin E.V., Savenko B.N. “Suppression of the antiferromagnetic state in $La_{0.82}Ba_{0.18}CoO_3$ cobaltite at high pressure”, JETP Letters, v. 101 (2015), p. 820-824.
6. Турченко В.А., Труханов А.В., Бобриков И.А., Труханов С.В., Балагуров А.М., “Исследование кристаллической и магнитной структуры $BaFe_{11.4}Al_{0.6}O_{19}$ в широком интервале температур”, Поверхность. Рентгеновские, синхротронные и нейтронные исследования, № 1 (2015), стр. 21-27. Turchenko V.A., Trukhanov A.V., Bobrikov I.A., Trukhanov S.V., Balagurov A.M., “Study of the crystalline and magnetic structures of $BaFe_{11.4}Al_{0.6}O_{19}$ in a wide temperature range”, Journal of Surface Investigation. X-ray, Synchrotron and Neutron Techniques, 2015, Vol. 9, Issue 1, pp. 17-23.
7. Ata-Allah S.S., Balagurov A.M., Hashhash A., Bobrikov I.A., Hamdy Sh., “Refinement of atomic and magnetic structures using neutron diffraction for synthesized bulk and nano nickel zinc gallate ferrite”, Physica B (2015), accepted.
8. Asgerov E.B., N.T. Dang, D.I. Ismayilov, S.E. Kichanov, R.N. Mehdiyeva, A.I. Madadzada, S.H. Jabarov, E.M. Kerimova, E.V. Lukin, “High-pressure effect on the chain-like crystal structure of the semiconductors $TlFeSe_2$ and $TlFeS_2$”, Modern Physics Letters B, v. 29 (2015), p. 1550024 (1-8).
9. Balagurov A.M., Bobrikov I.A., Pomjakushin V.Yu., Sheptyakov D.V., Yushankhai V.Yu., “Interplay between structural and magnetic phase transitions in copper ferrite studied with high-resolution neutron diffraction”, Journal of Magnetism and Magnetic Materials, Vol. 374 (2015), pp. 591-599.
10. Belozerova N.M., S.E. Kichanov, Z. Jirak, D.P. Kozlenko, M. Kacenka, O. Kaman, E.V. Lukin, B.N. Savenko “High pressure effects on the crystal and magnetic structure of nanostructured manganites $La_{0.63}Sr_{0.37}MnO_3$ and $La_{0.72}Sr_{0.28}MnO_3$”, Journal of Alloys and Compounds, v. 646 (2015), p. 998-1003.
11. Burzo E., M. Valeanu, D.P. Kozlenko, S.E. Kichanov, A.V. Rutkauskas, · B.N. Savenko “Magnetic and transport properties of $Ca_{1.5}La_{0.5}FeMo_{1-x}W_xO_6$ perovskites”, Journal of Alloys and Compounds, v. 621 (2015), p. 71-77.
12. Gorkovenko EA, Kichanov SE, Kozlenko DP, Belushkin AV, Wąsicki J, Nawrocik W, Mielcarek J, Dubrovinsky LS, Lathe C, Savenko BN “The Pressure-Induced Polymorphic Transformations in Fluconazole”, J Pharm Sci., doi: 10.1002/jps.24644 (2015).
13. Jirák, Z.; Kačenka, M.; Kaman, O.; Maryško, M.; Belozerova, N.; Kichanov, S.; Kozlenko, D. “Role of surface on magnetic properties of $La_{1-x}Sr_xMnO_{3+\delta}$ nanocrystallites”, IEEE Transactions on Magnetics, 51, 11 (2015), p. 1-4.
14. Karpinsky, D., I.O. Troyanchuk, N.V. Pushkarev, A. Dziaugys, V. Sikolenko, V. Efimov, A.L. Kholkin, “Evolution of electromechanical properties of $Bi_{1-x}Pr_xFeO_3$ solid solution across the rhombohedral-orthorhombic phase boundary: role of covalency”, J. Alloys. Comp., v. 638 (2015), p. 429-434.
15. Keppler, R., Ullemeyer, K., Behrmann, J.H., Stipp, M., Kurzawski, R.M. & Lokajícek, T., “Crystallographic preferred orientations of exhumed subduction channel rocks from the Eclogite Zone of the TauernWindow (Eastern Alps, Austria), and implications on rock elastic anisotropies at great depths”, Tectonophysics, v. 647-648 (2015), p. 89-104.
16. Kholmurodov Kh.T., Ibragimova S.A., Gladishev P.P., Vannikov A.V., Tameev A.R., Zelenyak T.Yu., “Molecular Dynamics Simulations of Perovskites: The Effect of Potential Function Representation on Equilibrium Structural Properties”, Open Journal of Physical Chemistry, v. 5(4) (2015).
17. Kozlenko D.P., E. Burzo, P. Vlaic, S. E. Kichanov, A. V. Rutkauskas & B. N. Savenko “Sequential Cobalt Magnetization Collapse in $ErCo_2$: Beyond the Limits of Itinerant Electron Metamagnetism” Scientific Reports, v. 5 (2015), p. 8620.
18. Kozlenko D.P., N. T. Dang, S. E. Kichanov, E. V. Lukin, A.M. Pashayev, S. G. Jabarov, L. S. Dubrovinsky, H.-P.Liermann, W. Morgenroth, A. I. Mammadov, R.Z.Mekhtieva, V.G. Smotrakov and B. N. Savenko “Competing magnetic states and structural modifications in multiferroic YMn_2O_5 at high pressure” Physical Review B v. 92 (2015), p. 134409 (1-7).
19. Sikolenko, V., I. Troyanchuk, M. Bushinsky, V. Efimov, L. Keller, J.S. White, F.R. Schilling, S. Schorr, “High pressure induced spins state crossover in $Sr_2CaYCo_4O_{10.5}$”, J. Phys.: Cond. Mat. v. 27 (2015), p. 046005.
20. Troyanchuk, I., M.V. Bushinsky, V. Sikolenko, V. Efimov,

N.V. Volkov, D.M. Többens, C. Ritter, B. Raveau, "Ferromagnetism in single-valent manganites", J. Alloys. Comp. v. 619 (2015), p. 719-725.
21. Troyanchuk, I., Bushinsky M.V., Volkov N.V., Sikolenko V., Efimova E.A., C. Ritter, "Role of Superexchange Interaction in the Ferromagnetism of Manganites", JETP, v. 120 (2015), p. 97-102.
22. Troyanchuk, I., M.V. Bushinsky, V. Efimov, S. Schorr, C. Ritter and V. Sikolenko "Ferromagnetic ordering in $La_{0.7}Sr_{0.3}Mn^{3+}{}_{0.85}Nb^{5+}{}_{0.15}O_3$ manganite", Powder Diffraction v. 30 (2015), S97-S100.
23. Troyanchuk, I., M.V. Bushinsky, D.V. Karpinsky, N.V. Tereshko, V.M. Dobryansky, D.M. Többens, V. Sikolenko, V. Efimov "Magnetic interactions in $La_{0.7}Sr_{0.3}Mn_{1-x}Me_xO_3$ (Me = Ga, Fe, Cr) manganites", J. Magn. Magn. Mater. v. 394 (2015), p. 212-216.
24. Troyanchuk, I., M.V. Bushinsky, D.V. Karpinsky, V.V. Sikolenko, M. Frontzek, V.V. Efimov "Magnetic ordering in $Ln_{0.7}Sr_{0.3}Mn_{0.85}Sb_{0.15}O_3$ (Ln = La, Nd, Sm, Eu)", Physics of the Solid State, v. 57 (2015), p. 1128-1133.
25. Troyanchuk, I., M.V. Bushinsky, N.V. Tereshko, V.M. Dobryanskii, V.V. Sikolenko, D.M. Többens "Magnetic properties of manganites doped with gallium, iron and chromium ions", JETP v. 120 (2015), p. 838-843.
26. Trukhanov A.V., Turchenko V.O., Bobrikov I.A., Trukhanov S.V., Kazakevich I.S., Balagurov A.M., "Crystal structure and magnetic properties of the $BaFe_{12-x}Al_xO_{19}$ (x = 0.1–1.2) solid solutions", Journal of Magnetism and Magnetic Materials, Vol. 393 (2015), pp. 253-259.
27. Tsvyashchenko A.V., D.A. Salamatin, V.A. Sidorov, A.E. Petrova, L.N. Fomicheva, S.E. Kichanov, A.V. Salamatin, A. Velichkov, D.P. Kozlenko, A.N. Nikolaev, G.K. Ryasny, O.L. Makarova, D. Menzel and M. Budzynski "Incommensurate antiferromagnetism induced by a charge density wave in the cubic phase of $TbGe_{2.85}$" Physical Review B v. 92 (2015), p. 104426 (1-7).
28. Valkov S., D. Neov, A. Beskrovny, D. Kozlenko, P. Petrov, "X - Ray and Neutron Diffraction of TiAl Alloys", Proceedings of the Sixth International Scientific Conference – FMNS, Blagoevgrad, Bulgaria, 10-14 June 2015, Vol.2, p. 80-85.

Nanostructured materials (small-angle scattering and diffraction)

29. Balagurov A.M., Bobrikov I.A., Bokuchava G.D., Vasin R.N., Gusev A.I., Kurlov A.S., Leoni M., "High-resolution neutron diffraction study of microstructural changes in nanocrystalline ball-milled niobium carbide $NbC_{0.93}$", Materials Characterization, Vol. 109 (2015), pp. 173-180.
30. Bokuchava G.D., Gorshkova Yu.E., "Analysis of small angle neutron scattering from nanocrystalline niobium carbide particles using global scattering functions", Journal of Optoelectronics and Advanced Materials, Vol. 17, Issue 7-8 (2015), pp. 985-990.
31. Bulavin L.A., S. O. Samoilenko, S. E. Kichanov, D. P. Kozlenko, O. I. Ivankov, V. S. Gurin, G. E. Rachkovska, G. B. Zaharevych, A. Kh. Islamov, B. N. Savenko "Nanoformation in doped silicate glass and its fractal dimensions", Nuclear Physics and Atomic Energy, v. 16 (2015), p. 152–156.
32. Kichanov S. E., D. P. Kozlenko, A. V. Belushkin, E. V. Tretyak, G. P. Shevchenko, G. E. Malashkevich, B. N. Savenko "Structural Aspects of the Formation of Optical Properties of Composite Garnet Phosphors" JINR News, № 2 (2015), p. 18-21.
33. Samoylenko S.A., E.V. Tret'yak, G.P. Shevchenko, S.E. Kichanov, D.P. Kozlenko, G.E. Malashkevich, A.P. Stupak, B.N. Savenko "Crystal Structure and Optical Properties of $Lu_3Al_5O_{12}$:Ce^{3+} Obtained by a Colloidal Chemical Synthesis Method" Journal of Applied Spectroscopy, v. 81(6) (2015), p. 1048-1055.

Soft matter, liquids (small angle scattering and diffraction)

34. Авдеев М.В., Петренко В.И., Феоктистов А.В., Гапон И.В., Аксенов В.Л., Векаш Л., Копчанский П. "Нейтронные исследования феррожидкостей", Укр. фiз. журн., т. 60 (2015), с. 728-736 (Avdeev M.V., Petrenko V.I., Feoktystov A.V., Gapon I.V., Aksenov V.L., Vekas L., Kopcansky P., Neutron investigations of ferrofluids. Ukr. J. Phys., 2015, 60(8), 728-736).
35. Авдеев М.В., Иванов А.О., Зубавичус Я.В., Велигжанин А.А., Эффекты взаимодействия в жидких коллоидных системах с магнитными наночастицами: аспекты исследования на синхротронных и нейтронных источниках, Вестник РФФИ, 2(86) 2015, с. 48–54. (Avdeev M.V., Ivanov A.O., Zubavichus Y.V., Veligzhanin A.A., Interaction effect in liquid colloidal systems with magnetic nanoparticles: aspects of research at sources of synchrotron radiation and neutrons, RFBR Journal, 2015, 2(86), 48-54 (in Russian))
36. Булавiн Л. А., М. В. Авдєєв, О. О. Ключников, А. В. Нагорний, В. І. Петренко. Нейтронографія магнітних рідинних систем. К.:Чорнобиль. 2015. 244с. (Монография на украинском языке).
37. Гапон И.В., Петренко В.И., Авдеев М.В., Булавин Л.А., Хайдуков Ю.Н., Солтведель О., Зависова В., Копчански П., Учет дифузного рассеяния при анализе зеркального отражения нейтронов на границе раздела магнитная жидкость - кремний, Поверхность. Рентгеновские, синхротронные и нейтронные исследования, №4 (2015), с. 8-13. (Gapon I.V., Petrenko V.I., Avdeev M.V., Bulavin L.A., Khaydukov Yu.N., Soltwedel O.,.Zavisova V, Antal I., Kopcansky P., Consideration of Diffuse Scattering in the Analysis of Specular Neutron Reflection at the Magnetic Fluid–Silicon Interface, Journal of Surface Investigation. X_ray, Synchrotron and Neutron Techniques, 2015, 9(2), 320–325.).
38. Жаргалан Н., Тропин Т.В., Авдеев М.В., Аксенов В.Л., Исследование кинетики растворения фуллерена С60 в растворителях разной полярности методом УФ-Вид спектроскопии, Поверхность. Рентгеновские, синхротронные и нейтронные исследования, №1 (2015), с. 16-20 (Jargalan N., Tropin T.V., Avdeev M.V., Aksenov V.L., Investigation of the dissolution kinetics of fullerene C60 in solvents with different polarities by UV-Vis spectroscopy,/ Journal of Surface Investigation. X-Ray, Synchrotron and Neutron Techniques, 2015, Vol. 9, No. 1, pp. 12-16).
39. Кизима Е.А., Томчук А.А., Булавин Л.А., Петренко В.И., Алмаши Л., Коробов М.В., Волков Д.С., Михеев И.В., Кошлань И.В., Кошлань Н.А., Блаха П., Авдеев М.В., Аксенов В.Л., Структура и токсичность водных растворов фуллерена С60. Поверхность. Рентгеновские, синхротронные и нейтронные исследования, № 1 (2015), с. 5–9 (Kyzyma E.A., Tomchuk A.A., Bulavin L.A., Petrenko V.I., Almasy L., Korobov M.V., Volkov D.S., Mikheev I.V., Koshlan I.V., Koshlan N.A., Blaha P., Avdeev M.V., Aksenov V.L., Structure and Toxicity of Aqueous Fullerene C60 Solutions Journal of Surface Investigation. X_ray, Synchrotron and Neutron Techniques, 2015, Vol. 9, No. 1, pp. 5–9).
40. Киселев М.А., Е.В. Земляная, Е.И. Жабицкая, В.Л. Аксенов, "Исследование однослойных везикул ДМФХ в

водных растворах сахарозы методами малоуглового рассеяния нейтронов и рентгеновских лучей", Кристаллография, т. 60, №1 (2015), с. 140-150.
41. Ковальчук М.В., Н.Н. Новикова, М.А. Киселев, С.Н. Якунин. Диагностика липидных наноструктур на основе высокоразрешающих структурно-чувствительных методов с использованием рентгеновского излучения и нейтронов. Вестник РФФИ № 2 (86) (2015), с. 11-15.
42. Лебедев В.Т., Вуль А.Я., Тропин Т.В., Нейтронные исследования и структурная диагностика функционализированных углеродных наноструктур в растворах, Вестник РФФИ, №2 (86) (2015), с. 55-61 (Lebedev V.T., Vul A.Ya., Tropin T.V., Neutron Research and Structural Characterization of Synthesized Vi Arcjet and Functionalized Carbon Nanostructures in Solutions, RFBR Journal, 2015, N2 (86), pp. 55-61).
43. Петренко В.И., Авдеев М.В., Булавин Л.А., Алмаши Л., Григорьева Н.А., Аксенов В.Л., "Влияние избытка ПАВ на устойчивость магнитных жидкостей на основе слабополярного растворителя по данным малоуглового рассеяния нейтронов", Кристаллография, 2015, в печати.
44. Тропин Т.В., Шмельцер Ю.В.П., Аксенов В.Л., "Современные аспекты кинетической теории стеклования", Успехи физических наук, 2015, принята в печать.
45. Фельдман, Т.Б. Иваньков, А.И. Муругова, Т.Н. Куклин, А.И. Шелякин, П.В. Яковлева, М.А. Горделий, В.И. Белушкин, А.В. Островский, М.А., "Исследование супрамолекулярной организации зрительного пигмента родопсина в фоторецепторной мембране методом малоуглового рассеяния нейтронов с вариацией контраста" Доклады Академии Наук, т. 465, № 5 (2015), с. 1-5.
46. Avdeev M.V., Petrenko V.I., I.V.Gapon, L.A.Bulavin, A.A.Vorobiev, O.Soltwedel, M.Balasoiu, L.Vekas, V.Zavisova, P.Kopcansky, "Comparative structure analysis of magnetic fluids at interface with silicon by neutron reflectometry", Applied Surface Science, v. 352 (2015), pp. 49–53.
47. Balasoiu M., V.T. Lebedev, I. Bica, Yu.L. Raikher, „Investigation of dimethyl siloxane magnetic elastomers by means of small-angle neutron scattering", in Actual problems of condensed matter physics, Ed. Yu.M. Raikher, ISBN 978-5-7691-2418-1 (Russ.), Perm 106-115 (2015).
48. M. Balasoiu, O. I. Ivankov, D.V. Soloviov, S.N. Lysenko, R.M. Yakushev, A-M. Balasoiu-Gaina, N. Lupu, "Microstructure investigation of a CoFe2O4/lauric acid/DDS-Na/H2O ferrofluid, Journal of Optoelectronics and Advanced Materials, v. 17 (7-8) (2015), p. 1114-1121.
49. Bica I., M. Balasoiu, M. Bunoiu, L. Iordaconiu, G. Cirtina, "Influence of the longitudinal magnetic field on the turning angle of a cylindrical bar-shaped magnetorheological elastomer", J. Optoelectron. Adv. Mater. v. 17 (9-10) (2015), p. 1379-1384.
50. Bodale, I., Oprisan, M., Stan, C., Tufescu, F., Racuciu, M., Creanga, D., & Balasoiu, M. "Nanotechnological Application Based on CoFe2O4 Nanoparticles and Electromagnetic Exposure on Agrotechnical Plant Growth. In 3rd International Conference on Nanotechnologies and Biomedical Engineering, Springer Singapore, p. 153-156, (2016).
51. Bulavin L.A., Soloviov D.V., et al. "Small-Angle X-Ray Scattering and Differential Scanning Calorimetry Studies of DPPC Multilamellar Structures Containing Membranotropic Agents of Different Chemical Nature", Ukrainian journal of physics, v. 60(9) (2015), p.908-913.
52. Bulavin, L. A., Soloviov, D. V., Gordeliy, V. I., Svechnikova, O. S., Krasnikova, A. O., Kasian, N. A., & Lisetski, L. N. "Lyotropic model membrane structures of hydrated DPPC: DSC and small-angle X-ray scattering studies of phase transitions in the presence of membranotropic agents". Phase Transitions, (2015), ahead-of-print, p. 1-11.
53. Dushanov E.B., Kholmurodov Kh.T., Koltovaya N.A., "Simulation of Mutant P32T Homo and Heterodimers of Human Inosine Triphosphate Pyrophosphatase hITPA", Biophysics, v. 60, No. 4 (2015), p. 529–537.
54. Eremin R.A., Kholmurodov Kh.T., Petrenko V.I., Avdeev M.V., Chapter 3. Oleic Acid in Benzene and Decalin Solutions: Solvation Shell Effect on Small-Angle Neutron Scattering – pp. 25-34. B Kholmurodov Kh. T. (Editor) Computational Materials and Biological Sciences. New York: Nova Science Publishers, 2015. – 188 P.
55. Eremin R.A., Kholmurodov Kh.T., Petrenko V.I., Rosta L., Grigoryeva N.A., Avdeev M.V. On the microstructure of organic solutions of mono-carboxylic acids: Combined study by infrared spectroscopy, small-angle neutron scattering and molecular dynamics simulations. Chemical Physics, v. 461 (2015), p. 1-10.
56. Gibhardt, H., Haramagatti, C. R., Islamov, A. K., Ivankov, O. I., Kuklin, A. I., & Eckold, G. "Ordering Phenomena in Surfactant Systems: From Micellar Solutions to Gel and Crystalline Phases", Zeitschrift für Physikalische Chemie, v. 229 (10-12) (2015), p. 1869-1885.
57. Gorshkova Yu.E., "Fusion of unilamellar DMPC vesicles in presence of the sulfoxides: Effect of time and concentration", Journal of optoelectronics and advanced materials, v. 17, No. 9-10 (2015), p. 1532-1537.
58. Gorshkova Yu.E., O.I. Ivankov, :Structure and phase transitions of the multilamellar DMPC membranes in presence of the DMSO and DESO sulfoxides", Journal of optoelectronics and advanced materials (2015), under review.
59. Itkis D.M., Velasco-Velez J.J., Knop-Gericke A., Vyalikh A., Avdeev M.V., Yashina L.V., „Probing of electrochemical interfaces by photons and neutrons in operando". ChemElectroChem, v. 2 (2015), p. 1427–1445.
60. Jargalan N., Tropin T.V., Avdeev M.V., Aksenov V.L., Investigation and modeling of evolution of UV-Vis spectra of C60/NMP solution. Nanosystems: physics, chemistry, mathematics, 2015, accepted.
61. Kenoufi A., Kholmurodov Kh.T., "Symbolic Regression of Inter-Atomic Potentials via Genetic Programming", Biological and Chemical Research, v. 2015 (2015), p. 1-10.
62. Kiselev M.A., E.V. Zemlyanaya, O.M. Ipatova, A.Yu. Gruzinov, E.V. Ermakova, A.V. Zabelin, E.I. Zhabitskaya, O.S. Druzhilovskaya, V.L. Aksenov, "Application of small-angle X-ray scattering to the characterization and quantification of the drug transport nanosystem based on the soybean phosphatidylcholine", J. Pharm. Biomed. Anal., v. 114 (2015), p. 288-291.
63. Kholmurodov Kholmirzo T. Editor. «Computational Materials and Biological Sciences» ISBN: 978-1-63482-541-2, Nova Science Publishers, New York (2015), 230 p.
64. Khusenov M.A., Dushanov E.B., Kholmurodov Kh.T., "Correlation Effect of the Van-der-Waals and Intramolecular Forces for the Nucleotide Chain - Metallic Nanoparticles Binding in a Carbon Nanotube Matrix of Periodic Boundaries", British Journal of Applied Science & Technology, v. 8(3) (2015), p. 313-323.
65. Khusenov M.A., Dushanov E.B., Kholmurodov Kh.T., "Molecular Dynamics Simulations of the Nucleotides and Metallic Nanoparticles Interaction on a Carbon Nanotube

Matrix", Materials Transactions, v. 56, No.9 (2015), p. 1390-1393.
66. Khusenov M.A., Dushanov E.B., Kholmurodov KH.T., Zaki M.M., Sweilam N.H., "Differences in behavior of purine and pyrimidine nucleotides on interactions with metallic nanoparticles inside of a carbon nanotube matrix", Journal of Basic and Applied Research International, v. 6(1) (2015), p. 45-56.
67. Kopcansky P., Siposova K., Melnikova L., Bednarikova Z., Timko M., Mitroova Z., Antosova A., Garamus V.M., Petrenko V.I., Avdeev M.V., Gazova Z., "Destroying activity of magnetoferritin on lysozyme amyloid fibrils", J. Magn. Magn. Mater., v. 377 (2015), p. 267–271.
68. Kyzyma O.A., Tomchuk A.V., Avdeev M.V., Tropin T.V., Aksenov V.L., Korobov M.V., "Structural researches carbonic fluid nanosystems", Ukr. J. Phys., v. 60, No. 9 (2015), p. 835-843 (Кизима Е.А., Томчук А.В., Авдеев М.В., Тропин Т.В., Аксёнов В.Л., Коробов М.В., Структурные исследования жидкостных углеродных наносистем, Укр. фіз. журн., 2015. Т. 60, № 9, с. 835-844)
69. Lombardo D., M. Kiselev, S. Magazu and P. Calandra, "Amphiphiles Self-assembly:Basic Concepts and Future Perspectives of Supramolecular Approaches" Advances in Condensed Matter Physics (2015), accepted.
70. Mamedov T.N., D.S. Andrievskii, M. Balasoiu, K.I. Gritsaj, V.N. Duginov, A.L. Getalov, E.N. Komarov, S.A. Kotov, A.E. Moroslip, I.I. Pavlova, V.G. Scherbakov, S.I. Vorob'ev, C. Stan, "Magnetic properties investigation of a ferrofluid with cobalt ferrite nanoparticles using polarized muons", J. Optoelectron. Adv. Mater. v. 17(7-8) (2015), p. 1086-1091.
71. Melníková L., Petrenko V.I., Avdeev M.V., Garamus V.M., Almásy L., Ivankov O.I., Bulavin L.A., Mitróová Z., Kopčanský P., "SANS contrast variation study of magnetoferritin structure at various iron loading", J. Magn. Magn. Mater., v. 377 (2015), p. 77–80.
72. Murugova T.N., A.V.Vlasov, O.I.Ivankov, A.V.Rogachev, D.V.Soloviov, A.Zhigunov, Yu.S.Kovalev, Yu.L.Ryzhykau, E.V.Zinovev, A.Round, V.I.Gordeliy, A.I.Kuklin "Low resolution structural sdudies of apoferritin via SANS and SAXS: The Effect of concentration", Journal of optoelectronics and advanced materials, v.17, No 9-10 (2015), p.1397-1402.
73. Nagornyi A.V., Petrenko V.I., Avdeev M. V., Solopan S. O., Elenich O. V. , Belous A. G. , Veligzhanin A. A. , Gruzinov A. Yu. , Zubavichus Ya. V. , Bulavin L. A., Structure of water-based magnetic liquids by small-angle x-ray scattering. Romanian Journal of Physics, accepted (2015).
74. Oprica, L., Nadejde, C., Andries, M., Puscasu, E., Creanga, D., & Balasoiu, M. "Magnetic contamination of environment-laboratory simulation of mixed iron oxides impact on microorganisms cells", Environmental Engineering and Management Journal, v. 14(3) (2015), p. 581-586.
75. Ordon M., Yu. Gorshkova, M. Ossowska-Chruściel, "Lithocholic acid derivative in the dimethyl sulfoxide presence: Morphology and phase transitions", Organic and Biomolecular Chemistry, (2015), submitted.
76. Petrenko V.I., Avdeev M.V., Garamus V.M., Bulavin L.A., Kopcansky P., "Impact of polyethylene glycol on aqueous micellar solutions of sodium oleate studied by small-angle neutron scattering", Colloids and Surfaces A, v. 480 (2015), p. 191–196.
77. Petrenko V.I., Bulavin L.A., Avdeev M.V., Kopcansky P., Book "Nanobiophysics: Fundamental and Applications". Chapter 5. Structure diagnostics of biorelevant associates and complexes in liquid nanosystems by small-angle scattering. Pan Stanford Publishing Pte Ltd. (2016) pp. 120-150. In press.
78. Petrenko V.I., Ivankov O.I., Avdeev M.V., Nikolaienko T.Yu., "Spatial structure of liquid systems with organic-coated magnetite nanoparticles". Bulletin of Taras Shevchenko National University of Kyiv Series Physics & Mathematics, 2015, 3, in press.
79. Prylutskyy Yu.I., Cherepanov V.V., Evstigneev M.P., Kyzyma O.A., Petrenko V.I., Styopkin V.I., Bulavin L.A., Davidenko N.A., Wyrzykowski D., Woziwodzka A., Piosik J., Kaźmierkiewicz R., Ritter U., "Structural self-organization of C60 and cisplatin in physiological solution", Phys.Chem.Chem.Phys., v. 17 (2015), p. 26084-26092.
80. Prylutskyy Yu.I., Evstigneev M.P., Cherepanov V.V., Kyzyma O.A., Bulavin L.A., Davidenko N.A., Scharff P., "Structural organization of C60 fullerene, doxorubicin, and their complex in physiological solution as promising antitumor agents", J. Nanopart. Res., 17:45 (2015).
81. Rajnak M., Petrenko V.I., Avdeev M.V., Ivankov O.I., Feoktystov A., Dolnik B., Kurimsky J., Kopcansky P., Timko M., "Direct observation of electric field induced pattern formation and particle aggregation in ferrofluids", Applied Physics Letters, v. 107 (2015), p. 073108.
82. Ryzhykau Yu., M. Nikolaev, D. Soloviov, O. Ivankov, Yu. Kovalev, T. Murugova, E. Zynoviev, A. Vlasov, A. Rogachev, V. Borshchevskiy, V. Gordeliy, A. Kuklin "Small-angle scattering studies of phospholipids phase transition in membrane mimicking systems", FEBS Journal, v 282, Issue Supplement s1 (2015), p. 235.
83. Schmelzer J.W.P., T.V. Tropin, "Kinetic criteria of glass-formation, pressure dependence of the glass-transition temperature, and the Prigogine-Defay ratio", Journal of Non-Crystalline Solids, v. 407 (2015), p. 170-178.
84. Tomchuk O.V., Volkov D.S., Bulavin L.A., Rogachev A.V., Proskurnin M.A., Korobov M.V., Avdeev M.V., "Structural characteristics of aqueous dispersions of detonation nanodiamond and their aggregate fractions by small-angle neutron scattering" Journal of Physical Chemistry C, v. 119 (2015), p. 794-802.
85. Tropin T.V., Schulz G., Schmelzer J.W.P., Schick C., "Heat capacity measurements and modeling of polystyrene glass transition in a wide range of cooling rates", Journal of Non-Crystalline Solids, v. 409 (2015), p. 63-75.
86. Vlasov A., T.Murugova, S.Grudinin, O.Ivankov, D.Soloviov, A.Rogachev, A.Round, Y.Ryzhykau, A.Mishin, T.Balandin, V.Borschevskiy, V.Gordeliy, A.Kuklin "Protein structure and structural ordering versus concentration dependence", FEBS Journal, v 281, Issue Supplement s1 (2015), p. 593.
87. Zhernenkov M., Bolmatov D., Soloviov D., et al. "Phonon-mediated passive transport in DPPC lipid bilayer across the phase transition", Journal of the American Chemical Society (2015), submitted.

Thin films (reflectometry, polarized neutrons)

88. Боднарчук В.И, П. Петров, Д.П. Козленко, Д. Дечев, Н. Иванов, И. Мартев, А.В. Нагорный, И.А. Касаткин, Исследование свойств многослойных нанопокрытий MeN/MeN, полученных методом DC-магнетронного распыления, Me = Ti, W, Поверхность. Рентгеновские, синхротронные и нейтронные исследования, принято в печать (2015).
89. Боднарчук В.И., Садилов В.В., Маношин С.А., Ерхан Р.В., Авдеев М.В., Ярадайкин С.П. «Геометрический фактор в методе спин-эхо малоугловом рассеянии нейтронов с линейно растущими во времени

магнитными полями», Поверхность. Рентгеновские, синхротронные и нейтронные исследования, принято в печать (2015).
90. Кожевников С.В., В.Д. Жакетов, А.В. Петренко, М.В. Булавин, А.Е. Верхоглядов, С.А. Куликов, Е.П. Шабалин, "Использование криогенного замедлителя на нейтронном рефлектометре РЕМУР", Поверхность, № 1 (2016), с. 1-11.
91. Никитенко Ю.В., "Рефлектометрия нейтронов в стационарном и осциллирующем магнитных полях", Поверхность, №7 (2015), с. 1-8.
92. Никитенко Ю.В., А.В. Петренко, Н.А. Гундорин, Ю.М. Гледенов, В.Л. Аксёнов, "Изотопно-идентифицирующая рефлектометрия нейтронов", Кристаллография, т.60, №3 (2015), с. 385-399.
93. Никитенко Ю.В., "Спин-эхо спектрометр нейтронов скользящей геометрии", Поверхность, №2 (2016), с. 1-9.
94. Рябухина М.В., Е.А. Кравцов, Д.В. Благодатков, Л.И. Наумова, Ю.В. Никитенко, В.В. Проглядо, Ю. Хайдуков, "Магнетизм сверхрешеток Fe/Cr/Gd", Поверхность. Рентгеновские, синхротронные и нейтронные исследования. № 1 (2015), с. 1-3.
95. Татарский Д.А., А.В. Петренко, С.Н.Вдовичев, О.Г.Удалов, Ю.В.Никитенко, А.А. Фраерман, "Невзаимная ячейка для нейтронов", Письма в ЖЭТФ, т. 102 (2015), с. 721-725.
96. Doroshkevych O.S., Shylo A.V., Kirillov A.K., Saprykina A.V., Danilenko I.A., Troitskiy G.A., Konstantinova T.E., Zelenyak T.Yu. "Magnetically Induced Electrokinetic Phenomena in the Surface Layers of Zirconia Nanoparticles", Journal of Surface Investigation. X-ray, Synchrotron and Neutron Techniques, v. 9, No. 3 (2015), pp. 564–572.
97. Kozhevnikov S.V., V.K. Ignatovich, Yu.V. Nikitenko, F. Ott, A.V. Petrenko, "System of neutron microbeams from a planar waveguide", Письма в ЖЭТФ, т. 102 (2015), с. 3-9.
98. Kozhevnikov S.V., F. Ott, F. Radu, "Neutron methods for the direct determination of the magnetic induction in thick films", J. Magn. Magn. Mater. (2015), accepted.
99. Ott F., S. Kozhevnikov, A. Thiaville, J. Torrejon, M. Vazquez, "Shaping micron-sized cold neutron beams", Nucl. Instrum. and Meth. A v. 788 (2015), p. 29-34.
100. Patroi D., V.D. Zhaketov, Yu.V. Nikitenko, M.M. Codescu, E.A. Patroi, E. Manta, "Neutron Depolarization Investigations of Spring Exchange Interaction Nanocomposites", J. Optoelectronics and Advanced Materials, Vol. 9, No. 9-10 (2015), p. 1328 – 1331.

Atomic and magnetic dynamics (inelastic neutron scattering)

101. Antonov A.S., Pozharskii A.F., Ozeryanskii V.A. Filarowski A., Suponitsky K.Yu., Tolstoy P.M., Vovk M.A. Ring lithiation of 1,8-bis(dimethylamino)naphthalene: another side of the 'proton sponge coin'. Dalton Transaction, 2015, DOI: 10.1039/C5DT02482J.
102. Drużbicki, K., Mielcarek, J., Kiwilsza, A., Toupet, L., Collet, E., Pajzderska, A., Wąsicki J.:'Computationally assisted (solid-state density functional theory) structural (X-ray) and Vibrational Spectroscopy (FT -IR, FT -RS, TDs-THz) characterization of the cardiovascular drug lacidipine,' Cryst. Growth. Des., v. 15 (6) (2015), p. 2817−2830.
103. Drużbicki, K., Mikuli, E., Pałka, N., Zalewski, S., Ossowska-Chruściel, M. D. 'Polymorphism of resorcinol explored by complementary vibrational spectroscopy (FT -RS, THz-TDS, INS) and firstprinciples solid-state computations (plane-wave DFT),' J. Phys. Chem. B, v. 19(4) (2015), p. 1681−1695.
104. Filarowski A., Lopatkova M, Lipkowski P., Van der Auwerar M., Leen V., Dehaen W. "Solvatochromism of BODIPY-Schiff base Dye", Journal of Physical Chemistry B, v. 119 (2015), p. 2576-2584.
105. Hetmańczyk J., Hetmańczyk Ł., Migdał-Mikuli A., Mikuli E., "Vibrations and reorientations of NH3 molecules in [Mn(NH3)6](ClO4)2 studied by Infrared Spectroscopy and theoretical (DFT) calculations", Spectrochim. Acta A v. 136 (2015), p. 1515-1522. DOI: 10.1016/j.saa.2014.10.044.
106. Hetmańczyk Ł., Hetmańczyk J., "Comparison of vibrational dynamics, thermal behaviour and phase transition in [Ni(NH3)4](ReO4)2 and [Ni(NH3)6](ReO4)2", J. Therm. Anal. Cal. v. 119 (2015), p. 1415-1428. DOI: 10.1007/s10973-014-4292-3.
107. Hołyńska M., Filarowski A., Kochel A., Twaróg K., "Why Does the 2,2′-Bipyridine-4-methyl-3,3′-Dicarboxylic Acid Not Form MOFs: Synthesis, Crystal Structure and Properties of a New Organic Ligand", Journal of Chemical Crystallography, v. 45 (2015), p. 363-368.
108. Kachalkina S.G., Borodkin G.S., Pozharskii A.F., Antonov A.S., Borodkina I.G., Maltsev Y.F., Filatova E.A., Filarowski A., Ozeryanskii V.A., "Base-promoted transformation of 2-C(O)R-1,8-bis(dimethylamino)naphthalenes into benzo[g]indole derivatives", Mendeleev Communications, v. 25 (2015), p. 182-184.
109. Kiwilsza A., Milanowski B., Drużbicki K., Emerson-Coy L., Grzeszkowiak M., Jarek M., Mielcarek J., Lulek J., Pajzderska A., Wąsicki J. 'Mesoporous drug carrier systems for enhanced delivery rate of poorly water-soluble drug: nimodipine', Journal of Porous Materials, v. 22 (3) (2015), p. 817−829.
110. Kozlecki T., Tolstoy P.M., Kwocz A., Vovk M.A., Kochel A., Polowczyk I., Tretyakov P.Yu., Filarowski A., Conformational state of β-hydroxynaphthylamides: Barriers for the rotation of the amide group around CN bond and dynamics of the morpholine ring", Spectrochimica Acta Part A: Molecular and Biomolecular Spectroscopy, v 149 (2015), p. 254-262.
111. Kwocz A., Kochel A., Chudoba D., Filarowski A. "Tautomeric design of ortho-hydroxyheterocyclic Schiff bases. Journal of Molecular Structure", v. 1080 (2015), p. 52-56.
112. Łuczyńska, K., Drużbicki, K., Lyczko, K, Dobrowolski, J. Cz.,'Experimental (X-ray , 13C CP/MASNMR, IR, RS, INS, THz) and Solid-State DFT Study on (1:1) Co-Crystal of Bromanilic Acid and 2,6-Dimethylpyrazine' J. Phys. Chem. B., v. 119 (2015), p. 6852−6872.
113. Mikuli E., Hetmańczyk J., Grad B., Kozak A., Wąsicki J.W., Bilski P., Hołderna-Natkaniec K., Medycki W., The relationship between reorientational molecular motions and phase transitions in polycrystalline [Mg(H2O)6](BF4)2, studied with the use of 1H and 19F NMR and FT-MIR, J. Chem. Phys. v. 142 (2015), p. 064507(1-10).DOI: 10. 1063/1.4907372.
114. Natkaniec I., Sheka E. F., Drużbicki K., Holderna-Natkaniec K., Gubin S. P, Buslaeva E. Y, Tkachev S. V. 'Computationally supported neutron scattering study of parent and chemically reduced graphene oxide', J. Phys. Chem C, v. 119(32) (2015), p. 18650−18662.
115. Ordon M., Gorshkova Y., Ossowska-Chruściel M., "Lithocholic acid derivative in the dimethyl sulfoxide presence: Morphology and phase transitions", Chemistry A European Journal 2015, (submitted).

3. PUBLICATIONS

116. Ordon M., Rudzki A., Juszyńska-Gałązka E., Ossowska-Chruściel M.D., Zając W., Chruściel J., Wojciechowska S., „Phase polymorphism and thermal stability of new cholesterol thioesters derivatives", Liquid Crystals, v. 42, Issue 10, (2015), p. 1405-1418.
117. Pajzderska, A., Drużbicki, K., Kiwilsza, A., Gonzalez, M.A., Jarek, M., Mielcarek, J., Wasicki, J.,'On the relaxation dynamics in active pharmaceutical ingredients: Solid-state 1H NMR, quasi-elastic neutron scattering and periodic DFT study of acebutolol hydrochloride' RSC Advances, v. 5 (71) (2015), p. 57502−57514.
118. Rudzki A., Ossowska-Chruściel M. D., Ordon M., Zając W., Chruściel J., „Thermal analysis and simulation model of natural lithocholic acid", J Therm Anal Calorim, DOI 10.1007/s10973-015-4656-3.
119. Sheka E. F., Natkaniec I., Melnikov V., Drużbicki K. 'Neutron scattering from graphene oxidepaper and thermally exfoliated reduced graphene oxide,' NANOSYSTEMS: PHYSICS, CHEMISTRY, MATHEMATICS, v. 6 (3) (2015), p. 378–393.
120. Szostak E., Hetmańczyk J., Migdał-Mikuli A., Inelastic and elastic neutron scattering studies of the vibrational and reorientational dynamics, crystal structure and solid-solid phase transition in [Mn(OS(CH3)2)6](ClO4)2 supported by theoretical (DFT) calculations, Spectrochim. Acta A, v. 145 (2015), p. 368-375. DOI: 10.1016/j.saa.2015.03. 037.

Applied studies (texture, stresses, geological materials)

121. Бокучава Г.Д., Папушкин И.В., Бобровский В.И., Катаева Н.В., "Эволюция дислокационной структуры аустенитной стали Х16Н15М3Т1 в зависимости от степени холодной пластической деформации", Поверхность. Рентгеновские, синхротронные и нейтронные исследования, № 1 (2015), с. 49-57. G.D. Bokuchava, I.V. Papushkin, V.I. Bobrovskii, N.V. Kataeva, "Evolution in the Dislocation Structure of Austenitic 16Cr–15Ni–3Mo–1Ti Steel Depending on the Degree of Cold Plastic Deformation", Journal of Surface Investigation. X-ray, Synchrotron and Neutron Techniques, 2015, Vol. 9, Issue 1, pp. 44-52.
122. Иванкина Т.И., Маттис З., "О развитии количественного текстурного анализа и применении его в решении задач наук о Земле". // ЭЧАЯ. Т. 46(3). 2015. С. 366-423.
123. Balagurov A.M., Bokuchava G.D., Sumin V.V., Papushkin I.V., "Investigation of precipitation-hardened steels using TOF neutron diffraction", Annex to IAEA-TECDOC-1773 (ISBN: 978-92-0-108915-1): Use of Neutron Beams for Materials Research Relevant to the Nuclear Energy Sector, IAEA, 2015, pp. 6-30.
124. Duliu O. G., Ivankina T.I., Herman E., Ricman C., Tiseanu I., "Orientation Distribution Function of Biotite Platelets Based on Optical, Thin Sections and μ-CT in an Outokumpu (Finland) Biotite Gneiss: Comparison with Neutron Diffraction Texture Analysis", Neues Jahrbuch fur Geologie und Paleontologie, 2015 (submitted).
125. Ivankina T.I., Zel I.Yu., Lokajicek T.,Kern H., Lobanov K.V., Zharikov A.V., "Elastic anisotropy of layered rocks: ultrasonic measurements of biotite gneiss versus texture-based theoretical predictions (effective media modeling)", Tectonophysics, 2015 (submitted).
126. Kaisheva D., Bokuchava G., Papushkin I., Petrov P., "Study of Microstructural Changes and Residual Stresses in Electron Beam Welding of Alloyed Steels", Proc. of Sixth International Scientific Conference of FMNS (FMNS-2015), 10-14 June 2015, Blagoevgrad, Bulgaria, Volume 2 "Physics and Technologies", pp. 48-54. ISSN 1314-0272.
127. Kanitpanyacharoen W., Vasin R., Wenk H.-R., Dewhurst D.N. "Linking preferred orientations to elastic anisotropy in Muderong Shale, Australia", Geophysics, 2015, Vol. 80, №1, pp. C9-C19.
128. Lychagina T., D. Nikolayev, A. Sanin, J. Tatarko, K. Ullemeyer, "Investigation of wheel steel crystallographic texture changes due to modification and thermo-mechanical treatment", IOP Conference Series: Materials Science and Engineering, v. 82 (2015), p. 012107.
129. Lychagina, T. & Nikolayev, D. Quantitative comparison of the measured crystallographic textures, J. Appl. Cryst. (2015), submitted.
130. Nikolayev, D., Lychagina, T., Rusetzky, M. Ulyanenko, A. & Sasaki, S., "Internal optimization of the texture component approximation method", IOP Conference Series: Materials Science and Engineering v. 82 (2015), 012007.
131. Papushkin I., Kaisheva D., Bokuchava G., Petrov P., "Evaluation of Residual Stress and Microstrain in Electron Beam Welded Gear Wheel by Neutron Diffraction", Proc. of FIT'2015 - the 28-th International Scientific Conference of the Faculty of Industrial Technology of TU-Sofia, September 11-13, 2015, Sozopol, Bulgaria, pp. 131-136. ISBN 978-954-438-624-5.
132. Petrov P., Kaicheva D., Bokuchava G., Papushkin I., "A neutron diffraction study of residual stress due to electron beam welding", Proc. of 3rd IIW South-East European Welding Congress "Welding and Joining Technologies for a Sustainable Development and Environment", June 3-5, 2015, Timisoara, Romania, pp. 108-112. ISBN 978-606-554-955-5.
133. Petrov P., Bokuchava G., Kaicheva D., Papushkin I., "Neutron diffraction study of residual stresses due to the electron-beam welding in the automotive transmission gears", Proc. of FABTECH 2015, Nov 9-12 2015, Chicago, USA.
134. Ullemeyer K., Lokajicek T., Keppler R., Vasin R.N., Behrmann J.H. "Bulk rock elastic moduli at high pressures, derived from the mineral textures and from extrapolated laboratory data", IOP Conference Series: Materials Science and Engineering, Vol. 82 (2015), pp. 012093 (1-4).

Instruments and Methods

135. Аксенов В.Л., Балагуров А.М., "Дифракция нейтронов на импульсных источниках (к 100-летию со дня рождения Ф.Л.Шапиро)" УФН (2015), в печати.
136. Балагуров А.М., Бобриков И.А., Бокучава Г.Д., Журавлев В.В., Симкин В.Г., "Корреляционная фурье-дифрактометрия: 20-летний опыт эксплуатации на реакторе ИБР-2", ЭЧАЯ, т. 46, № 3 (2015), стр. 453-501. Balagurov A.M., Bobrikov I.A., Bokuchava G.D., Zhuravlev V.V., Simkin V.G., "Correlation Fourier Diffractometry: 20 Years of Experience at the IBR-2 Reactor", Physics of Particles and Nuclei, 2015, Vol. 46, Issue 3, pp. 249-276.
137. Бокучава Г.Д., Васин Р.Н., Папушкин И.В., "Применение нейтронной стресс-дифрактометрии для изучения остаточных напряжений и текстуры в промышленных металлических изделиях, обработанных различными способами", Поверхность.

Рентгеновские, синхротронные и нейтронные исследования, № 5 (2015), стр. 3-14. G.D. Bokuchava, R.N. Vasin, I.V. Papushkin, “Application of neutron stress diffractometry for the study of residual stress and texture in industrial metal products processed in various ways”, Journal of Surface Investigation. X-ray, Synchrotron and Neutron Techniques, Vol. 9 (2015), Issue 3, pp. 425–435.

138. Руткаускас А.В., Козленко Д.П., Кичанов С.Е., Бокучава Г.Д., Лукин Е.В., Савенко Б.Н., “Исследование нейтронных спектров пропускания материалами, перспективными для создания монокристаллических и поликристаллических фильтров”, Поверхность. Рентгеновские, синхротронные и нейтронные исследования, № 4 (2015), с. 5-7. Rutkauskas A.V., Kozlenko D.P., Kichanov S.E., Bokuchava G.D., Lukin E.V., Savenko B.N., “Investigation of the Neutron Transmission Spectra of Materials Promising for the Manufacturing of Crystalline and Polycrystalline Filters”, Journal of Surface Investigation. X-ray, Synchrotron and Neutron Techniques, 2015, Vol. 9, Issue 2, pp. 317-319.

139. Kichanov S.E., D.P. Kozlenko, T.I. Ivankina, A.V. Rutkauskas, E.V. Lukin, B.N. Savenko “The Neutron Tomography Studies of the Rocks from the Kola Superdeep Borehole”, Physics Procedia, v. 69 (2015), p. 537 – 541.

140. Kozlenko D.P., S.E. Kichanov, E.V. Lukin, A.V. Rutkauskas, G.D. Bokuchava, B.N. Savenko, A.V. Pakhnevich, A.Yu. Rozanov “Neutron Radiography Facility at IBR-2 High Flux Pulsed Reactor: First Results” Physics Procedia, v. 69 (2015), p. 87-91.

141. Kozlenko D. P., S. E. Kichanov, E. V. Lukin, A. V. Rutkauskas , A. V. Belushkin, G. D. Bokuchava, B. N. Savenko ”Experimental Station of Neutron Radiography and Tomography at the Pulsed High-Flux IBR-2 Reactor: First Results”, JINR News, № 1 (2015), p. 31-34.

142. Lukin E.V., D.P. Kozlenko, S.E. Kichanov, A.V. Rutkauskas, G.D. Bokuchava, B.N. Savenko “First attempts on energy-selective neutron imaging at IBR-2”, Physics Procedia, v. 69 (2015), p. 271 – 274.

143. Zhabitskaya E.I., E.V. Zemlyanaya, M.A. Kiselev. Numerical analysis of SAXS data from vesicular systems by asynchronous differential evolution method. Математическое моделирование, т.27, №7 (2015), с. 58-64.

DEPARTMENT OF IBR-2 SPECTROMETERS COMPLEX

144. Кирилов А.С., Петухова Т.Б. "Набор компонентов для построения GUI в системах управления нейтронными спектрометрами на основе PyQt№. Сообщение ОИЯИ, P10-2015-38.

145. Кирилов А.С., Мурашкевич С.М., Петухова Т.Б. "Адаптация Sonix+ для управления дифрактометром ДЗ" Сообщение ОИЯИ, P10-2015-39.

146. Кирилов А.С. "Новые версии программ юстировки и визуализации спектров для рефлектометров реактора ИБР-2". Препринт ОИЯИ, P10-2015-40. Принят к публикации в журнале ЭЧАЯ.

147. Кожевников С. и др. Использование криогенного замедлителя на нейтронном рефлектометре РЕМУР // Поверхность. Рентгеновские, синхротронные и нейтронные исследования. – 2016. – №1. – с. 1-11.

148. Манощин С., Белушкин А., Иоффе А. Развитие методов моделирования нейтронных спектрометров и виртуальных экспериментов в ЛНФ ОИЯИ, Обзорная статья, отправлена в юбилейный сборник ЭЧАЯ-2015 ОИЯИ.

149. Bellyakov A. et al. Control system of pelletized cold neutron moderator of the IBR-2 reactor / // Physics of particles and nuclei letters. – 2015. – Vol. 12, №6. – P. 773-777.

150. Bolshakova I. et al. Experimental evaluation of stable long term operation of semiconductor magnetic sensors at ITER relevant environment // Nuclear Fusion. – 2015. – Vol. 55. – №8. – P. 083006-083016.

151. Bodnarchuk V., Sadilov V., Manoshin S., Erhan R., Avdeev M.,. Ioffe A, Monte Carlo simulation of SESANS experiment with time-gradient magnetic fields, Submitted to NIM A

152. Shabalin E. et al. Spectrum and density of neutron flux in the irradiation beam line №3 of the IBR-2 reactor // Physics of particles and nuclei letters. 2015. Vol. 12, №2. pp. 336-343.

153. Verkhogliadov A [et al. Irradiation facility at the IBR-2 reactor for investigation of material radiation hardness // Nuclear instruments and methods in physics research B. 2015. Vol. 343. – pp. 26-29.

NUCLEAR PHYSICS DEPARTMENT

Experimental investigations

154. Abbas Mahmoud I., Badawi M. S., Ruskov I.N., El-Khatib A.M., Grozdanov D.N., Thabet A.A., Kopatch Yu.N., Gouda M.M., Skoy V.R., Calibration of a single hexagonal NaI(Tl) detector using a new numerical method based on the efficiency transfer method, Nuclear Instruments and Methods in Physics Research Section A: Accelerators, Spectrometers, Detectors and Associated Equipment, 771 (2015) 110-114, http://www.sciencedirect.com/science/article/pii/S0168900214012133.

155. Adam J., Baldin A.A., Chilap V., Furman W. et al. Measurement of high energy neutron flux on the surface of the natural uranium target assembly QUINTA irradiated by deuterons of 4 and 8 GeV energy, Physics Procedia 80, (2015) 94-97

156. Adam J., Chilap V., Furman W. et al., Study of secondary neutron interaction with 232Th, 129I and 127I nuclei with the uranium assembly QUINTA at 2, 4 and 8 GeV deuteron beams of JINR Nuclotron accelerator, Applied Radiation and Isotopes, on line.

157. Ahmadov F., Ahmadov G., Abdullaev X., Garibov A., Guliyev E., Khorev S., Madatov R., Muxtarov R., Naghiyev J., Sadigov A., Sadygov Z., Suleymanov S., Zerrouk F. Development of compact radiation detectors based on MAPD photodiodes with Lutetium Fine Silicate and Stilbene scintillators Journal of Instrumentation, 2015, vol.10, p.1-7

158. Ahmadov G.S., Kopatch Yu.N., Telezhnikov S.A., Ahmadov F.I., Granja C., Garibov A.A., Pospisil S. Detection of ternary and quaternary fission fragments from 252Cf with a position-sensitive ΔE-E telescope based on

silicon detectors. Physics of Particles and Nuclei Letters 07/2015; 12(4):542-549.
159. Borzakov S.B, Gundorin N.A, Pokotilovski Yu.N, Experimental search for the singlet meta-stable deuteron in the radiative n-p capture. Phys. of Part. and Nuclei Letters, 12 (2015) 536-541.
160. Chietera A., Stuttgé L., Gönnenwein F., Kopatch Yu., Mutterer M., Guseva I., Gagarski A., Chernysheva E., Dorvaux O., Hambsch F.J., Hanappe F., Mezentseva Z., Telezhnikov S., Neutron Emission Anisotropy in Fission, Proc. of the Int. Seminar on interaction of neutrons with nuclei, ISINN-22, http://isinn.jinr.ru/proceedings/isinn-22/pdf/chietera.pdf
161. Enik T.L., Mitsyna L.V, Popov A.B., Salamatin I.M., Angular anisotropy of slow neutrons scattered at IREN facility with Vanadium as sample. In: ISINN-22, Dubna, May 27-30, 2014, JINR E3-2015-13, p.91 (2015).
162. Garibov Adil, Madatov Rahim, Mustafayev Yusif, Ahmadov Farid, Ahmadov Gadir, Jahangirov Murad, Structural and Optical Properties of GaS Single Crystals Irradiated by Hydrogen. Journal of Electronic Materials 2015, Volume 44, Issue 10, pp 3375-3379.
163. Grozdanov D.N., Issatov A.T., Kopach Yu.N., Skoy V.R., Negovelov S.I., Ruskov I.N., Energy and Time Resolution of Gamma-ray Detectors, Proc. of ISINN-22, http://isinn.jinr.ru/proceedings/isinn-22/pdf/grozdanov.pdf.
164. Han Jinhua, Liu Jiaming, Liu Xiang, Fan Xiao, Wang Zhiming, Chen Jinxiang, Zhang Guohui, Gledenov Yu. M., Sedysheva M.V., Krupa L., Khuukhenkhuu G., Szalanski P.J., Differential and angle-integrated cross sections for the 40Ca(n,α)37Ar reaction from 4.0 to 6.5 MeV. European Physical Journal, 2015, vol. 51:12, pp. 1-10.
165. Ignatovich V.K., Salamatin I.M., Salamatin K.M., Senner A.E. Automation of Neutron Spectrometry Experiments Using Network Technologies // Proceedings of ICANS XXI: 21st International Collaboration on Advanced Neutron Sources, 29Sep-3Oct 2014 in Mito, Ibaraki, Japan. (in press, 2015)
166. Ignatovich V.K., Salamatin I.M., Salamatin K.M., Senner A.E. Unification of Experiment Procedure Control Tools for the Experiment Automation Systems in the Field of Neutron Spectrometry Using Network Technologies // Proceedings of the Seminar ISINN-22 (Dubna, May 27-30, 2014); Dubna E3-2015-13, Dubna: JINR, 2015, p. p. 105-111
167. Kopatch Yu., Chietera A., Stuttgé L., Gönnenwein F., Mutterer M., Gagarski A., Guseva I., Chernysheva E., Dorvaux O., Hambsch F.-J., Hanappe F., Mezentseva Z., Telezhnikov S., Detailed Study of the Angular Correlations in the Prompt Neutron Emission in Spontaneous Fission of 252Cf, Physics Procedia, Volume 64, 2015, Pages 171-176
168. Kozhevnikov S.V., Ignatovich V.K., Nikitenko Yu.V., Ott F., Petrenko A.V. System of neutron microbeams from a planar waveguide. Письма в ЖЭТФ, v. 102, n. 1, p. 3-9; (Jetp Lett. p. 1-6) 2015
169. Kulin G.V., Frank A.I., Goryunov S.V., Kustov D.V., Geltenbort P., Jentschel M., Strepetov A.N., Bushuev. V.A., Spectrometer for new gravitational experiment with UCN. NIM A, Vol.792 (2015) 38-46
170. Lychagin E.V., Muzichka A.Yu., Nekhaev G.V., Nesvizhevsky V.V., Sharapov E.I., Strelkov A.V., UCN Source at an external beam of thermal neutrons. Advances in High Energy Physics, Volume 2015, Article ID 547620, (2015).
171. Lychagin E.V., Muzychka A.Yu., Nekhaev G.V., Nesvizhevsky V.V., Sharapov E.I., and Strelkov A.V., http://www.hindawi.com/ journals/ahep/2015/547620/ 2015.
172. Madzharski T.P., Ivanov I.Zh., Ruskov I.N., Kopach Yu.N., Statistical Modeling Method for “Romashka”-type 4π Detector System, Proc. of the Int. Seminar on interaction of neutrons with nuclei, ISINN-22, http://isinn.jinr.ru/proceedings/isinn-22/pdf/madzharski.pdf.
173. Oprea A., Oprea C., Gledenov Yu. M., Sedyshev P.V., Sedysheva M.V. Cross Sections Evaluation in Nuclear Reactions with Fast Neutrons .XXII International Seminar on Interaction of Neutrons with Nuclei (ISINN22) Frank Laboratory for Neutron Physics - Joint Institute for Nuclear Research (FLNP-JINR), Dubna, Russian Federation. Proceedings of the Seminar, JINR Dubna Publishing Department, 2015, pp. 198-20
174. Oprea C., Oprea A., Mihul A. Numerical Evaluation of Sn Isotope Cross Sections by Photoneutron Activation Method. XXII International Seminar on Interaction of Neutrons with Nuclei (ISINN22) Frank Laboratory for Neutron Physics - Joint Institute for Nuclear Research (FLNP-JINR), Dubna, Russian Federation. Proceedings of the Seminar, JINR Dubna Publishing Department, 2015, pp. 192-197.
175. Paradela C., Calviani M., Tarrio D. et al., High-accuracy determination of the 238U/235U fission cross section ratio up to ≈ 1 GeV at n_TOF at CERN, Phys. Rev. C91, 024602(2015)
176. Ruskov I. N., Kopatch Yu. N., Bystritsky V. M., Skoy V. R., Shvetsov V. N., Hambsch F.-J., Oberstedt S., CapoteNoy R.,. Sedyshev P. V., Grozdanov D. N., Ivanov I. Zh., Aleksakhin V. Yu., Bogolubov E. P., Barmakov Yu. N., Khabarov S. V., Krasnoperov A. V., Krylov A. R., Obho J., Pikelner L. B., Rapatskiy V. L., Rogachev A. V., Rogov Yu. N., Ryzhkov V. I., Sadovsky A. B., Salmin R. A., Sapozhnikov M. G., Slepnev V. M., Sudac D., Tarasov O. G., Valković V., Yurkov D. I., Zamyatin N. I., Zeynalov Sh. S., Zontikov A. O., Zubarev E. V., TANGRA-Setup for the Investigation of Nuclear Fission Induced by 14.1 MeV Neutrons, Physics Procedia 64 (2015) 163-170, ISSN: 1875-3892, Elsevier, http://www.sciencedirect.com/science/article/pii/S1875389215001388
177. Ruskov I.N., Universal Monitor of Low Intensity Mixed Neutron-Gamma Radiation Fields Utilizing the Computer Sound Card as Multichannel Pulse Analyzer, Proc. of ISINN-22, http://isinn.jinr.ru/proceedings/isinn-22/pdf/ruskov.pdf.
178. Sadigov A., Ahmadov F., Ahmadov G., Ariffin A., Khorev S., Sadygov Z., Suleymanov S., Zerrouk F., Madatov R. A new detector concept for silicon photomultipliers. Nuclear Instruments and Methods in Physics Research Section A Accelerators Spectrometers Detectors and Associated Equipment 2015.
179. Seestrom S.J., Adamek Evan R., et al. (30 authors, including E. I. Sharapov), Upscattering of ultracold neutrons from gases, Physical Review C, in press (2015).
180. Snow W.M., Anderson E., Barron-Palos L., et al. (30 authors, including E.I. Sharapov), A slow neutron polarimeter for measurements of parity-odd neutron rotary power. Rev. Sci. Instr., v. 86, 055101 (2015)
181. Tang Z., Alarson R., Askanazi E., et al. (54 authors, including E.I. Sharapov), Measurement of parity violation in gamma emission from the capture of polarized neutrons on Al. Physical Review C, in press (2015).
182. Telezhnikov S.A., Ahmadov G., Kopatch Yu.N., Granja C., Pospisil S., Energy Calibration of Timepix Pixels below 60 keV, Proc. of the Int. Seminar on interaction of neutrons with nuclei, ISINN-22, http://isinn.jinr.ru/proceedings/isinn-22/pdf/telezhnikov.pdf
183. Vesna V.A., Gledenov Yu.M., Nesvizhevsky V.V.,

Sedyshev P.V., Shulgina E.V., Left-Right Asymmetry in Integral Spectra of γ-Quanta in the Interaction of Nuclei with Polarized Thermal Neutrons. Physics of Atomic Nuclei, 2015, Vol. 78, Issue 7, pp. 801-804.

184. Wang Z., Hoffbauer V.A., Moris C.L., et al. (36 authors, including E.I. Sharapov), A Multilayer surface detector for ultracold neutrons, Arxiv: 1503.03424, April 2015, NIM A, in press (2015).

185. Wang Zhimin, Fan Xiao, Zhang Luyu, Bai Huaiyong, Chen Jinxiang, Zhang Guohui, Gledenov Yu.M., Sedysheva M.V., Krupa L., and Khuukhenkhuu G. Cross sections of the 56Fe(n,α)53Cr and 54Fe(n,α)51Cr reactions in the MeV region". Phys. Rev. C 92, 044601, 1-7 (2015).

186. Zavorka L., Adam J., Baldin A. et al., Neutron induced transmutation reactions in 237Np, 238Pu and 239Pu at massive uranium spallation target, Nucl. Instr. and Methods in Phys. Res. B,349 (2015) 31-38Zontikov

187. A.O., Grozdanov D.N., Ruskov I.N., Kopatch Yu.N., Neutron-gamma field intensity and absorbed doses simulation at some points of “Romashka” experimental setup, Proc. of ISINN-22, http://isinn.jinr.ru/proceedings/isinn-22/pdf/zontikov.pdf

188. Бушуев В.А., Франк А.И., Кулин Г.В., Многоволновая динамическая теория дифракции нейтронов на движущейся фазовой решетке. Труды XIX Международного симпозиума “Нанофизика и наноэлектроника” (Нижний Новгород, 10-14 марта 2015), Т. 1 (2015) 324-325

189. Быстрицкий В.М., Валкович В., Грозданов Д.Н., Зонтиков А.О., Иванов И.Ж., Копач Ю.Н., Крылов А.Р., Рогов Ю.Н., Русков И.Н., Сапожников М.Г., Ской В.Р., Швецов В.Н., Многослойная пассивная защита сцинтилляционных детекторов на основе кристаллов BGO, NaI(Tl) и стильбена, работающих в интенсивных нейтронных полях с энергией 14,1 МэВ, Письма в ЭЧАЯ, Том:12, № 2, Страницы: 486-504, eISSN:1814-5973, Изд: ОИЯИ, http://www1.jinr.ru/Pepan_letters/panl_2015_2/18_bystr.pdf. Bystritsky V.M., Valkovic V., Grozdanov D.N., Zontikov A.O., Ivanov I.Zh., Kopatch Yu.N., Krylov A.R., Rogov Yu.N., Ruskov I.N., Sapozhnikov M.G., Skoy V.R., Shvetsov V.N., Multilayer passive shielding of scintillation detectors based on BGO, NaI(Tl), and stilbene crystals operating in intense neutron fields with an energy of 14.1 MeV, Physics of Particles and Nuclei Letters12(2) (2015) 325-335, MAIK Nauka/Interperiodica; http://link.springer.com/article/10.1134/S1547477115020089.

190. Суховой А.М., Новая практическая модель каскадного гамма-распада нейтронного резонанса. Основные положения и достижимая точность. ЯФ 2015, т. 78, 3-4, стр. 256-271. (Sukhovoj A.M., New model of the cascade gamma decay of neutron resonances for practitioners: Basic concepts and attainable precision. Physics of atomic nucleus, 2015 v.78, 2, pp.230-245.)

Theoretical investigations

191. Ignatovich V.K., Closer Look at EPR Paradox and Bell’s Inequality, American Journal of Modern Physics and Application, v.2, n. 2, p. 16-20, 2015,

192. Ignatovich V.K., Batkov K., An Attempt to Describe Quantum Interference on two Slits in Classical Terms, American Journal of Modern Physics ans Applications v.2, n. 3, p. 36-39, 2015

193. Ignatovich V.K., Neutron interferometry, by Helmut Rauch and Samuel A. Werner. Oxford, UK, Oxford University Press, Crystallography Reviews, (book review) v.21, n. 4, p. 307-310, 2015.

194. Ignatovich V.K., A Singular Solution for a Hydrogen Atom as a Way Toward Cold Nuclear Fusion, Open Science Journal of Modern Physics, v. 2, n. 5, p. 83-88, 2015

Applied research

195. Aleksiayenak Yu.V., Frontasyeva M.V., Ostrovnaya T.M., Okin O.I. Moss biomonitoring echnique, NAA and AAC for air pollution in Belarus. Problems of Reginal Ecology. No. 4, 2015 (Алексеенок Ю.В., Фронтасьева М.В., Островная Т.М., Окина О.И.. Метод мхов-биомониторов, НАА и ААС в исследовании воздушных загрязнений Беларуси. Проблемы региональной экологии, № 4, 2015).

196. Allajbeu Sh., Yushin N.S., Qarri F., Lazo P., Duliu O.G., Frontasyeva M.V.. Atmospheric deposition of rare earth elements in Albania studied by the moss biomonitoring technique, neutron activation analysis and GIS technology. JINR Preprint, E-18-2015-64, Dubna, 2015, pp. 18. Submitted to Env Sci Poll Research.

197. Antonova Landysh, Demikhov Timofey, Troitskii Alexey, Didyk Alexander, Kobzev Alexander, Yurasov Alexander, Samoilenkov Sergey, and Mikhailova Halina, Effect of 2.5 MeV proton irradiation on the critical parameters of composite HTS types. Physica Status Solidi C. Volume 12, Issue 1-2, (2015), pp.94-97.

198. Arafa W.M., Badawy W.M., Fahmi N.M., Ali K., Gad M.S., Duliu O.G., Frontasyeva M.V., Steinnes E.. Geochemistry of sediments and surface soils from the Nile delta and lower Nile valley studied by epithermal neutron activation analysis. Journal of African Earth Sciences, No. 107, 2015, p. 57-64. Elsevier.

199. Badawy W.M., Ali K., El-Samman H.M., Frontasyeva M.V., Gundorina S.F., Duliu O.G., Instrumental Neutron Activation Analysis of Soil and Sediment Samples from Siwa Oasis, Egypt. Physics of Particles and Nuclei. Vol. 12, No. 4, p. 637-644.. ISSN 1547-4771. Pleiades Publishing, 2015.

200. Barandovski L., Frontasyeva M.V., Stafilov T., Šajn R., Ostrovnaya T.M.. Multi-element atmospheric deposition in Macedonia studied by the moss biomonitoring technique. Environmental Science and Pollution Research. ISSN 0944-1344. 06, 2015 DOI 10.1007/s11356-015-4787-x, 2015.

201. Bezuidenhout J., Nicole Dames N.,, Alfred Botha A., Frontasyeva M.V., Goryainova Z.I., Pavlov D.F. Trace elements in Mediterranean mussels Mytilus galloprovincialis from the South African west coast. Accepted by Ecological Chemistry and Engineering S.

202. Cepoi L., Rudi L., Chiriac T., Valuta A., Zinicovscaia I., Duca Gh., Kirkesali E., Frontasyeva M.V., Culicov O., Pavlov S.S., Bobrikov I., Biochemical changes in cyanobacteria during the synthesis of silver nanoparticles. Canadian Journal of Microbiology; Jan 2015, Vol. 61 No. 1, 2015, pp. 13.

203. Doroshkevich N.V., Frontasyeva M.V., Doroshkevich V.S., Lygina O.S., Shylo A.V., Ostrovnaya T.M., Pavlov S.S., Pirko N.N., Zelenyak T.Yu., Konstantinova T. E., Lyubchyk S.B., Doroshkevich A.S., Zirconia nanoparticles impact on morphophysiological data and mineral composition of P. ostreatus. Ecological Chemistry and Engineering, Vol. 22, No. 2, 2015, p. 169-188.

204. Fiałkiewicz-Kozieł B., Smieja-Król B., Ostrovnaya T.M., Frontasyeva M.V., Siemińska A., Lamentowicz M., Peatland microbial communities as indicators of the extreme atmospheric dust deposition. Water, Air, & Soil Pollution, 01/2015.
205. Gorbunov A.V., Granovskaya G.A., Ermolaev B.V., Lyapunov S.M., Ilchenko I., Frontasyeva M.V., Pavlov S., Assessment of mercury in diagnostic biomaterials of different population groups of urban areas of Moscow Region. Ecology of Urbanized Territoriers, No. 2, 2015, p. 16-24 (Горбунов А.В., Грановская Г.А., Ермолаев Б.В., Ильченко И.Н., Ляпунов С.М., Фронтасьева М.В., Павлов С.С., Авдосьева М.В.. Оценка содержания ртути в диагностических биоматериалах различных групп населения урбанизированных территорий Московского региона. Экология урбанизированных территорий. № 2, 2015, с. 16-24).
206. Gorbunov A.V., Lyapunov S. M., Okina O.I., Chamov N.P., Frontasyeva M. V., Pavlov S. S., Avdoseva M. V., Assessing biomonitoring opportunities in the study of technogenic pollution of the environment of the Yamal Peninsula. Ecology of Urbanized Territoriers, No.1, 2015, p. XX (Горбунов А.В., Ляпунов С.М., Окина О.И., Чамов Н.П., Фронтасьева М.В., Павлов С.С., Авдосьева М.В., Оценка возможностей биомониторинга при изучении техногенного загрязнения природной среды п-ова Ямал. Экология урбанизированных территорий, № 1, 2015, p. 253-270).
207. Gorbunov A.V., Lyapunov S.M., Frontasyeva M.V., Pavlov S.S., Intake of Cl, Br, I, Se in human body with food in Central Regions of the European Part of Russia. Food and Nutrition Sciences, No. 6, 2015, p. 168-178. Published Online January 2015 in Sci Res. http://www.scirp.org/journal/fns; http://dx.doi.org/10.4236/fns.2015.61018.
208. Gorelova S.V., Frontasyeva M.V., Gorbunov A.V., Lyapunov S.M., Mochalova E.G., Okina O.I. Biogeochemical activity of Introducents in the conditions of industrially developed ecosystems. Vestnik of I. Kant Baltic Federal University, Vol, 1, 2015, p.92-106. (Горелова С.В., Фронтасьева М.В., Горбунов А.В., Ляпунов С.М., Мочалова Е.Г., Окина О.И.. Биогеохимическая активность интродуцентов в условиях промышленно развитых урбанизированных экосистем. Вестник Балтийского Федерального университета им. И. Канта. Вып. 1, 2015, с. 92-106).
209. Harmens H., Mills G., Hayes F., Sharps K., Frontasyeva M., Aboal J.R., Aherne J., Alber R., Alekseev A., Alonso R., Aleksiayenak Y., Anicic M., Balint A., Barandovski L., Baggard M., Bassin S., Batic F., Bender, T. Berg, V. Bermejo, O. Bethenod, O. Blum, S. Boltersdorf, K. Borowiak, S. Braun, A. Briolat, P. Büker, V. Calatayud, H. Cambridge J., Carballeira Ocaña A., Castell J.-F., Chaligava O., Chursin A., Cieslik S., Cinderby S., Cooper D., Coskun M., Cotrozzi L., Cucu-Man S. M., Dam M., Danielsson H., Davies B., Dott D., Dunaev A.M., Eler K., Emberson L., Ene A., Fares S., Fernández I.G., Fernández Escribano J. Á., Finco A., Fränzle S., Frolova M., Fuhrer J., Fumagalli I., Fusaro L., Galsomiès L., Garrec J.-P., Gerosa G., Gluschenko V., Godzik B., Goltsova N., Grünhage L., Hall J., Hoydal K., Ibrahimov Z., Infante Olarte M., Izquieta S., Jančík P., Jeran Z., Jones L., Kalabegeshvili T., Kapusta P., Karlsson G. P., Karlsson P. E., Kirkesali E., Koroleva Y., Kosior G., Krmar M., Krüger G., Kvietkus K., Kubin E.,. Las Heras R. T, Lazo P., Lebedeva N. A., Leblond S., Liiv S., Magnússon S., Mammadov E., Manes F., Manninen S., Maňkovská B., Martínez-Abaigar J., de Marco A., Marzuoli R., Mastrorilli M., Maxhuni A., Mehrabova M., Melece I., Meyer M., Milanovic I., Minkova-Gecheva G., Marinova S., Nali C., Nickel S., Norris D., Núñez-Olivera E., Omarova N., Paoletti E., Pavlikova I., Piispanen J., Pihl Karlson G., Pleijel H., Poikolainen J., Popescu I. V., Purvis W., Qarri F., Rana G., Radnovich D., Radulescu C., Repellin A., Ruttens A., Saitanis C., Salvatori E., Santamaría J., Schaab M., Schaub M., Schlabach M., Schröder W., Shetekauri S., Sicard P. L., Skudnik M., Sogo H.C., Soja G., Solodukhin V., Spiric Z., Stafilov T., Steinnes E., Stihi C., Suchara I., Sucharová J., Szarek-Łukaszewska G., Ie Thiec D., Thöni L., Tibor K., Todoran R., Turk B., Uggerud H., Urbaniak J., Vandermeiren K., Velissariou D., Vergel K. N., Vikhrova I. V., Vitale M., Volk M., Waegeneers N., Werner W., Zechmeister H. G., Zeiko G., Zlobin V., Air Pollution and Vegetation, ICP Vegetation, Annual Report 2014/2015, H. Harmens, G. Mills, F. Hayes, K. Sharps, M. Frontasyeva, (Eds.), ICP Vegetation Programme Coordination Centre, Centre for Ecology and Hydrology, Environment Centre Wales, Bangor, Gwynedd, UK, Moss Survey Coordination Centre, Frank Laboratory of Neutron Physics, Joint Institute for Nuclear Research, Dubna, Moscow Region, Russian Federation, September, 2015.
210. Harmens H., Norris D.A., Sharps K., Mills G., Alber R., Aleksiayenak Y., Blum O., Cucu-Man S.-M., Dam M., De Temmerman L., Ene A., Fernandez J.A., Martinez-Abaigar J., Frontasyeva M., Godzik B., Jeran Z., Lazo P., Leblond S., Liiv S., Magnússon S.H., Mankovska B., Pihl Karlsson G., Piispanen J., Poikolainen J., Santamaria J.M., Skudnik M., Spiric Z., Stafilov T., Steinnes E., Stihi C., Suchara I., Thoni L., Todoran R., Yurukova L., Zechmeisteret H.G. al. Heavy metal and nitrogen concentrations in mosses are declining across Europe whilst some "hotspots" remain in 2010. Environmental Pollution, No. 200, 2015, p. 93-104.
211. Harmens H., Schröder W., Zechmeister H.G., Steinnes E., Frontasyeva M. V. Comments on Fernandez J.A., Boquete M.T., Carballeira A., Aboal J.R. (2015). A critical review of protocols for moss biomonitoring of atmospheric deposition: Sampling and sample preparation. Science of the Total Environment, Vol. 517, 2015, p. 132-150.
212. Horodek P., Siemek K., Kobets A.G., Kulik M., Meshkov I.N., Positron beam and RBS studies of thermally grown oxide films onstainless steel grade 304. Applied Surface Science. Volume 333, (2015), pp. 96–103.
213. Hristozova G., Goryaynova Z., Marinova S., Frontasyeva M.V. Preliminary results of soil contamination with toxic metals and trace elements in the area affected by Kardzhali lead-zinc smelter. FLNP Annual Report 2014, Dubna, 2015.
214. Hristozova G., Marinova S., Strelkova L.P., Goryainova Z., Frontasyeva M.V., Stafilov T.. Milti-element atmospheric deposition study in the area of lead-zinc plant in Kardzhali, Bulgaria. American Journal of Analytical Chemistry, USA, Vol. 5, 2015, p. 920-931.
215. Ignatenko O.V., Konovalova A.V., Komar V.A., Leonchik S. V., Shempel N. A., Aleksiayenak Yu. V., Frontasyeva M.V., Shvetsov V.N., Ene A., Cantaragiu A., Comparative characteristics of synthetic diamond powder obtained in systems Fe-Ni-C and Mn-Ni-C, Proceedings of the 2nd International Conference on Modern Applications of Nanotechnology, 6-8 May 2015, Minsk, Belarus, 3 pp.
216. Kalabegishvili T.L., Murusidze I.G., Kirkesali E.I., Rcheulishvili A.N., Ginturi E.N., Gelagutashvili E.S., Kuchava N.E., Bagdavadze N.V., Janjalia M.V., Pataraya D.T., Gurielidze M.A., Frontasyeva M.V., Zinicovscaia I.I., Pavlov S.S., Tsertsvadze G.I., Gabunia V.N., Possibilities of physical methods in development of microbial nanotechnology. European Chemical Bulletin, Vol. 4, No.

1, 2015, p. 43-49.
217. Keränen A., Leiviskä T., Zinicovscaia I., Frontasyeva M.V., Hormi O., Tanskanen J., Quaternized pine sawdust in the treatment of mining wastewater. Environmental Technology, 2015 Nov 20, 1-23.
218. Kosior G., Prell M., Samecka-Cymerman A., Stankiewicz A., Kolon K., Kryza R., Brudzińska-Kosior A., Frontasyeva M., Kempers A. J., Metals in Tortula muralis from sandstone buildings in anurban agglomeration. Ecological Indicators, No. 58, 2015, p. 122-131.
219. Kravtsova A.V., Milchakova N.A., Frontasyeva M. V.. Levels, spatial variation and compartmentalization of trace elements in brown algae Cystoseira from marine protected areas of Crimea (Black Sea). Marine Pollution Bulletin. No. 3, 2015, p. 97-99.
220. Maňkovská B., Frontasyeva M. V. and Ostrovnaya T.M. Temporal and spatial trends (1990−2010) of trace element atmospheric deposition in Slovakia − assessment based on moss analysis. Chapter of a book “Air Pollution”, INTECH, Open Access Publisher, 2015.
221. Nekhoroshkov P.S., Frontasyeva M.V., Tokarev Yu.N., Biophysical parameters and muli-element content of phytoplankton communities of the Black Sea in the coastline zone of Crimea. Water: chemistry and ecology. (www.watchemec.ru) 2015) (Нехорошков П.С., Фронтасьева М.В., Токарев Ю.Н.. Биофизические параметры и многоэлементный состав фитопланктонных сообществ Черного моря в прибрежной зоне Крыма. Вода: химия и экология (www.watchemec.ru), № 8, 2015. с. 10-17б 2015).
222. Nekhoroshkov P.S., Kravtsova A.V., Frontasyeva M.V., Tokarev Yu.N.. Neutron activation analysis for assessment of elemental content of phytoplankton coastal assemblages from the near-shore zone of Sevastopol (the Black Sea). FLNP Annual Report 2014, Dubna, 2015.
223. Oprea C., Szalansky P. J., Gustova M. V., Oprea I. A., Buzguta V. Trace element distribution in human teeth by x-ray fluorescence and multivariate analysis. Romanian Reports in Physics, ISSN:1221-1451, Romanian Academy of Science, 2015 v. 67, Nr. 2, pp. 452-459
224. Oprea A. I., Oprea C., Mihul A. A. Neutron Transmission Study of Environmental Gd Romanian Reports in Physics, ISSN:1221-1451, Romanian Academy of Science, 2015, v. 67, Nr. 3, pp. 854-864
225. Oprea C., Oprea A. Neutron Transmission Computer Experiment for Gd Isotopes Determination. XXII International Seminar on Interaction of Neutrons with Nuclei (ISINN22) Frank Laboratory for Neutron Physics - Joint Institute for Nuclear Research (FLNP-JINR) Dubna, Russian Federation Proceedings of the Seminar, JINR Dubna Publishing Department, 2015, pp. 121-127
226. Pjevie D., Marinkovi T., Savi J., Bundaleski N., Obradovii M., Milosavljevic M., Kulik M., Influence of substrate temperature and annealing on structural and optical properties of TiO2 films deposited by reactive e-beam evaporation. Thin Solid Films. Volume 591, part B, (2015) pp. 224-229.
227. Qarri F., Lazo P., Bekteshi L., Stafilov T., Frontasyeva M., Harmens H., The effect of sampling scheme in the survey of atmospheric deposition of heavy metals in Albania by using moss biomonitoring, Environmental Science and Pollution Research, Vol. 22, No. 3, 2015, p. 2258-2271.
228. Qarri F., Stafilov T., Bektrshi L., Kane S., Allajbeu Sh., Frontasyeva M.V.. Risk assessment in heavy metal atmospheric deposition in Albania by using mosses as bioindicator and ICP/AES and ENAA analysis. Submitted to Ecological Indicators.
229. Shetekauri L.S., Shetekauri T., Kvlividze A., Chaligava O., Kalabegeshvili T., Kirkesali E.I., Frontasyeva M.V., Chepurchenko O.E., Preliminary results of atmospheric deposition of major and trace elements in the Greater and Lesser Caucasus Mountains studied by the moss technique and neutron activation analysis. Annali di Botanica (Italy), Ann. Bot. (Roma), No. 5, 2015, p. 89–95.
230. Spankova M., Rosova A., Dobrocka E., Chromik S., Vavral., Strbik V., Machajdik D., Kobzev A.P., Sojkova M. Structural properties of epitaxial La0,67Sr0,33MnO3 films with increased temperature of metal-insulator transition grown on MgO substrate. Thin Solid Films. Volume 583,(2015), pp. 19 – 24.
231. Tserenpil Sh., Baljinnyam N., Frontasyeva M.V., Gundorina S.F.. Neutron activation analysis of urban soils from Mongolia. FLNP Annual Report 2014, Dubna, 2015
232. Tugulan C., Duliu O.G., Voica Bojar A., Dumitras D., Zincovskaya I., Culicov O.A., Frontasyeva M.V. Late Quaternary climatic conditions in Dobrogea (Romania) as reflected by loess geochemistry. Quaternary International, 08/2015; DOI: 10.1016/j.quaint.2015.06.062.
233. Vuković G., Aničić-Urošević M., Goryainova Z., Pergal M., Škrivanj S., Samson R., Popović A.. Activemoss biomonitoring for extensive screening of urban air pollution: Magnetic and chemical analyses. Science of the Total Environment. Vol. 521–522, p. 2015, p. 200–210.(IF: 4.099)
234. Vuković G., Aničić-Urošević M., Pergal M., Janković M., Goryainova Z., Tomašević M., Popović A.. Residential heating contribution to level of air pollutants (PAHs, major, trace, and rare earth elements): a moss bag case study. Environmental Science and Pollution Research. 2015. DOI 10.1007/s11356-015-5096-0.(IF: 2.828).
235. Xuesong Li, Hristozova G., Nekhoroshkov P.S., Frontasyeva M.V., Neutron activation analysis of constituent elements of edible and medicinal plant of iron stick yam (Dioscorea opposita Thunb). Accepted by International Research Journal of Public and Environmental Health, 2 November, 2015.
236. Zinicovscaia I., Cepoi L., Chiriac T., Culicov O. A., Frontasyeva M. V., Pavlov S.S., Kirkesali E., Akshintsev A., Rodlovskaya E. Spirulina platensis as biosorbent of chromium and nickel from wastewaters. Desalination and Water Treatment, 2015, DOI:10.1080/19443994.2015.1042061.
237. Бажажина Н.В., Мареев Ю.Д., Пикельнер Л.Б., Седышев П.В., Швецов В.Н., Анализ элементного и изотопного состава образцов методом нейтронной спектроскопии на импульсном источнике нейтронов ИРЕН. Письма в ЭЧАЯ, 2015, т. 12, №4, стр. 895-903. (Bazhazhina N.V., Mareev Y.D., Pikelner L.B., Sedyshev P.V., Shvetsov V.N., 2015, Analysis of Element and Isotope Composition of Samples by Neutron Spectroscopy at the IREN Facility.Physics of Particles and Nuclei Letters, Volume 12, No. 4, pp. 578–583)
238. Дидык А.Ю., Бондаренко Г.Г., Ерискин А.А., Кобзев А.П., Никулин В.Я., Силин П.В., Волобуев И.В., Белоус В., Васяк Я., Хаевска Е. Распределение дейтерия и водорода в Zr, Ni и Ti сборках фольг при воздействии импульсной дейтериевой высокотемпературной плазмы. Препринт ОИЯИ Р13 – 2015 – 62.
239. Игнатенко О.В., Коновалова А.В., Комар В.А, Леончик С.В., Шемпель Н.А., Алексеенок Ю.В., Фронтасьева М.В., Швецов В.Н., Ене А., Cantaragiu A., Влияние состава ростовой системы на характеристики синтетических алмазных порошков. Сборник материалов международного симпозиума «Перспективные материалы и технологии», 27-29 мая 2015 г., г. Витебск, Беларусь.

MISCELLANEOUS

- At the 7th European Exhibition of Creativity and Innovation (16 May 2015, Iasi, Romania), a young JINR FLNP scientist from Moldova (Institute of Chemical Research of the Academy of Sciences of Moldova, Kishinev, Moldova), **Inga Zinicovskaia**, won the gold medal.

- The PAC meeting for Condensed Matter Physics held a competition for the best poster presentation among young scientists. The poster “Study of crystal and magnetic structures of nanostructured lanthanum-strontium manganites in a wide pressure and temperature range” presented by **N. Belozerova** was selected as the best poster presentation. The PAC also noted two other high-quality posters: “Research of the coexistence of ferromagnetism and superconductivity in layered nanostructures” by **V. Zhaketov** and “Detector ASTRA. New detector elements and data acquisition system” by **V. Milkov**.

AYSS AND FLNP FELLOWSHIPS

In 2015, within the framework of the competition of the Association of Young Scientists and Specialists of JINR, the scholarships were awarded to:

1. grant for young PhD researchers
   I.I. Zinicovscaia
   A.V. Nagornyi
   V.I. Petrenko

2. grant for young specialists
   A.V. Kutergin
   A.N. Likhachev
   E.V. Lukin
   I.A. Markovnikov
   K.A. Mukhin

3. grant for young researchers
   M.V. Bulavin
   K.N. Vergel
   A.V. Verhogladov
   I.V. Papushkin
   P.S. Nehoroshkov
   A.V. Tomchuk

4. grant for young workers
   R. V. Chepurchenko

Since 2002, in FLNP a scholarship named after Academician of the USSR Academy of Sciences and first Director of the Laboratory of Neutron Physics **I.M. Frank** has been established in order to stimulate scientific and methodical research of young scientists.

In 2015 I.M. Frank scholarships were awarded to:

- In Neutron Nuclear Physics: **A.O. Zontikova**
- In Condensed Matter Physics: **T.V. Tropin**
- In Methodical Investigations: **V.S. Popov**
- In Development of basic facilities: **E.A. Golubkov, A.I. Ivankov**

In 2015 **F.L. Shapiro scholarships** were awarded to:

- In «Neutron Spectroscopy» **D. Berikov, R.N. Vasin, S.V. Goryunov.**

JINR PRIZES

JINR Prizes are awarded annually for the best scientific, technical, methodical and applied research studies. In 2015, the following studies performed by the FLNP specialists or in collaboration with the employees from other JINR Laboratories or scientific institutions were awarded with the prizes of various degrees:

Scientific and technical applied research:

First prize

“Structure diagnostics and investigations of powders and liquid suspensions of detonation nanodiamonds by small angle scattering of thermal neutrons”

Authors: Avdeev Mikhail Vasilyevich, Aksenov Viktor Lazarevich, Ivankov Oleksandr Igorevich, Rogachev Andrey Vyacheslavovich, Tomchuk Olexandr Vasilyevich, Bulavin Leonid Anatolyevich, Rosta Laszlo, Garamus Vasil Mikhaylovich, Rozhkova Natalia Nikolaevna, Osawa Eiji

Encouraging prizes

“Neutron activation analysis in wastewater treatment”

Authors: Zinicovscaia Inga, Frontasyeva Marina Vladimirovna, Culicov Otilia Ana, Pavlov Sergey Segeevich, Gundorina Svetlana Fedorovna, Cepoi Liliana, Chiriac Tatiana, Rudi Liudmila, Valuta Ana, Mitina Tatiana

FLNP SEMINARS

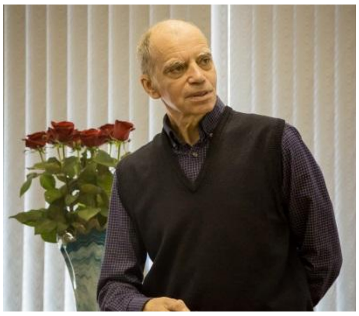

A.M. Balagurov

- **A.M. Balagurov** (FLNP DNICM). *50th anniversary of neutron diffraction on the IBR pulsed reactors (dedicated to the 100th anniversary of F.L. Shapiro's birth).* (19.01.2015)
- **J. Teixeira** (Laboratoire Léon Brillouin, Saclay, France). *Anomalous properties of low temperature water. A view at molecular scale probed by scattering experiments.*(13.05.2015)
- **A.M. Balagurov** (FLNP DNICM)**, J.-H. Behrmann** (GEOMAR Helmholtz-Zentrum, Kiel, Germany) *In commemoration of Prof.Anatoly N.Nikitin and Dr.Klaus Ullemeyer "Geologists impassioned with neutron physics".* (14.05.2015)
- **U. Filges** (Neutron Optics and Scientific Computing Group, Paul Scherrer Institut, Switzerland). *Preparation of SINQ Upgrade,* **V. Talanov** (Radiation Transport and Multiphysics Group, Paul Scherrer Institut, Switzerlan). *Target and Moderator Developments for the Neutron Sources at PSI.* (09.06.2016)

Ch. Alba-Simonesco

- **Ch. Alba-Simonesco** (LLB, Saclay, France) *Information about Laboratoire Leon Brillouin.* (23.10.2015)
- **D. Kolodynska** (Marie Curie-Sklodowska university, Lublin, Poland) *Organic-inorganic hybrid materials and their applications* (29.10.2015)
- **T. Yamamoto** (Waseda University, Okubo, Shinjuku, Tokyo) *X-ray Absorption Near-Edge Structure Analysis for Functional Materials with the Aid of the First-Principles Calculations* (07.12.2015)
- **Ye.P.Shabalin** (FLNP JINR) *Neutron source of the future in FLNP* (24.12.2015)

CONFERENCES AND MEETINGS

- On May 25-29, 2015 the JINR International Conference Centre hosted the **23rd International Seminar on Interaction of Neutrons with Nuclei:** Fundamental Interactions & Neutrons, Nuclear Structure, Ultracold Neutrons, Related Topics **(ISINN-23).** The Seminar is organised by the Laboratory of Neutron Physics annually at the end of May. This year it was dedicated to the 100th anniversary of the birth of the outstanding Soviet physicist, one of the founders of the LNP – Corresponding Member of the USSR Academy of Sciences F.L. Shapiro.The Seminar was attended by about 70 staff-members from different laboratories of JINR, about 40 scientists from Russia and the CIS, and about 20 representatives of a wide range of countries: Bulgaria, Great Britain,

ISINN-23, Dubna, Russia

Vietnam, Germany, Iran, Romania, Serbia, Slovakia, France and the United States. Within 4 working days 60 oral reports and 50 poster presentations on the subject of the Seminar were given to the participants.

- **The 6th European Conference on Neutron Scattering** (ECNS-2015) was held in Zaragoza, Spain, from August 30 to September 4. The Conference is organized every four years since 1996 under the auspices of the European Neutron Scattering Association (ENSA). ECNS-2015 brought together over 600 representatives of the European neutron scattering community to discuss recent developments and advances in all branches of science in which neutron scattering is used. The Conference's topics covered a wide range of relevant interdisciplinary problems of physics of condensed and soft matter, biology and medicine, chemical design, magnetism and spintronics, fundamental neutron physics, diagnostics of functional materials and objects of cultural heritage, geology and investigations of matter under extreme conditions. The Conference provided a platform for discussion of the current status and prospects of the available and future European neutron sources (nuclear research reactors and accelerator-based spallation sources), development of specialized neutron moderators and instruments on neutron sources, as well as proposals for the implementation of new methods and approaches for investigations of matter using neutron scattering.

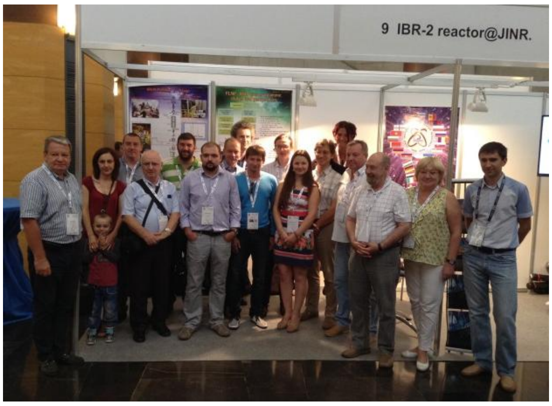

6th ECNS, Zaragoza, Spain

JINR was represented at ECNS-2015 by a delegation of twenty FLNP scientists who reported their results of the investigations conducted at the Laboratory neutron sources — IBR-2 and IREN. An important part of the ECNS program was an exhibition of the world's leading neutron centers, in which JINR participated with great success. The FLNP stand provided the Conference participants with an opportunity to become acquainted with the operation and plans of development for the neutron sources in JINR. The presentation was primarily focused on the implementation of the user policy at the IBR-2 pulsed reactor after its recent modernization. Numerous visitors of the stand could get the most comprehensive information about the possibilities of the existing spectrometers and find out the details of obtaining experimental beamtime at the IBR-2.

- **The International Conference 'Condensed Matter Research at the IBR-2'** (CMR-2015) was held in the Frank Laboratory of Neutron Physics on October 11-15, 2015. A series of these conferences was launched in 2014, aimed at providing a platform for discussion of the results of interdisciplinary studies of condensed matter using neutron scattering at the IBR-2 reactor, as well as for analysis of prospects of future research and improvement of instrumentation

CMR IBR-2, Dubna, Russia

and methodological base. The CMR-2015 was dedicated to the 100th anniversary of the birth of the outstanding Soviet physicist Fyodor Shapiro, the event which was celebrated in JINR throughout 2015. Fyodor Shapiro is recognized as one of the founders of the Frank Laboratory of Neutron Physics, who made a significant contribution to the development of scientific research areas and basic facilities of the Laboratory.

The Conference was attended by over 120 participants from scientific organizations and universities of the Russian Federation, Azerbaijan, Belarus, Bulgaria, Vietnam, Germany, Latvia, Moldova, Mongolia, Romania, Serbia, Slovakia and Ukraine.

EDUCATIONAL PROGRAM

- **The VI International School for Young Scientists and Students "Instruments and Methods of Experimental Nuclear Physics. Electronics and Automatics of Experimental Facilities"** was held on November 9-14, 2015 in FLNP. The School was organized by the Frank Laboratory of Neutron Physics with the support of the JINR Directorate and Plenipotentiary of Kazakhstan. Seventy two attendees from the JINR Member States (Belarus, Kazakhstan, Russia, Ukraine) took part in the School. The most representative group of participants came from Dubna, Obninsk, Kharkov, Astana, Moscow, Almaty, Tomsk, Dimitrovgrad. Among them were 4th year students (28 participants), 5th and 6th year students (27 participants), 3d year students (7 participants), 2nd year students (3 participants), 4 postgraduates and 3 researchers.

VI IMENP, Dubna, Russia

Summer student practice, 2015, IBR-2, Dubna, Russia

- The FLNP successfully collaborates with the **JINR University Centre** in the organization of **summer practical work for students from the JINR Member States** (Belarus, Czech Republic, Poland, Romania, Slovakia,) and Associated countries (Egypt, South Africa).

Lectures and excursions to the FLNP facilities for teachers of physics from Russia and the JINR Member States were organized.

VISITS AT OUR FACILITIES

- On February 05, a delegation of German Embassy visited FLNP.
- On June 09, Dr. Uwe Filges from Paul Scherrer Institut, Switzerland visited the FLNP.
- On June 16, the participants of the Brasilia-JINR Forum “Frontiers in Nuclear, Elementary Particle and Condensed Matter Physics” held in JINR from June 15 to June 19, 2015, visited the Laboratory. Members of the delegation met the Laboratory Directorate and visited the facilities on the IBR- 2 reactor.
- On August 07, a delegation of Turkish Embassy visited FLNP.
- On October 22-23, 2015 a delegation from Laboratoire Léon Brillouin, Saclay, France headed by Dr. Ch. Alba-Simonesco visited FLNP. The guests met with the Laboratory Directorate and visited the IBR-2 reactor.
- On October 28-29, 2015 Dr. Dorota Kolodynska from Marie Curie-Sklodowska university, Lublin, Poland visited FLNP.
- On November 29 – December 1, 2015 a delegation from the European Spallation Source (ESS), Sweden visited FLNP. Members of the delegation met the Laboratory Directorate and visited the facilities on the IBR- 2 reactor. The workshop on research and development of equipment for neutron scattering instruments on external beams was organized.
- Director of the Institute of Condensed-Matter Science, Waseda University, Tokyo, Dr. Tomoyuki Yamamoto visited FLNP in December 2015.

6. ORGANIZATION

STRUCTURE OF LABORATORY AND SCIENTIFIC DEPARTMENTS

Directorate:	
Director	*V.N. Shvetsov*
Deputy Director	*O.A. Culicov*
Deputy Director	*E.V. Lychagin*
Deputy Director	*N. Kucerka*
Deputy Director	*S.V. Kozenkov*
Chief engineer:	*A.V. Vinogradov*
Scientific Secretary	*D.M.Chudoba*
Laboratory Scientific Leader	*V.L. Aksenov*
Advisor to Directorate	*V.D. Ananiev*
Advisor to Directorate	*L.B.Pikelner*

Reactor and Technical Departments	Head
IBR-2 reactor	Chief engineer: *A.V. Dolgikh*
Mechanical maintenance division	*A.A. Belyakov*
Electrical engineering department	*V.A. Trepalin*
Design bureau	*A.A. Kustov*
Experimental workshops	*A.N. Kuznetsov*

Scientific Departments	Head
The Division of Condensed Matter Research and Developments	*A.V. Belushkin*
Nuclear physics department	*V.N. Shvetsov*
Sector of Raman Spectroscopy	*G.M. Arzumanyan*

Administrative Services
Secretariat
Finances
Personnel

Scientific Secretary Group
Secretariat
Translation
Graphics

DIVISION OF CONDENSED MATTER RESEARCH AND DEVELOPMENTS
DEPARTMENT OF NEUTRON INVESTIGATION OF CONDENSED MATTER

Sub-Division	Title	Head
Head of the Department		*D.P.Kozlenko*
Sector 1: Neutron Diffraction. Head: *G D. Bokuchava*		
Group No.1	HRFD	*A.M. Balagurov*
Group No.2	DN-2	*A.I. Beskrovnyi*
Group No.3	DN-12	*B.N. Savenko*
Group No.4	Geomaterials	*D.M.Levin*
Group No.5	SKAT /Epsilon	*Ch. Scheffzük*
Sector 2: Neutron Optics. Head: *M.V. Avdeev*		
Group No.1	REMUR	*Yu.V. Nikitenko*
Group No.2	REFLEX	*V.I. Bodnarchuk*
Group No.3	GRAINS	*V.I.Petrenko*
Small angle scattering group		*A.I. Kuklin*
Inelastic scattering group		*D. Chudoba*

DEPARTMENT OF IBR-2 SPECTROMETERS COMPLEX

Sub-Division	Title	Head
Head of the Department		*S.A. Kulikov*
Group No.1	Detectors	*A.V. Churakov*
Group No.2	Electronics	*A.A. Bogdzel*
Group No.3	Information technologies	*A.S. Kirilov*
Group No.4	Sample environment and choppers	*A.P. Sirotin*
Group No.5	Cryogenic investigations	*A.N. Chernikov*
Group No.6	Cold moderators	*M.V. Bulavin*

SECTOR OF RAMAN SPECTROSCOPY

Sub-Division	Title	Head
Head of the Sector		*G.M. Arzumanyan*
Group of biomolecular spectroscopy		
Group of luminescence and structural analysis		

NUCLEAR PHYSICS DIVISION

Sub-Division	Title	Head
Sector 1.	investigations of neutron-nuclear interactions	*Y.N. Kopatch*
Sector 2.	Investigation of neutron fundamental properties.	*Ye.V. Lychagin*
Sector 3.	Neutron Activation Analysis and Applied Research:	*M.V. Frontasyeva*
IREN facility		*V.G. Pytaev*

6.ORGANIZATION

PERSONNEL

Theme	Departments	People
-1104-	Nuclear Physics Department	104
	The Division of Condensed Matter Research and Developments	1
-1121-	Department of neutron investigation of condensed matter	100
-1122-	Department of IBR-2 spectrometers complex	50
	Sector of Raman Spectroscopy	9
-1105-	IBR-2 reactor Mechanical and Technical Department Electric and Technical Department Central Experimental Workshops Nuclear Safety Group Design Bureau	46 48 31 36 8 7
	FLNP infrastructure: Directorate Services and Management Department Scientific Secretary Group Supplies Group	 10 27 5 5
Total		**487**

PERSONNEL FROM THE JINR MEMBER STATES (BESIDES THE RF)

Country	People	of which young specialists (≤35 years)
Azerbaijan	11	10
Belarus	1	1
Bulgaria	6	3
Georgia	1	
Germany	1	
Kazakhstan	11	11
Moldova	2	2
Mongolia	9	9
Poland	11	3
Romania	8	3
Slovakia	2	1
Ukraine	12	9
Uzbekistan	1	1
Vietnam	4	

TOTAL	80	53

OUR PhD STUDENTS

In 2015 23 PhD students from 10 countries conducted their experimental research at the FLNP facilities.

Name	Country	PhD student of
Alekseenok Yu.V.	Belarus	International Sakharov Environmental University
Hristozova G.	Bulgaria	Paisii Hilendarski University
Sanislo A.	Hungary	Obuda University
Bagdaulet M.	Kazakhstan	Al-Farabi Kazakh National University
Hramco C.	Moldova	University of the Academy of Science of Moldova
Nyamsuren B.	Mongolia	National University of Mongolia
Luczynska K.	Poland	Institute of Nuclear Chemistry and Technology
Ordon M.	Poland	Siedlce University of Natural Sciences and Humanities
Jaketov V.D.	Russia	JINR University centre
Rumyantsev I.	Russia	JINR University centre
Rutkauskas A.V.	Russia	JINR University centre
Halansky D.A.	Russia	Dubna International University for nature, Society and Man
Husenov M.A.	Russia	Moscow State University of Technology „STANKIN“
Zelenyak T.Y.	Russia	Dubna International University for nature, Society and Man
Vergel K.	Russia	Dubna International University for nature, Society and Man / FLNP JINR
Kravtsova A.V.	Russia	A.O. Kovalevsky Institute of biology of the Southern Seas
Nekhoroshkov P.	Russia	A.O. Kovalevsky Institute of biology of the Southern Seas
Ndlovu N.B.	South Africa	Stellenbosch University
Eze P.	South Africa	Western Cape University
Gapon I.V.	Ukraine	National University of Kyiv
Popiuk T.V.	Ukraine	National University of Kyiv
Samoylenko S.A.	Ukraine	National University of Kyiv
Tomchuk A.V.	Ukraine	National University of Kyiv

In 2015, 2 BSc theses, 8 MSc theses and 7 PhD theses were defended using the experimental material obtained in FLNP.

INTERNATIONAL COOPERATION

In 2015 the Frank Laboratory of Neutron Physics collaborated with 240 institutions from 41 countries.

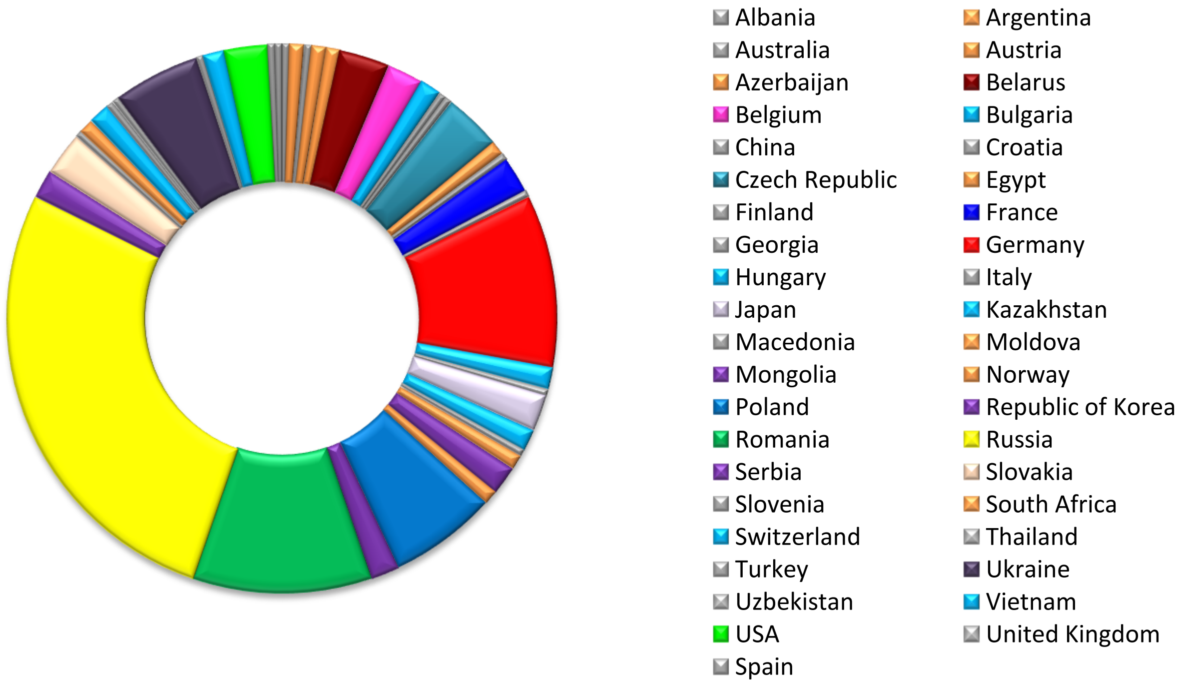

USER INTERACTION

In 2015 were two calls for proposals for experiments at the modernized IBR-2 reactor (01 September – 15 October 2013; Call-II: 01 March – 15 April 2014). A total of 197 proposals for conducting experiments were received from 19 different countries. The received proposals covered the broad spectrum of neutron research in physics, materials science, chemistry, geosciences, biology and applied sciences. 174 received proposals were admitted for realization.

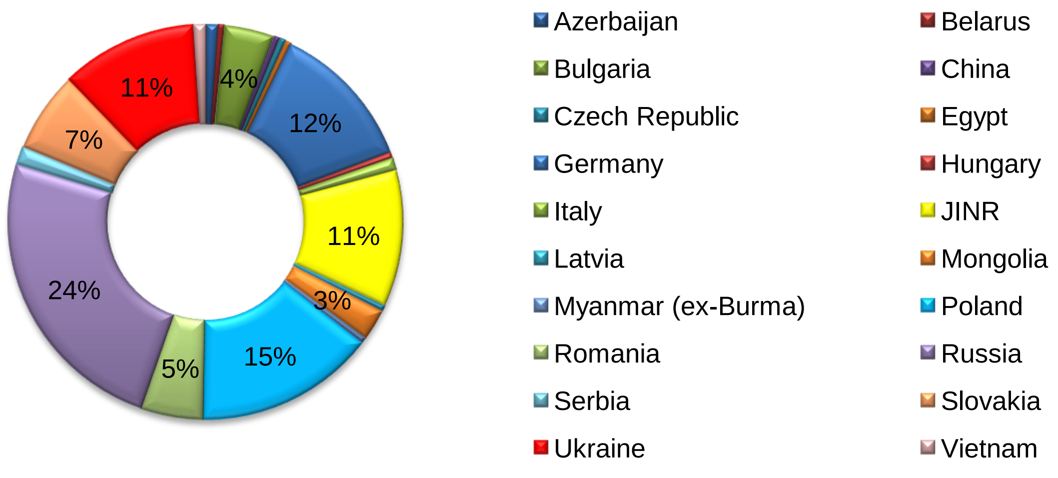

Proposal distribution by science (left) and by facilities (right).

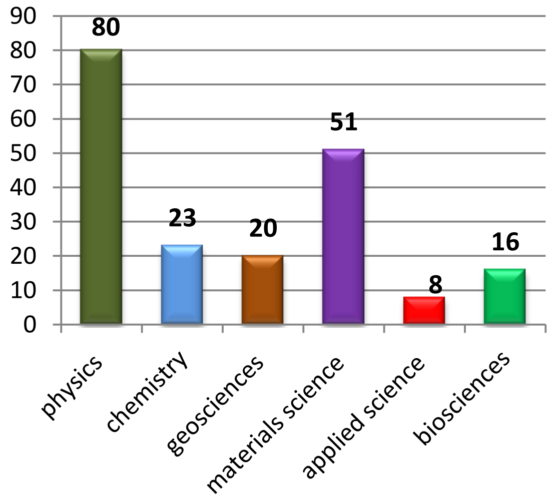

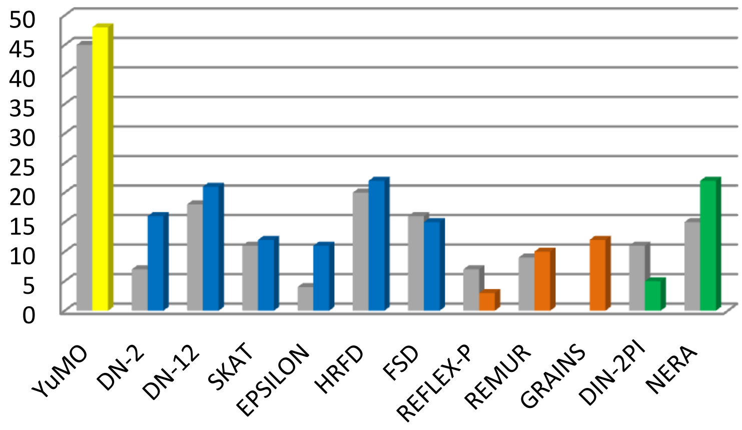

List of Visitors from the Member States or Associated Members of JINR in 2015

Country	Nr of visitors
Azerbajan	2
Belarus	2
Bulgaria	8
Czech Republic	10
Georgia	2
Germany	19
Egypt	3
Kazakhstan	1
North Korea	6
Moldova	2
Mongolia	3
Poland	12
Romania	5
Serbia	3
Slovakia	5
Ukraine	7
RSA	4
Vietnam	3

List of Visitors from the not Member States or Associated Members of JINR in 2015

Country	Nr of visitors
China	1
France	3
Japan	4
Latvia	1
Norwey	1
Tajikistan	4
Sweden	6
Swizerland	2

8. FLNP AND MASS-MEDIA

In the year 2015 Frank Laboratory of Neutron Physics was at center of interest of mass media

Телеканал Дубна
March 2015

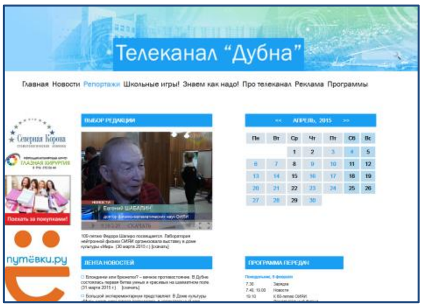

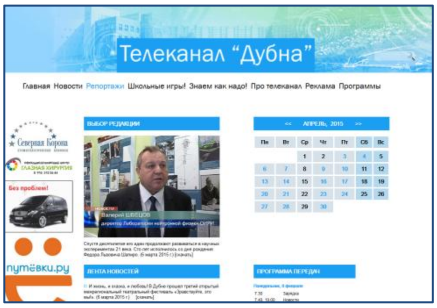

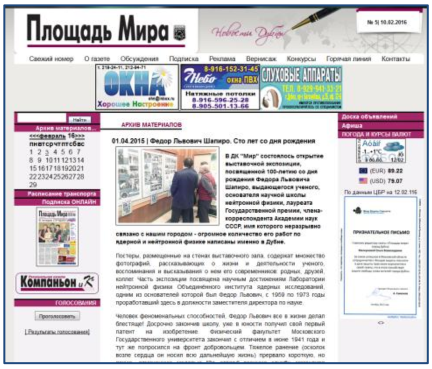

Площадь Мира
April 2015

Встреча
April 2015

ДУБНА
June 2015

Наука - практике

Реакторное материаловедение на ИБР-2

Advertising feature

Fast pulsed reactor IBR-2

The IBR-2 pulsed reactor is a powerful neutron source operating at the Frank Laboratory of Neutron Physics of Joint Institute for Nuclear Research. It operates at a mean power of 2 MW.

The main part of the reactor, as shown schematically in Figure 1, is an irregular hexahedron composed of fuel element subassemblies. The cooling system has three circuits and two loops. In the first and second circuits the coolant is liquid sodium and in the third it is air. The core is installed in a double-walled steel vessel and is surrounded by a number of stationary reflectors, control and safety units among them. Around the reactor there are water moderators scanned by 16 horizontal channels for neutron extraction. Two of the moderators are grooved. After modernization of the IBR-2 reactor (2006-2011) a pelletized cold-neutron moderator based on solid mesitylene was installed.

Its main difference from other reactors consists in mechanical reactivity modulation by a movable reflector (Figure 2).

The movable reflector is a complex mechanical system providing reliable operation of two parts, which determine the reactivity modulation: the main movable reflector and the auxiliary movable reflector. The rotors of the main and auxiliary movable reflectors rotate in opposite directions with different velocities. When both reflectors coincide near the reactor core, a power pulse is generated. The IBR-2 reactor with its unique technical approach produces one of the most intense pulse neutron fluxes at the moderator surface among the world's reactors: ~10^{16} n/cm²/s, with a power of 1850 MW per pulse.

Currently, the spectrometer complex of the IBR-2 pulsed reactor consists of 13 instruments available for scientific research: 7 diffractometers, 1 small-angle neutron scattering spectrometer, 3 reflectometers and 2 inelastic neutron scattering spectrometers (Figure 3). There are also 2 new facilities under construction: neutron imaging instrument for radiography and tomography studies (NRT) and Fourier spectrometer for stress measurements (FSS).

The IBR-2 is used mainly for condensed matter physics and applied research. Experiments usually take 2500 hours of operation time per year.

Figure 1. Main part of IBR-2 reactor.

Figure 2. Core of IBR-2 reactor with movable reflector.

Figure 3. Layout of IBR-2 spectrometer complex.

Contact
The Frank Laboratory of Neutron Physics, JINR, Joliot-Curie str. 6, Dubna, Moscow reg., Russia, 141980
Tel (7-49621) 65-657
E-mail shv@nf.jinr.ru
Web http://flnp.jinr.ru/25/

Physics World, Focus on Neutron Science
October 2015

Neutron News
November 2015

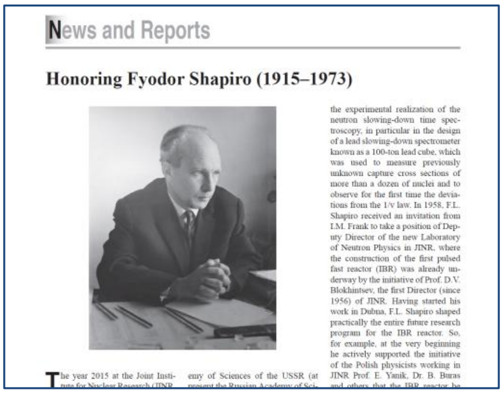

News and Reports

Honoring Fyodor Shapiro (1915–1973)

the experimental realization of the neutron slowing-down time spectroscopy, in particular in the design of a lead slowing-down spectrometer known as a 100-ton lead cube, which was used to measure previously unknown capture cross sections of more than a dozen of nuclei and to observe for the first time the deviations from the 1/v law. In 1958, F.L. Shapiro received an invitation from I.M. Frank to take a position of Deputy Director of the new Laboratory of Neutron Physics in JINR, where the construction of the first pulsed fast reactor (IBR) was already underway by the initiative of Prof. D.V. Blokhintsev, the first Director (since 1956) of JINR. Having started his work in Dubna, F.L. Shapiro shaped practically the entire future research program for the IBR reactor. So, for example, at the very beginning he actively supported the initiative of the Polish physicists working in JINR Prof. E. Yanik, Dr. B. Buras and others that the IBR reactor be